Theses and Dissertations

2017

Optimization Procedure to Identify Blockages in Pipeline Networks via non-invasive Technique based on Genetic Algorithms

Mohanad Abdulzahra Ani Khazaali
Lehigh University

Follow this and additional works at: http://preserve.lehigh.edu/etd

Part of the Civil and Environmental Engineering Commons

Optimization Procedure to Identify Blockages in Pipeline Networks via

non-invasive Technique based on Genetic Algorithms

By

Mohanad Khazaali

A Thesis

Presented to the Graduate and Research Committee

of Lehigh University

in Candidacy for the Degree of

Master of Science

in

Structural Engineering

Lehigh University

MAY- 2017

Approval

This thesis is accepted and approved in partial fulfillment of the requirements for the Master of Science.

_____

Date

_____

Thesis Advisor

_____

Chairperson of Department

Acknowledgements

I would like to express my deep and sincere gratitude to my supervisor Dr. Paolo Bocchini for his support, his effort and his time during my study. I would like to thank him for providing me with useful information, remarks and engagement through the entire process of my thesis. Also, I would like to thank Dr. Marzani for his dedicated involvement in contributing to my study and his support on my way. Moreover, I would like to thank Prof. Herman Nied for his attendance and his useful comments during the experimental part of the study.

Furthermore, my deep gratitude to the seven undergraduate students (Diana, Amanda, Jill, Ilais, Le. Fang, Jeff and Zhuojie Ji) who helped me throughout the experimental work. They had willingly shared their precious time during the experiment setups. I would also like to thank Dr. Richard Weisman and Prof. David Angstadt for their valuable lectures addressing the fluid dynamic concepts.

I would like to thank our research group, my colleagues and my friends, who have offered help by revising my thesis or supporting throughout the entire process. Finally, I would like to thank the Higher Committee of Education Development in Iraq (HCED) for their support and funding my master's degree. At the same time, I would like to thank Lehigh University for funding my experimental work and made it possible.

Last but not the least, I would like to express my affection, respect and gratitude to my parents for bestowing their unyielding support to educate me and encourage me to pursue my career. Special love and great thanks to my brother who sacrificed his life to protect my country.

A huge thank you to my sisters and my other youngest brother for supporting and taking care of my parents.

Table of Contents

List of Tables

List of Figures

X

Notation

L: The original pipe length

D: The original pie diameter

fr: The friction coefficient

h_L: Head loss of *Darcy* formula

Q: The pipe flow

e: The roughness of a pipe

Re: Reynolds number in a pipe

ρ: The fluid density

V: The fluid velocity

μ: Fluid dynamic viscosity

T: The fluid temperature

$\widehat{D_e}$:   The equivalent uniform diameter

g: The gravitational acceleration

n_p: Total number of pipes

n: Total number of nodes

α: Normalized diameter reduction

K: Global stiffness

h: Global vector of pressure heads

R: Global vector of residuals

J :   The fitness function

Φ_h: The head loss discrepancy function

Φ_Q: The discharge discrepancy function

nl_h: Head loss noise level

nl_Q: Flow noise level

γ: The penalty factor

z: Nodal elevation

β^h, β^Q: The independent standard Gaussian random variables

ΔQ: The volumetric flow rate

Δh: The change in pressure heads

Abstract

The existence of blockages in pipeline networks leads to serious issues that affect the efficiency of the infrastructure, losses of services and environmental risks. To these regards, this study proposes a technique to identify the pipes that are blocked within pipeline or a complex pipe network. This thesis focuses on detecting blockages by using a technique based on a ***few measurements that are usually gathered from normal operational conditions*** of the pipeline system. The same approach can be implemented in different fields of engineering to identify the damage, which it is the object of recent interest and development.

Such technique can provide significant economic benefits especially for the gas and oil industries (i.e., this pipe blockage detection method leads to time and monetary savings compared to traditional inspection techniques which are more expensive). Long term blockages have the potential to cause permanent damage inside the pipes. To this respect, an optimization procedure that relies upon noninvasive measurements of the flow rate and pressure head, is used to assess the system functionality through Genetic Algorithms (GAs) that aim to solve this problem and perform the optimization procedure. The framework of this technique relies on both a Finite Element-like simulator and GAs to perform the optimization procedure. More investigations have been done experimentally and numerically in this study to determine the occlusions that occur inside looped or branched pipeline networks. The main contribution of the following study explores the validity, sensitivity and accuracy of such methodology by considering different blockage scenarios through two major parts:

Part 1 (Experimental work) - A series of experiments were designed and performed by our team, involving myself and 7 more students from the civil and mechanical engineering departments under my supervision, in the span of 12 weeks to validate the robustness of the proposed technique empirically. The study was proven numerically by some researchers with real cases [Marzani et al., 2013 and Bocchini et al., 2014], while there has not been any research publicly available to validate this technique experimentally. For the first time, a comprehensive empirical study has examined the capability of this technique to identify the presence of blockages within different pipeline networks (evaluate the accuracy and the sensitivity). Several looped and branched networks by utilizing PVC pipes were tested throughout this study. The experimental data (flow in pipes and nodal pressure heads) acquired from the testing were analyzed and used to validate the proposed technique. Based on empirical data, it is evident that the technique could successfully identify the location of blockages inside the pipes with a reasonable degree of accuracy. More importantly, the proposed technique can cope even with missing measurements. Such technique is still a valid option for detecting the blockage in pipeline system, but with limitation in the accuracy based on several parameters (i.e., the structure of the network itself, the selected objective function and boundary conditions). Results, errors and conclusions are presented thereafter.

Part 2 (Theoretical work) – Several numerical tests have been conducted to improve the technique by considering parametric studies. The theoretical work is focused on assessing the accuracy, robustness, computational efficiency and limits of applicability of the methodology. Many parameters are taken into consideration, such as friction factor (fr), objective function ($J(\alpha)$) and other design criteria (i.e., the input data) to observe its effect

on the technique's sensitivity. As a part of this study, strategies to improve the technique are investigated and summarized. Then, real cases are considered to evaluate the overall performance of the suggested technique. The results of blockage identification, advantages and disadvantages of the procedure for practical implementation are presented.

Chapter 1

INTRODUCTION TO BLOCKAGE IDENTIFICATION

1. Introduction

Long term blockages in pipeline networks have the potential to cause enduring damage inside the pipes. This affects the efficiency and reliability of the infrastructure, which can lead to significant economic losses as well as severe disruption of the normal operational conditions. More specifically, occlusions are a prevalent issue that can happen in the components that are used to transmit the fluid (i.e. pipelines or ducts). The fluid can be water, oil, gas or even waste water. Blockage is a serious problem that can affect the entire network. It has considerable economic and environmental cost. Obstructions may generate due to waste deposition, aging pipelines and corrosion in pipes. The presence of a blockage or multiple blockages can reduce the cross-sectional area of the pipe and the flow, and increase the roughness on the inner surface of the pipe. In most cases, it is critical to identify the exact location of the pipes that are blocked and then through further inspection, a remedial action can be taken. It is important to take immediate action for such issue. The early detection of blockages has a great impact on the economy (i.e., early pipe blockage detection leads to time and monetary savings and prevents structural damage) [Bocchini et al., 2014].

Interestingly, a new technique has been proposed by Marzani et al., [2013] that is based on non-invasive steady state measurements that can be usually gathered during the normal operational conditions of the system. This approach can provide significant economic benefits, especially for the gas and oil industries, when compared to traditional inspection techniques, which are costly. Marzani et al., [2013] and Bocchini et al., [2014] have validated the technique numerically under fifteen blockage scenarios of pipeline networks in collaboration with the Italian Hydrocarbon Company (ENI S.p.A.). The

identification method includes an optimization procedure that is used to assess the system functionality through Genetic Algorithms (GAs). The framework of this technique relies on both a Finite Element-like simulator and GAs to perform the optimization procedure [Bocchini et al., 2014]. Nonetheless, there has not been any research publicly available to validate this technique experimentally.

This thesis focuses on detecting blockages in a pipeline and complex pipe networks by using such technique. A detailed study has examined experimentally for the first time the ability to identify different blockages with different designs of the pipeline networks (evaluate the accuracy and sensitivity). Experimental work on looped and branched network has been conducted to validate the proposed technique. Also, several numerical applications have been considered to assess the accuracy, robustness, computational efficiency and limits of applicability of the methodology. Furthermore, new strategies have been suggested to improve the procedure.

The main purpose of this method is to identify the blockage in each individual segment of the pipelines. There are several methods that can be used to further analyze the pipe that is obstructed. Most of the common techniques that can be used to do this task are summarized in the following.

The "Discrete Blockage Detection in Pipelines Using the Frequency Response Diagram" depends also on non-invasive measurements to detect location and size of discrete blockages for each pipe by extracting the behavior of the system in the form of a frequency diagram [Lee et al., 2008]. This technique requires dynamics analysis using eigenvalues to find the frequencies for each mode. Therefore, it requires time and a high cost to be implemented. Other techniques presented by Sattar et al., [2008] and Mohapatra

et al., [2006] utilize the frequency response as well. The "Friction Loss Technique" enables to identify the blockages according to variations in pressure and flow measurements, but it works with limitations (e.g., it has been validated to detect the wax deposit in the Valhall subsea pipelines) [Marshall et al., 1990]. The "Evaluation of the Backpressure Technique" proposed by Scott and Satterwhite [1998] allows to detect the pipes that are partially obstructed as a result of comparing "a production data" (pressure and flow) to "a baseline performance curve". Moreover, some techniques have been proposed based on fluid transients [see, among others, Adewumi et al., 2003, Wang et al., 2005 and Duan et al., 2014]. Adewumi et al., [2003] proposed a technique which has successfully been applied to detect multiple blockages with a reasonable accuracy by utilizing "the interaction between a pressure pulse propagating in pipe with the blockages therein and characterization". More recently, new techniques have been proposed to perform the same purpose and most of them validated under different field of study (e.g., hydraulics and mechanics). The technique based on transient overpressures is the more recent study used in detecting location, size and length of overall blockages inside the pipes. However, it requires very high efficiency devices to record the high pressures and the time history analyses, which makes it very costly to be implemented.

Dedicated devices, high cost, and sophisticated measurements that interrupt the operational conditions are essential parts for all above mentioned methods. Also, most of these techniques have been successfully proved only under laboratory conditions with a single pipe and have limited applicability. However, the technique studied in this thesis is based on simple, available measurements that do not affect the normal operational conditions and have low relevant economic impact. With respect to all above stated

methods, the proposed technique provides further benefits and enhancements in blockage identification. The technique is successfully validated to identify the blockages in the entire pipelines network. This method can work with any type of network, whether simple, complex, looped or branched. Since the technique takes into consideration the surrounding temperature of the pipes, it can be used with pipes at any location, whether underground, in the desert, or submerged in the sea [Marzani et al., 2013].

The fluid properties, pipe network characteristics and type of fluid are taken into consideration during the identification procedure. The blockage identification is performed by minimizing the discrepancy between the empirical available measures (pressure heads and flow) and the computed measures via Finite Element Modeling, FEM. Each pipe is modeled as a two node element. The entire network is analyzed by considering two main variables: pipe flows (Q) and nodal pressure heads (h). The next step of the optimization problem is determined by GAs, which is a popular heuristic technique that works quite well for such proposed methodology. GAs are particularly appropriate "for this application because they can cope quite easily with the presence of local minima and do not require a closed form expression of the objective function" [Bocchini et al., 2014].

The main contribution of the following study embeds two major parts of the blockage identification (experimental work and theoretical work). Numerical and experimental applications are investigated to determine the occlusions that occur inside the loops or the branches of pipeline networks. Several parametric studies are conducted to prove the efficiency, accuracy, and limitation of applicability of such methodology.

1.1 Objective of the Methodology

The research aims to identify the blockages in pipe networks through a non-invasive technique based on steady state measurements and GAs to perform the optimization procedure. Several scenarios of obstructions in different networks are inspected. The purpose of this study is to validate the proposed technique numerically and experimentally by using simple and complex pipeline networks. Also, it attempts to improve the accuracy, robustness, computational efficiency and limits of applicability of such methodology by testing the most critical parameters (i.e., the friction factor, GAs parameters and objective function) that affect results. Likewise, the study aims to provide a better understanding about the stability of the pipeline networks (the appropriate location to impose boundary conditions). The ultimate goal is to customize the technique for different designs of the pipeline networks by proposing more relevant strategies.

1.2 Motivation for the Study and Statement of the Proposed Approach

The preference of the proposed methodology among others that were previously mentioned, can be beneficial for many reasons. Most of the techniques that have been discussed require dynamic analysis to obtain the frequency diagram, which is used in blockage identification. The dynamic analysis itself is time consuming and costly. Other techniques that have been examined depend on transient analysis and flow-pressure diagram. These methods require complicated measurements at each pipe segment and the process will interrupt the normal operational conditions, which leads to negative economic impact. Nowadays, engineers are looking for simple and rational solutions with a reasonable degree of accuracy. It is necessary for any applications to take into

consideration many aspects to achieve the optimal solutions with a cost effectiveness and decent accuracy. In fact, the suggested technique can easily attain these conditions. This method relies on simple measurements that are usually gathered from the normal operational conditions. Moreover, the technique provides a deep understanding about the entire behavior of the network, and it can detect the blockages at any location without going into details about what has happened inside individual pipes. More importantly, this procedure compared with others, can be used with pipes at any location, whether in ground or submerged in water.

The identification procedure can be done by using a FEM- like simulator and GAs that solve the optimization problem. Also, the user can easily apply GAs without going into details. GAs do not require a closed-form expression of the objective function. The technique does not require sophisticated steps, it requires simple measures to detect the occlusion in the entire network. The technique also provides a very good accuracy even in case of a few missing measurements (i.e., the pressure head and pipe flow are not available). This case can happen when pipes are inaccessible.

In case of large or complex pipeline networks, it is difficult, if not impossible, to apply other previously discussed methods with suitable accuracy. It is illogical to take measurements in each segment of pipe since this is considered neither realistic nor, often, interesting. For this reason, in many cases it is preferred for large infrastructure to be subdivided, which facilitates the identification procedure. Hence, the proposed technique is appropriate to deal with the most complex infrastructure, and it can analyze the various parts individually. The technique successfully identifies the blockages with sufficient

accuracy regardless of their size and length, whether the entire pipe is blocked or only a portion of it.

It has been noticed that further enhancement of using multi-phase fluid within the pipe can be accomplished during the improvement and adjustment of such methodology by implying a more complex set of finite elements [Bocchini et al., 2014].

1.3 Background Information

The proposed technique depends primarily on the measurements of flow and pressure head, which essentially depict the nature of the fluid and what is occurring inside the pipes. For example, the measurements of flow at any pipe can provide insight about the fluid behavior, whether turbulent, transient or laminar. These measurements are considered the most important parameters needed to examine the fluid state inside the system. It is notable that a major portion of analysis methods in fluid mechanics are formulated for finding flow rate and changes in pressure. Thus, it is important to understand the methodology, philosophy, and overall need of those measurements. In other words, it would be impossible to validate such technique without the flow and pressure measurements. The more measurements are available, the more accurate and reliable are the results that can be achieved. Generally, in fluid mechanics, all applications and most of the mathematical formulas rely on the flow measurements. The flow is also valuable for computing other quantities in fluid mechanics. When the flow measurement is available, other dependent variables can be easily computed. For instance, fluid flow is used to calculate the velocity via *Bernoulli* equation (the most popular formula in fluid dynamics), or pressure losses through *Darcy's* formula, and can also provide a good indicator about

the fluid flow behavior (i.e., laminar or turbulent flow). In some cases, just the flow measurement data is of importance. Either numerically or empirically, several methods can be used to find the flow quantity. However, the user should know the purpose of the measurements to assess their accuracy. Time should be taken to clearly define the need for such measurements. Depending on the flow measurement tool, it is important to understand if the measured value is to be used as is, or should be processed. To obtain meaningful results all these factors should be considered.

As important and necessary the flow rate is in fluid mechanics, so is pressure for many applications. The availability of precise pressure measuring tools is still limited, thus obtaining accurate pressure measurements is difficult compared with flow measurements. The needed pressure in many applications can be classified in three different categories; (1) absolute pressure, which refers to the absolute value of force per unit area, (2) gage pressure, which is the difference between absolute and local atmospheric pressure and (3) differential pressure, which is the measurement of pressure at any point referenced to a second, unknown, pressure at a different location [Heeley, 2005]. Therefore, it is necessary to select appropriately the type of pressure measurement. Moreover, it is imperative to have a basic understanding about the fluid's physical properties and their effect on its state (i.e., density, specific weight, temperature, viscosity, and compressibility).

The blockages can be identified by implementation of FEM and GAs, a function that represents the discrepancy between the measured data and the values simulated numerically. The output of the methodology is α of each pipe [Marzani et al., 2013].

Chapter 2

FUNDAMENTAL PROPERTIES AND DESCRIPTION OF THE PROPOSED TECHNIQUE

Abstract

This chapter discusses the most relevant fluid properties, which are one of the important features that clearly need to be defined. These properties are density, specific weight, viscosity and temperature, which can be changed in the model according to the type of fluid. For example, natural gas has its specific properties that are different from those of water.

It also presents the detailed steps of the proposed technique. Obstructions are detected as a result of minimizing the discrepancy between measured and computed quantities through an optimization procedure. Ways of solving nonlinear FEM, and the steps of applying GAs to perform the identification procedure are discussed in details.

2.1 Introduction

It is useful to provide a brief review of the relevant concepts of fluid mechanics. It can be defined as one of the oldest branches of physics and the foundation for the understanding of many other aspects of applied sciences and engineering [Yuan, 1967]. Recently, it has become an interesting and widespread subject in all fields of engineering. It is important to understand the nature of the fluid flow and distinguish how the physical properties vary when the fluid is either liquid or gas. Hence, the fluid properties are indicators to provide insight about how fluids can be used in various fields and give indication on the fluid behavior.

This chapter particularly describes in detail the framework of the identification procedure within three sections. The first section focuses predominantly on the characteristics of the pipe network (location of nodes, elevations, connectivity, physical and thermal properties of the fluid). The second section offers a detailed study about the

14

flow simulation by using nonlinear finite elements. Also, it includes the mathematical approach that formulates the FE model and several ways of solving it (i.e., Newton Raphson method used in the proposed technique). The third section contains a brief overview about GAs and how they can be implemented. Moreover, the identification procedure that is a result of minimization of the discrepancy between empirical and theoretical measurements is discussed in detail.

Finally, the most important basic properties of fluid, the characteristic of networks, the proposed methodology framework and its operation, and the identification procedure are discussed in full details.

2.2 Fluid Properties and Network Requirements

Fluid mechanics is a complicated branch of science, but it is necessary to comprehend the behavior of fluids inside pipeline networks. When the behavior is understood, it becomes simple to apply the appropriate formulas that facilitate the solution finding. Fluid mechanics is an advanced science, and it would be impossible to cover all the physical properties involved. for this reason, this section explains only the most important basic properties, which are essential in comprehending the proposed technique. They depend on a fluid type and are not influenced by a fluid motion. In other words, this sections discusses the fluid properties that will not change depending on whether the fluid flow is laminar or turbulent. Also, most of these properties are highly dependent on the change in temperature.

a. Pressure (P) is defined as the force exerted per unit area [Bayley, 1958]. Pressure measurements in any structure are complicated because of several requirements, and they are very sensitive to change in barometric pressure. Often, most pressure measurements require to be modified by considering the surrounding climate variations.

15

b. Density (ρ) is the mass per unit volume of a fluid. It can be expressed by the following mathematical formula:

$$\rho = \frac{mass}{volume}$$

Whereas, specific weight (γ) is the value of density multiplied by the acceleration of gravity (g).

$$\gamma = \rho.g$$

c. Viscosity (μ) is considered the most important property in the analysis of fluid behavior and its movement (the fluid motion). It can be defined as the amount of fluid resistance to the shear stress [Yuan, 1967 and Sankararaj, 2013]. Fluid viscosity can be divided into two types: (1) Kinematic viscosity that describes the behavior of flow; and (2) Dynamic viscosity that is known as shear viscosity. Temperature has a noticeable impact on viscosity (e.g., in liquid, viscosity decreases as temperature increases, while in gas, viscosity increases as temperature increases).

d. Temperature (T), as temperature varies throughout the day, the previous properties will be affected as well. The temperature of the fluid inside and outside the pipe is taken into consideration in the proposed technique. Therefore, the suggested methodology can easily work with pipes that are situated at any location.

These properties are required to be defined as input data in the suggested technique before running any optimization procedure. The system identification requires to define these properties in consistent units as inputs, as well as the characteristics of the network itself. The input of GAs includes all characteristics of the network to solve the optimization problem (i.e., location and elevation of the nodes, as well as connectivity matrix), of the individual pipes (i.e., length, design diameter, roughness, distributed head-losses, and

average temperature), and of the boundary conditions (i.e., the imposed pressure heads and flow). Furthermore, it requires for empirical measurements of flow and/or piezometric head to exist at some of the nodes [Marzani et al., 2013].

Pipe flow quantities are simulated numerically via FEM. Nonlinear FEM has been used, which applies a formula similar to that seen in structural mechanics. Additionally, GAs are selected as an engine to perform the optimization procedure by implementation of the objective function. FEM along with GAs are discussed in detail within the following successive sections.

2.3 Formulation of Finite Element Method (FEM)

As it is known among engineers, FEM is considered one of the most important approximate methods used successfully in many fields of engineering. It has been applied effectively in solving complex problems in structural analysis and fluid mechanics as well. The method was originally established to study the stresses in complex air-frame structures [Clough, 1960]. Later on it was extended to include all fields of continuum mechanics [Zienkiewicz and Cheung, 1965]. In many practical cases using closed-form expression is not impossible but difficult to some extent, or very time consuming. Hence, FEM is the best way to overcome this issue, and it is a preferable solution among engineers. Nowadays FEM is receiving substantial interest in education and in industry. It has become one of the qualification requirements in industry for many engineering jobs. FEM can deal with all types of problems, regardless of their complexity. The diversity and flexibility of FEM allow for its use in many applications. This thesis deals with single phase flow in steady state, thus, it is not necessary to use a complex FE model to simulate the pipe flow. Each

17

pipe is treated as a one-dimensional two-node element. However, it would be necessary to develop sophisticated elements in the case of multi-phase fluid (i.e., liquid and gas).

Recently, among the various numerical methods that have evolved over the year, FEM has received a considerable attention in the structural applications, [Nithiarasu et al., 2004]. Figure 2.1 shows and summarizes the scheme for the procedure of modeling a structure by FEM.
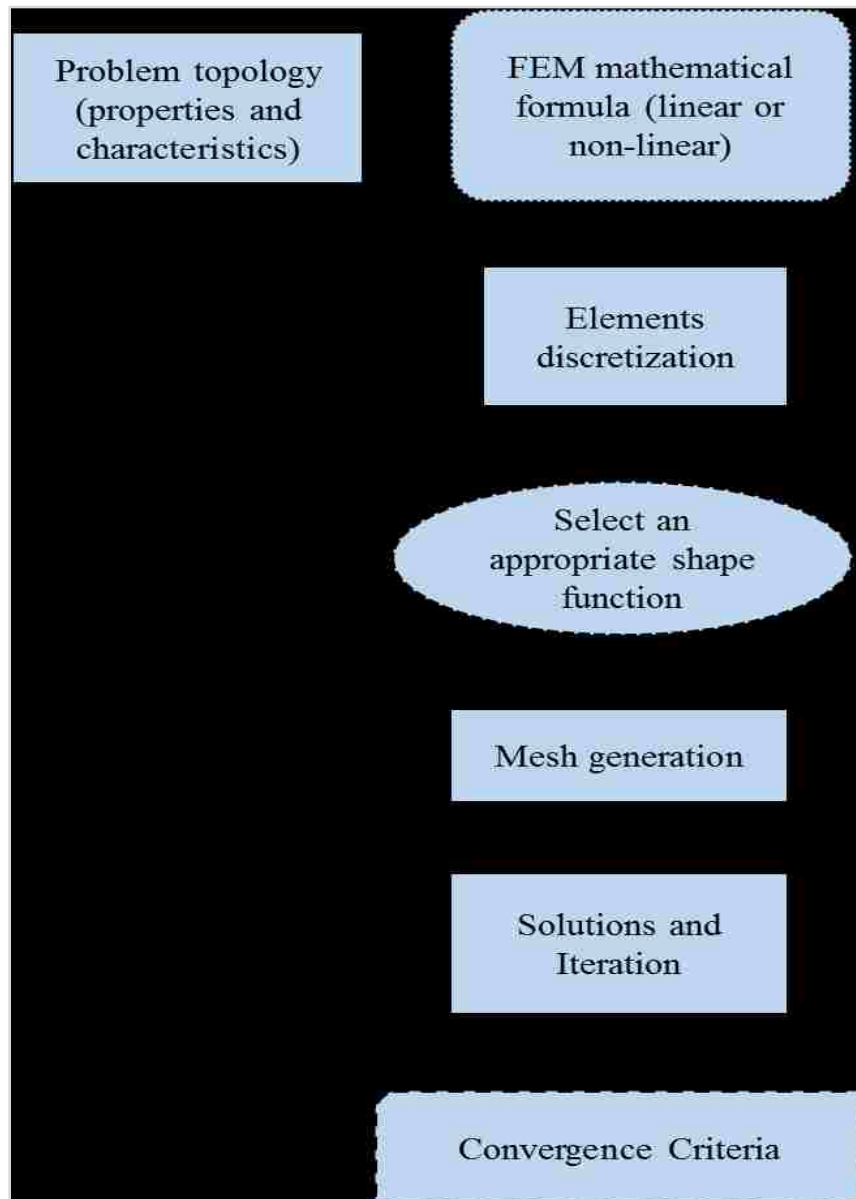
Figure 2.1:   FEM model of a structural element

2.3.1 Physical and Mathematical Descriptions

It is important to emphasize that the system identification depends on the measurements of the outputs and also on how the physical properties of the fluid in inputs can influence the system. Once the user understands the relation between the inputs and outputs of the suggested methodology, it does not need to investigate the details of what is actually happening inside the system. The idealization of a physical problem to a mathematical model requires certain assumptions that together lead to the (non-linear) equations governing the mathematical model [Bathe, 2014]. The suggested methodology uses FEM to simulate pipes flow quantities through an iterative solution. In this study, a mathematical formula that depends on the pressure head and flow as basic terms is used to simulate the flow quantities. Since the FEM is an approximate model with an iterative solution, it is important to tune specific parameters that provide good accuracy. In other words, it is necessary to evaluate the solution accuracy. If the accuracy criteria are not reached, "the numerical solution has to be repeated with refined solution parameters (such as finer meshes) until a sufficient accuracy" is obtained [Bathe, 2014].

"The finite element solution will solve only the selected mathematical model and all assumptions in this model will be reflected in the predicted response." Thus, to understand the total performance of the network system, it is important to choose an appropriate mathematical model [Bathe, 2014].

The formulation that is utilized in such technique is an extension of the expression represented by Mohtar et al., [1991]. The proposed technique in this thesis relies on the mathematical formula that is modified to include additional parameters compared with the

Mohtar et al. formulation. In particular, it includes the basic physical properties of fluid (i.e., density, viscosity, and temperature).

For each pipe, the model adopts the *Darcy Weisbach* formula that connects pressure head losses with the flow quantity such as:

$$h_L = \frac{8.fr.l}{\pi^2 g (\alpha D)^5} Q^2$$

Where:

h_L : Head loss

fr : Friction factor that depends on pipe roughness, diameter, and Reynolds number

L: Pipe length

g : Acceleration of gravity

D: Original diameter of the pipe

Q: pipe discharge

α : Parameter of reduction percentage of the original diameter.

The factor $'\alpha'$ is used to provide a quantitative assessment of the blockage in each pipe. When $\alpha = 100\%$ the pipe is completely clean, whereas, $\alpha = 0$ means that the pipe is entirely clogged.

Reynolds number (Re) is necessary to understand the conduct of the flow inside the pipe (i.e., laminar, transient or turbulent).

$$Re = \frac{\rho \upsilon D_H}{\mu}$$

Where:

D_H: The hydraulic diameter of the pipe

ρ: Fluid density

v: Average flow velocity

μ: The dynamic viscosity of the fluid that varies with fluid temperature

The threshold of Re to determine the flow type differ in the literature, but the most common one is as follows: $Re < 2100$ means the flow is laminar; if Re ranges between 2100 and 4000, it means the flow is transient; otherwise the flow will be turbulent. In many cases the transient flow is considered as turbulent flow. In the proposed technique, it is considered either laminar or turbulent flow.

The friction factor (fr) can be computed by using a close-form expression that depends on the flow type. If the flow is laminar, it can be calculated easily by the following formula:

$$fr = \frac{64}{Re}$$

While in the case of a turbulent flow, there are several ways to calculate fr explicitly or implicitly, which will be mentioned in detail in Chapter 4.

The term αD in *Darcy Weisbach* is equivalent to D^{eq}, which is the residual equivalent diameter. It can be defined as a diameter of a uniform pipe that has the same head loss of a real blocked pipe. The methodology aims to find blockages in term of D^{eq}, but it cannot detect any information about length or size of the obstructions. In other words, occlusions are modeled as a uniform reduction of the pipe diameter. Most of the pipes are partially blocked, sometimes pipes are completely blocked. Therefore, the product αD carries the same name of "residual equivalent diameter" [Marzani et al., 2013]. Figure 2.2 represents all the pipe concepts that have been explained above
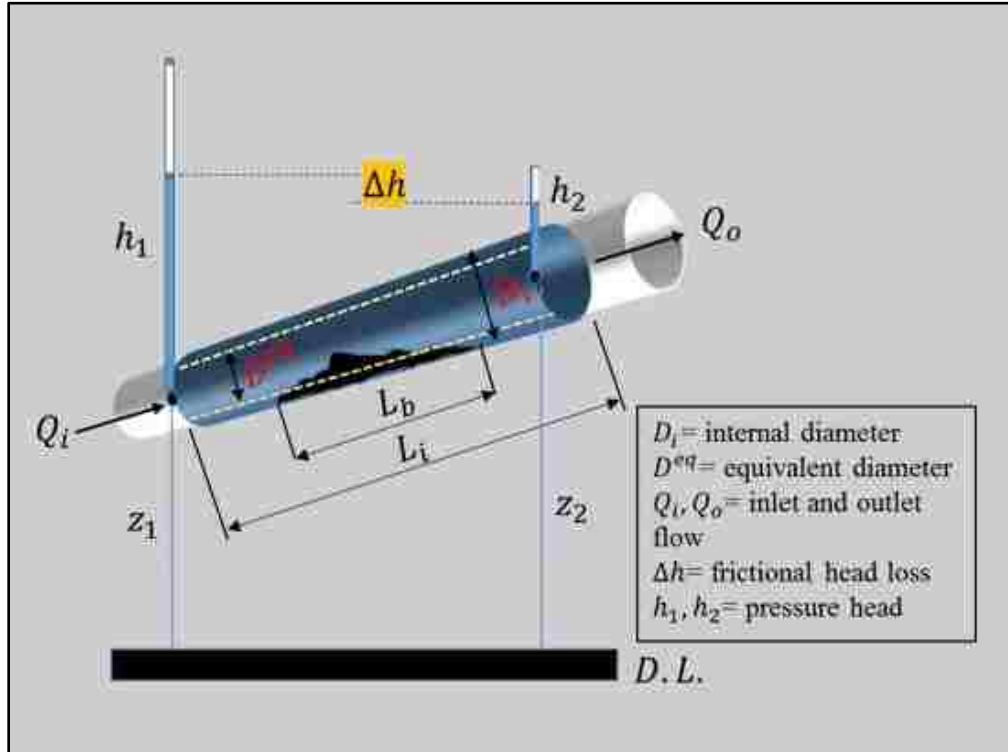
Figure 2.2: Modeling of the blocked pipe via FEM

The equivalent diameter can be calculated numerically for such pipe (partially blocked) by modeling it as two segments in series. The first segment with its length equals the length of the clean portion $(L_i - L_b)$, whereas the second portion has a length that equals the blockage length (L_b). By using the same *Darcy* formula, the equivalent diameter for partially obstructed pipe can be computed as follows [Mazzotti et al., 2008]:

$$D^{eq} = \left[\frac{L_i}{(L_i - L_b)/D_i^5 + L_b/D_b^5} \right]^{1/5}$$

In which:

L_i: Original length of the pipe

L_b: Blockage length

D_i: Original diameter of the pipe

D_b: Blockages residual diameter

For the purpose of the identification procedures, the diameter reduction is actually handled by a non- dimensional factor [Marzani et al., 2013]:

$$\alpha = \frac{D^{eq}}{D}$$

The main goal of the proposed technique is to identify the exact location of blockages in pipeline networks. The outcome of the procedure is α , which can provide useful indication about the blockage severity inside the system. The suggested methodology can successfully detect the pipe that is blocked without any side effects on the networks operability. The fluid properties and the selected mathematical model have a direct impact on the simulated measurements. Hence, it is crucial to introduce a model that provides insight about the predicted response. Therefore, *Darcy* equation can be used to introduce a system of non-linear algebraic equations, [Mohtar et al., 1991], such as

$$K(\alpha)h(\alpha) - z = R(\alpha)$$

Where:

K: is the global "stiffness matrix"

h: is the pressure heads

z: is the sum of the global vector connected with nodal elevation and external nodal demand

R: is the global vector of residuals

The formula above is equivalent to what has been seen in nonlinear mechanical problems. Thus, it can be solved by using the same approach that have been used in mechanical analysis. The next section will address this in detail.

2.3.2   Suggested Methods of Solving Nonlinear FEM

In many engineering applications it is preferable to analyze a set of linear algebraic equations by FEM. The stiffness of a linear structural system is easy to handle and compute. Indeed, the solution of linear problems can be simply solved in the following form:

$$Ka = f$$

However, non-linear problems always lead to a complicated set of algebraic equations, which are difficult to handle without iterative solutions. The common formula of non-linear FEM used to solve mechanical problems is presented by Zienkiewicz and Taylor, [2000].

$$\Psi(a) = f - P(a) = 0$$

Where (a) is the set of discretization parameters, and is also equivalent to α in the proposed method, while f is equivalent to z.

Since the solution procedure of FEM in fluid mechanics is similar to that applied in structural engineering, it is possible to use all the techniques that are well-known in the structural engineering field (e.g. the Newton Raphson for non-linear equations [Reddy, 2004] and the methodologies applied in structural damage detection [Bocchini et al., 2013]) with fluid dynamic problems. There are many other approaches that can serve the same purpose (i.e., Modified Newton Raphson and Incremental-secant or quasi-Newton methods) [Zienkiewicz and Taylor, 2000]. Also, it is possible to solve non-linear FEM by using Picard iterations [Muccino and Luo, 2004]. This study implements the Newton-Raphson method to solve the algebraic set of the non-linear finite element equations because of it is one of the most commonly combined with FEM.

The Newton-Raphson method requires iterations. It is important to define the essential parameters for such methods (i.e., tolerance and maximum number of Newton-

Raphson iterations). Furthermore, since the system is not linear, the tangent and secant stiffness matrices are required, which are dependent on nodal elevations (z) and pressure heads (h).

In most cases of structural analysis, FEM is applied in finding the displacements at any node. The widespread equation has been established in the structural engineering community for the solution of a non-linear problem as follows:

$$R(u) = F - K(u)u = 0$$

Which is equivalent to the formula that is used in the proposed technique, but the flow and pressure head are used as main parameters. For such equation, the "residual matrix" R is an implicit nonlinear function of the unknown solution of the next iterative step ($i.e.,$ $i\ is\ known, but\ i + 1\ is\ unknown$) making iteration necessary, which is a typical requirement of implicit methods. When the solution of the previous step is known, a Taylor series can be used to find the solution of the next iteration:

$$R(u) = R\big(u^{(i-1)}\big) + \left(\frac{\partial R}{\partial u}\right)^{(i-1)} \delta u + \cdots = 0$$

By eliminating all the high order terms and substituting $K_T^{(i-1)}$ instead of $\left(\frac{\partial R}{\partial u}\right)^{(i-1)}$, the equation becomes:

$$K_T^{(i-1)} \delta u = -R(u^{(i-1)}) \qquad (1)$$

Therefore, the residual vector (R) of the starting point for the iteration can be computed as follows:

$$-R\big(u^{(i-1)}\big) = F - K(u^{(i-1)})u^{(i-1)} \quad (2)$$

By solving Equations (1) and (2) simultaneously, the increment in displacement can be determined as:

$$\delta u = (K_T^{(i-1)})^{-1}[F - K(u^{(i-1)})u^{(i-1)}]$$

Now, it is possible to solve for the next step:

$$u^{(i)} = u^{(i-1)} + \delta u$$

The program will compare the error of new value of $u^{(i)}$ with the required tolerance according to the convergence criteria. The iteration will continue until the solution satisfies the convergence conditions.

2.4 Optimization Procedure by using Genetic Algorithms (GAs)

The subject of optimization is important in many applications. Several fields of mathematics and engineering have used the theory of optimization. In fact, engineers pursue the optimal solution that attains good performance and requires low cost.

Optimization is a task that is applied in different fields of research, and it can be defined as a process that finds the best solution within constraints. Three points are essential to be considered in the application of optimization, 1) an objective function is needed that provides a scalar quantitative performance measure that needs to be minimized or maximized. In the proposed technique, the objective function has been set to minimize the discrepancy between simulated and measured quantities. 2) A predictive model is needed to comprehend the system behavior. 3) Variables that develop in the predictive model must be tuned to satisfy the convergence criteria ["Introduction to Process Optimization", n.d.]. GAs are one of the preferable evolutionary tools that used to perform the optimizations. GAs have been used in many research studies to optimize a wide variety of complex system. Thus, GAs are selected as an engine in this technique to perform the optimization and are suitable to obtain sufficient accuracy.

2.4.1   Concepts of GAs

GAs are heuristic techniques that perform a search based on evolutionary sets of trial solutions (generations) [Marzani et al., 2013]. Nowadays, GAs are the most broadly applicable approach used among the evolutionary computation methods. The best GAs are developed by Holland, [1975]. It is imperative to have deep insight about the principles of GAs, which are summarized by Michalewicz, [1996] as follows:

1. A generic representation of solutions to the problem

2. Generate an initial population of solutions

3. An assessment function valuing solutions in terms of fitness

4. Genetic operators that change the genetic arrangement of children during reproduction

5. Values for the parameters of GAs

As a result, GAs are the best way to accomplish the optimization problem in the suggested methodology of blockage identification. GAs provide the solution to problems (simple or complex) reliably and accurately. The optimization procedure is used to determine the residual factor (α) that provides a quantitative assessment of blockage in each pipe.

MATLAB is used to perform the GAs analysis, which is based on *Darwin's* theory of survival. GAs comprise several parameters that should be defined in regards to the type of problem and the convergence criteria. GAs begin with a set of solutions represented by chromosomes, called population [Rahul et al., 2011]. Then the new population will be generated by recombining trial the old population. The new population can be created as a result of valuing each member of the current population by its fitness. Ranking individual

scores helps select parents based on the fitness with the elite individuals (the individuals in the current population that have lower fitness) passing to the next population. Children are produced from the parents either by mutation or crossover to generate the next population. This process will repeat until the condition of convergence criteria is achieved. Generally, as the number of generations increases, the individuals in the population get closer together and approach the minimum point. For the convergence condition to be satisfied, it is necessary to take into consideration the most basic parameters that affect the accuracy and efficiency of the optimization procedure. The fundamental parameters of GAs that need to be defined are: the number of generation, population size, crossover rate, type of crossover and mutation rate. All the stated above steps are outlined in the flowchart shown in Figure 2.3.
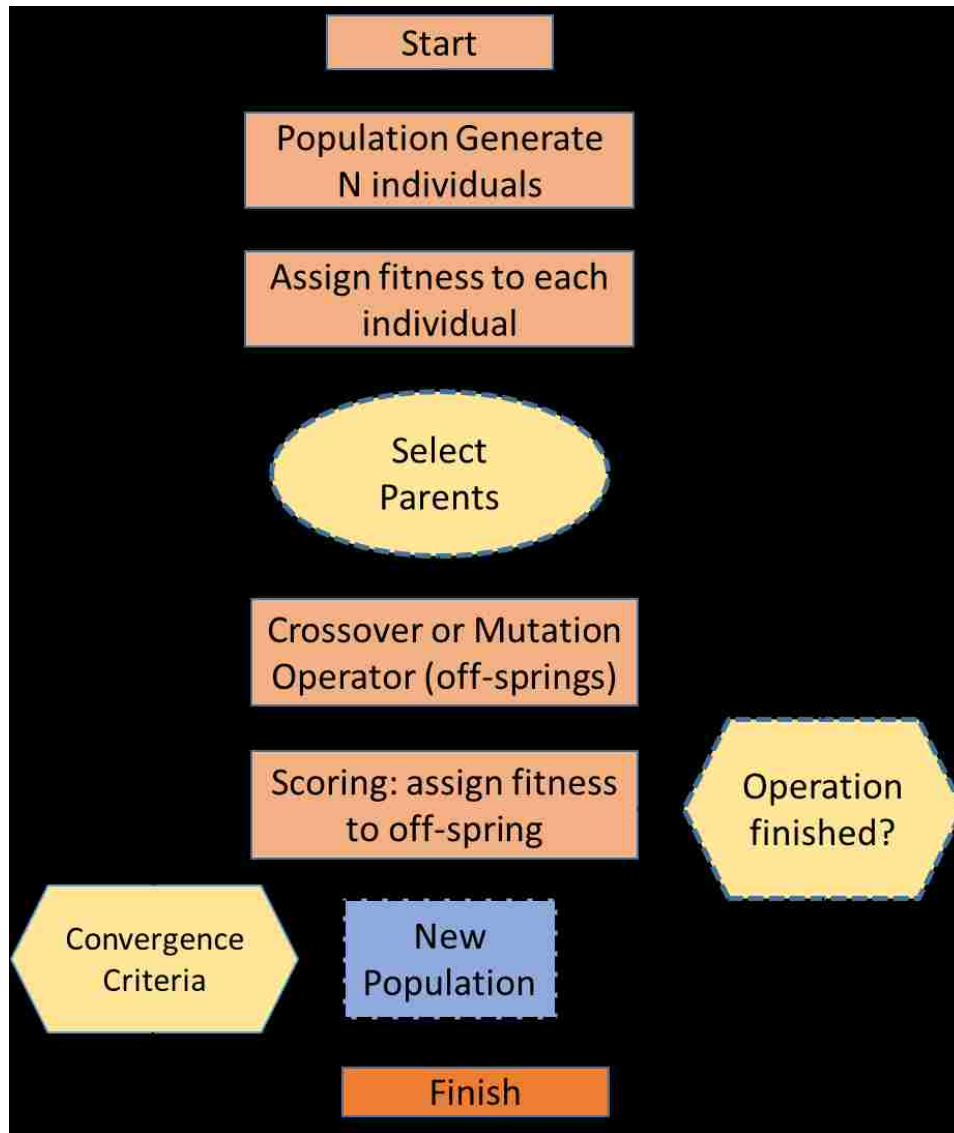
Figure 2.3: Flow-chart representation of genetic algorithms (GAs)

To recapitulate what has been explained above about FEM and GAs, it can be simply said that GAs perform most of identification procedure while FEM simulate the flow quantities as described in Figure 2.4.
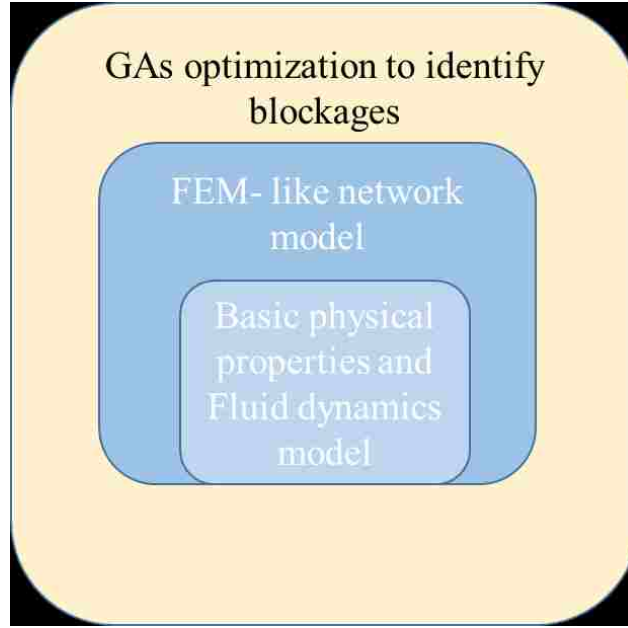
Figure 2.4: Proposed approach model

2.4.2   Blockages Identification Procedure

The final step of blockage detection in pipeline networks can be executed by minimizing the discrepancy between experimentally measured (Q^{exp} and h^{exp}) and numerically computed (Q^c and h^c) pipe flows and nodal pressure heads. The Q^{exp} and h^{exp} values can be obtained empirically by using the flowmeter and pressure gauge respectively, as will be discussed in next Chapter. However, in the absence of real data or for validation purposes, the pseudo-experimental data can be computed numerically by adding noise to the measurements that were calculated theoretically, such as:

$$Q^{exp} = Q^c\left(1 + nl_Q.\beta_p^Q\right) \forall\, p \quad and \quad h^{exp} = h^c(1 + nl_h.\beta_n^h) \,\forall\, n$$

Where nl_Q and nl_h are the noise levels for the flows and pressures respectively, while β_p^Q and β_n^h are independent random variables with standard normal distribution. The procedure

of the proposed technique can be outlined in the following steps [Marzani et al., 2013 and Bocchini et al., 2014]:

1- "A population of individuals $(\alpha_1, \alpha_2, \alpha_3, \ldots.)$ is initially generated. In the first generation of the GAs procedure each element of one individual of the population is set equal to 1, e.g. $\alpha_{1,s} = 1 \forall s$." The rest of the individuals of the population are arbitrarily generated to achieve the upper and lower boundaries, which are between 0 and 1. Later, in the next generations each value of α_i for individual in entire set will be varied between upper and lower bounds (i.e., α will range between 0 and 1).

2- For each individual, FEM will provide numerical values of flow rates and pressure heads in each pipe and node respectively $(i.e., Q^c \text{ and } h^c)$.

3- Apply an appropriate objective function (fitness value) that represents the discrepancy in measured and simulated data. For instance, Bocchini et al., [2014] used the objective function $J(\alpha)$, which can be computed in this way:

$$J(\alpha) = \log(\Phi_h) + \log(\Phi_Q) - \frac{\gamma}{n} \sum_{p=1}^{n} \alpha_p$$

Where:

n: is number of pipes

γ: is a penalty factor presented to improve the results. Value of γ usually included in the range (10-25)

Φ_h: is a metric of discrepancy between numerically computed pressure heads (h_i^C) and the n_h measured pressure heads (h_i^{exp}). It can be determined as:

$$\Phi_h = \sum_{i=1}^{n_h} \left[\frac{h_i^C - h_i^{exp}}{h_i^{exp}} \right]^2$$

In the same way Φ_Q is a metric of discrepancy between numerically computed flow (Q_i^C) and the n_Q measured flow (Q_i^{exp}). It can be computed as:

$$\Phi_Q = \sum_{i=1}^{n_Q} \left[\frac{Q_i^C - Q_i^{exp}}{Q_i^{exp}} \right]^2$$

Most importantly, n_h and n_Q are not necessarily equal to the actual number of nodes and pipes of the network. In other words, missing measurements are allowed in this technique and would still produce efficient results.

4- Rank individuals by scores according to their fitness to organize the population. Next, the convergence criteria should be checked. GAs will stop when they achieve the convergence conditions, and the best individual will be obtained.

5- If the convergence criteria is not satisfied, reproduction operation will be implemented by using the crossover and mutation operators to generate the next generation.

6- Then, a new set of trial solutions α_i are taken, and the algorithm restarts from step 2 continuing the same procedure until the convergence criteria is reached.

Figure 2.5 provides a schematic diagram that represents the identification procedure steps discussed above.
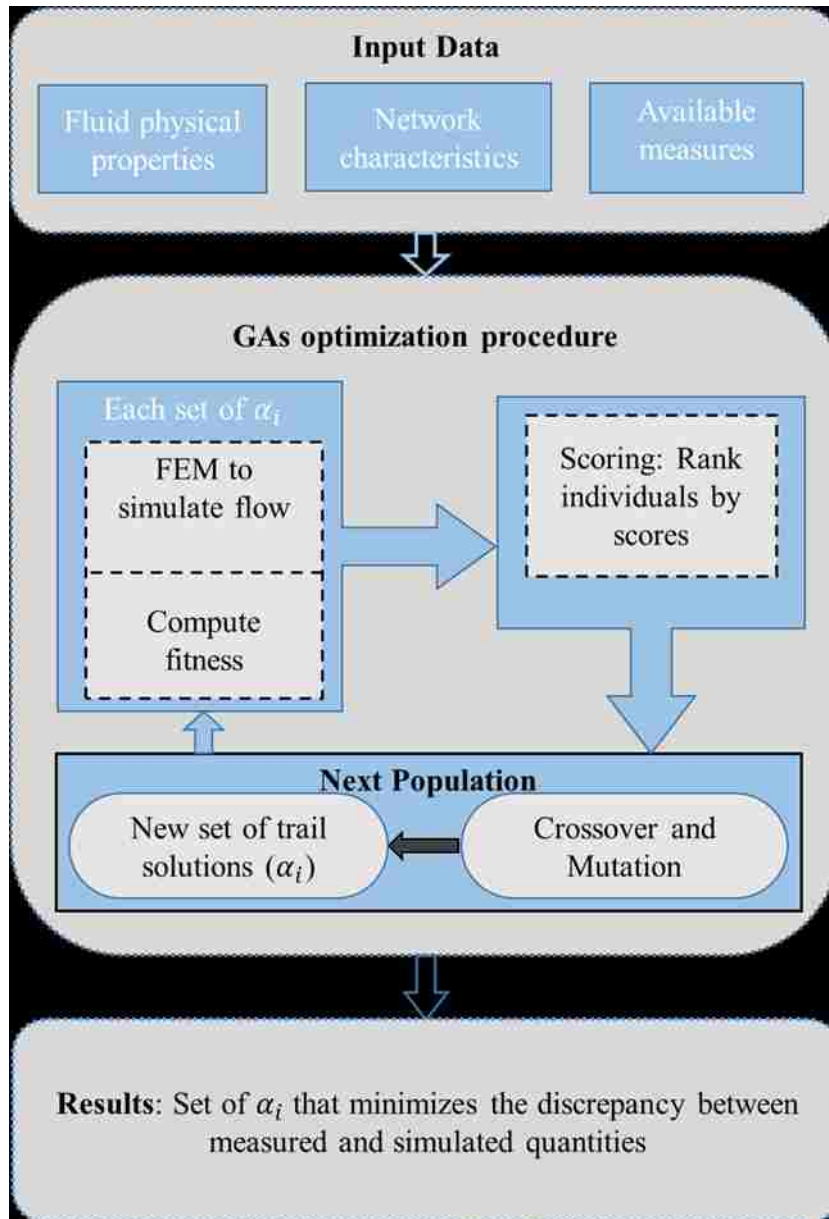
Figure 2.5: Block diagram representation of blockage detection

The MATLAB code includes multiple files, such as an input file and a main file used to run the optimization procedure. The construction of blockage identification exploits the Finite Element-like simulator of flow quantities in the system of pipes and GAs to perform the optimization procedure. An example is presented below to explain the basic features that have been described in Sections 2.3 and 2.4.

33

Example: A branched network is designed with different nodal elevations (z) and all pipes have a diameter equal to 250 mm, except 1 and 2 that have diameter 500 mm. The temperature range is assumed between $22°$ and $28°$, and the roughness of each pipe is $5E10^{-4}$. The network consists of 14 segments of pipe and 14 nodes and is filled with a single phase fluid (i.e., water). A piezometric head of 10 m is imposed at node 1 and all pits have piezometric head of 150 m over node 1. Flow measurements are collected in all pipes, except pipes 5 and 14, whereas the nodal pressure heads are taken in all nodes excluding nodes 6 and 11. Figure 2.6 shows the layout of the examined network. FEM is used to smilate the flow quantites, however the measured quantities are modified with a noise of 5% to simulate the measurement errors. The results of simulation for flow rates and pressure heads are presented in Figure 2.7. Blockage identification is determined as a result of an optimazition procedure, which is solved via GAs as shown in Figure 2.8. For simplicity, the framework of GAs consists of 20 individuls per generation and a maximuam of 200 generations. It is assumed that all pipes are completely clean, so it is expected that the "residul factor", α, is equal to 100% for all pipes.

The results indicate that the methodology is capable to obtain an extraordinary accuracy, nevertheless some measurements were missing.

34
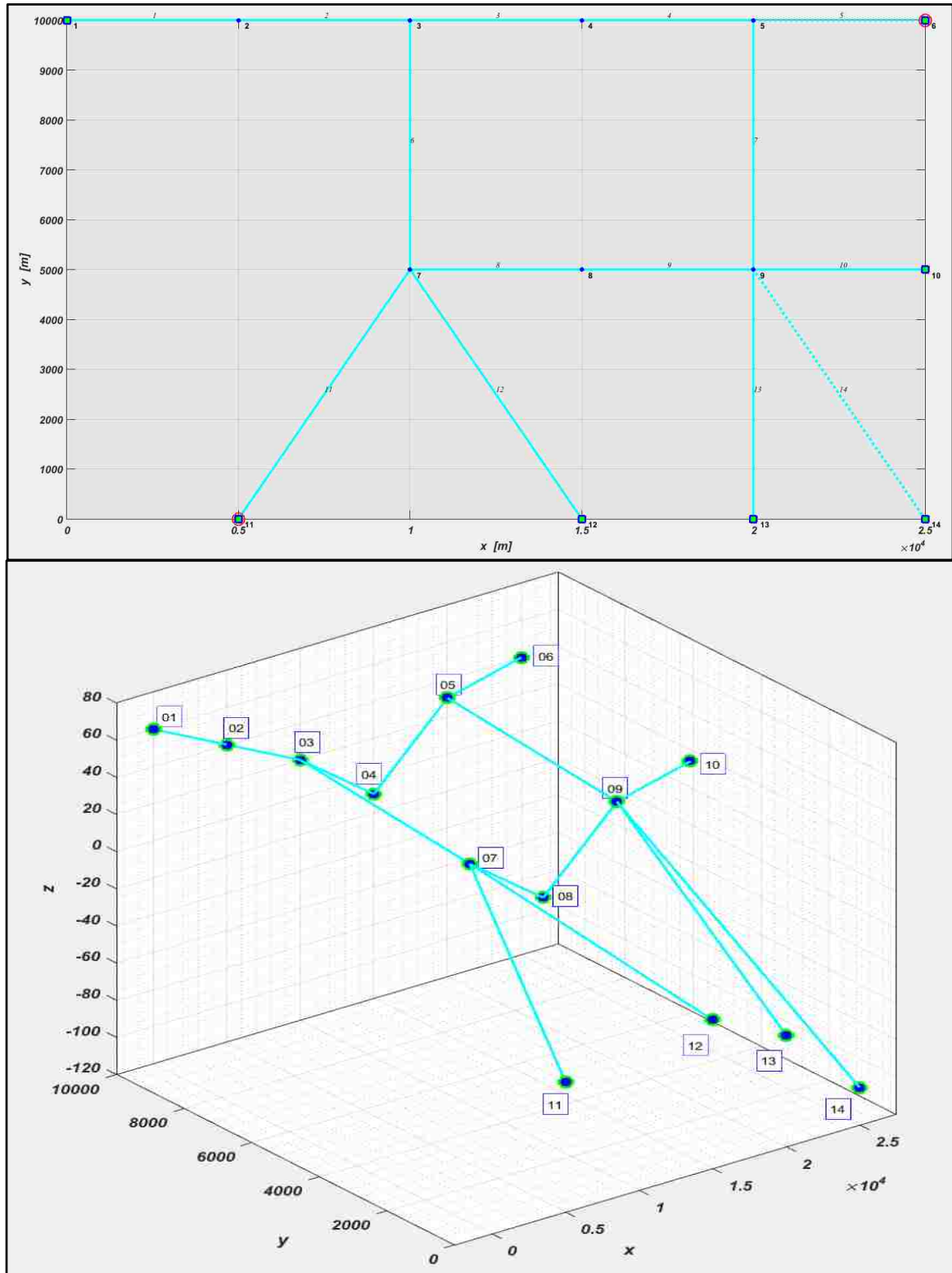
Figure 2.6: Layout of the investigated network

```
FLOW IN PIPES

    pipe              node i      node j       Q (m^3/s)
        1                2            1         0.15975
        2                3            2         0.15977
        3                4            3         0.066093
        4                5            4         0.066089
        5                6            5         0.036548
        6                7            3         0.09364
        7                9            5         0.02955
        8                8            7         0.024347
        9                9            8         0.024345
       10               10            9         0.019114
       11               11            7         0.034656
       12               12            7         0.034656
       13               13            9         0.019112
       14               14            9         0.015679
```

```
ALTITUDE AND PIEZOMETRIC HEAD AT NODES

      nodo           z (m)          h (m)         HGL(m)
         1             60             10             70
         2             40          39.128         79.128
         3             20          68.259         88.259
         4            -10          154.53         144.53
         5             30          170.8           200.8
         6             40          180             220
         7             10          185.31         195.31
         8            -20          224.62         204.62
         9             20          193.93         213.93
        10             30          190             220
        11            -50          270             220
        12            -40          260             220
        13            -60          280             220
        14           -100          320             220
```

Figure 2.7: Results of the flow rate and pressure heads
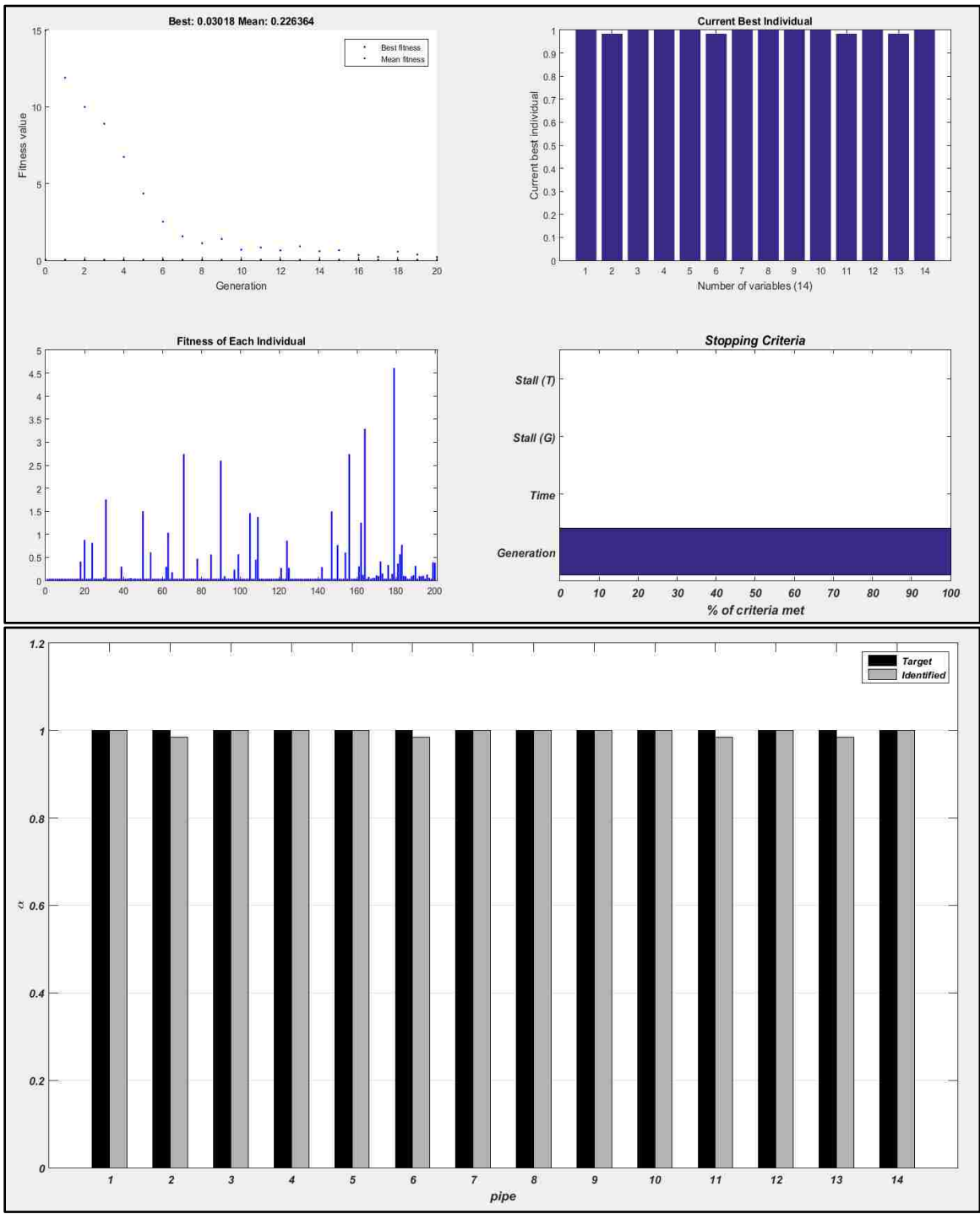
Figure 2.8: Blockage Identification as a result of optimization procedure via GAs

Chapter 3

EXPERIMENTAL WORK

Abstract

This chapter discusses the most relevant experimental work that consists in a series of experiments. The chapter intends to validate the proposed technique empirically. For the first time, a detailed study investigated the capability of such technique by using real field data. MATLAB code is modified according to the experimental work. Different designs of pipeline networks (branched and looped), utilizing water as a fluid, were taken into consideration. The experimental data (flow in pipes and nodal pressure heads) were analyzed and used to validate the proposed technique by minimizing the discrepancy between the empirical data and those measurements that were simulated numerically. Based on empirical data, it is evident that the technique could successfully identify the location of blockage inside the pipes. Finally, results, error analysis and conclusions are presented thereafter.

3.1 Introduction

The proposed methodology has been proven numerically by Marzani et al., [2013] and Bocchini et al., [2014]. However, there has not been any published research to validate this technique experimentally. For the first time, a comprehensive experimental study has examined the ability of such technique to identify the presence of blockages within different pipeline networks. In other words, several experimental setups were conducted to analyze the accuracy and sensitivity of the suggested technique. The experimental setups resemble a simplified scaled-down pipeline network as seen in oil pipelines. The work was accomplished by designing and performing a sequence of experiments using PVC pipes to build such network. A team of eight students, involving myself and seven other students from the civil and mechanical engineering departments worked together in the span of 12

weeks to come up with a suitable set of result for real field data flow and pressure measurements. The experiments were performed by utilizing only one type of single-phase fluid, liquid water, at a relatively constant temperature (outside temperature in midsummer of 2016, roughly ranging from 20 to 35 degrees Celsius), in a small-scale setup. The investigation of the technique by experiments was limited due to several conditions (i.e., funding, allowed time, and location regulations). Based on the empirical data, the suggested technique is a valid option for the blockage detection with minimal discrepancy due to several parameters that are discussed in detail in next chapter.

3.2 Experiments Setup

To acquire the required input data (flow in each pipe and nodal pressure heads), a flowmeter and a pressure gauge were used. The flowmeter consists of two transducers, one of them installed in the direction of upstream flow while the other in the downstream flow to capture the reading of discharge inside the pipe. The flowmeter is very sensitive to the distribution of the fluid in the entire pipe diameter. In other words, the flowmeter can capture the flow measurements only when the pipe is completely filled with fluid. Thus, throughout the work, the flow rate measurements were taken at horizontal pipes, which were always full. Due to the inability of the flowmeter to capture discharge accurately in other pipes that are not completely filled with fluid, those measurements have been disregarded. Similarly, pressure measurements were taken at each node by utilizing the pressure gauge. Due to the difficulty of taking pressure measurements exactly at the node, multiple pressure measurements were collected at approximately 3 inch from the intersection of each pipe. In an effort to minimize error, these measurements were averaged. Also, the pressure measure was not taken directly at the node because of the

unpredictable turbulence, pressure loss, and changes in velocity patterns within each joint.

The materials pertinent to these measurements are described briefly in the Figures.

Figure 3.1: Wayne Self-Priming Cast Iron Portable Transfer Water Pump: The pump boosts line pressure up to 50 PSI, has a motor speed of 7500 RPM, and gives a flow rate of 1,450 GPH.

Figure 3.2: Pressure Gauge: the DPG8001 series digital measures pressure with a 0.25% full scale terminal point accuracy.

Figure 3.3: FDT-21 Ultrasonic Flowmeter: The flowmeter measures fluid velocity by the use of transducers that send and receive sound waves and measure transit time. Once velocity is found, the flowmeter calculates flow rate based on the inputted pipe diameter.

3.3 Procedure and Design Criteria

This section explains in detail the design of two types of the networks (i.e., looped and branched) that have been implemented and used often during this work. The first design comprised of two closed loops at different levels. The design included a rectangular loop of pipes at the ground level and a pentagonal loop of pipes at 2.5 ft level from the ground. The rectangular loop had dimensions of 8.5ft × 3.5ft (measured from center to center of the pipes), while the pentagonal loop had dimensions of 4.3ft × 5ft. The two loops were linked together with a horizontal pipe of length 2.5ft and an inclined pipe of length 3ft. To overcome the inability of the flowmeter to collect the flow measurements at the pipes that are not filled with liquid, different nodal elevations were taken into consideration. In other words, it was made sure that the pipes were completely filled with liquid without any gaps. Consequently, the first level was at a lower elevation than that of the second, to ensure all pipes were completely filled with water before the measurements were taken. This was necessary as the flowmeter only gives accurate reading when there are no air pockets in the system. The pipes were connected to each other by using different types of joints. A variety of joints were used in the system, including a double wye, a tee section, and elbows of both 45 and 90 degrees. Each type of joint was associated with a different minor pressure loss, and therefore added complexity to the design (i.e., the sharp change in the network leads losses in pressure heads).

A 50 gal tank was used to feed the system with water. The network was supplied with pressure by utilizing a water pump that boosts line pressure up to 50 psi. The pump took the water from the tank and distributed it inside the system. Based on the experimental procedure and water distribution through the network, the inlet pressure and the flow rate

were 20.85 psi and 0.570 l/s respectively. As mentioned previously, the proposed technique used the fluid in its steady state. To guarantee sufficiently long operation, the water flowed within the system and was returned to the tank via a plastic hose.

Initially, a system without blockages ($\alpha = 100\%$) was analyzed by the use of only 2 inch PVC pipes (schedule 40). The tested network included 6 elbows 90^0, 4 elbows 45^0, 3 tee sections and one wye intersection as shown in Figure 3.4. The measurements were taken, and considered as a benchmark for other designs. Once the data was collected, experiments were conducted in which blockages were present. In reality, the obstruction can be found in any shape, however it is difficult to introduce such blockages empirically inside the pipes, especially when the pipe is partially obstructed. Thus, this study handled blockages as uniform over the entire length of the pipe or part of it. The uniform blockage was simulated by replacing some of the 2 inch pipes with pipes of smaller diameters. For example, replacing 2inch pipes with 1.5 inch or 1inch pipes leads to uniform reductions in diameter by 25% and 50% respectively. The investigated scenario is characterized by inserting the occlusion in pipes 2 and 14 by uniform reduction of 25% from the original diameter as presented in Figure 3.5. As a result, it was expected that the technique should identify α_2 and α_{14} in the range of (75-80)% and α of the remaining pipes should be 100%. Special adapters were used to insert blockages into the system, which helped to make the motion of the flow to a smaller pipe more gradual, natural, and smoother, and to minimize unintended potential pressure loss.
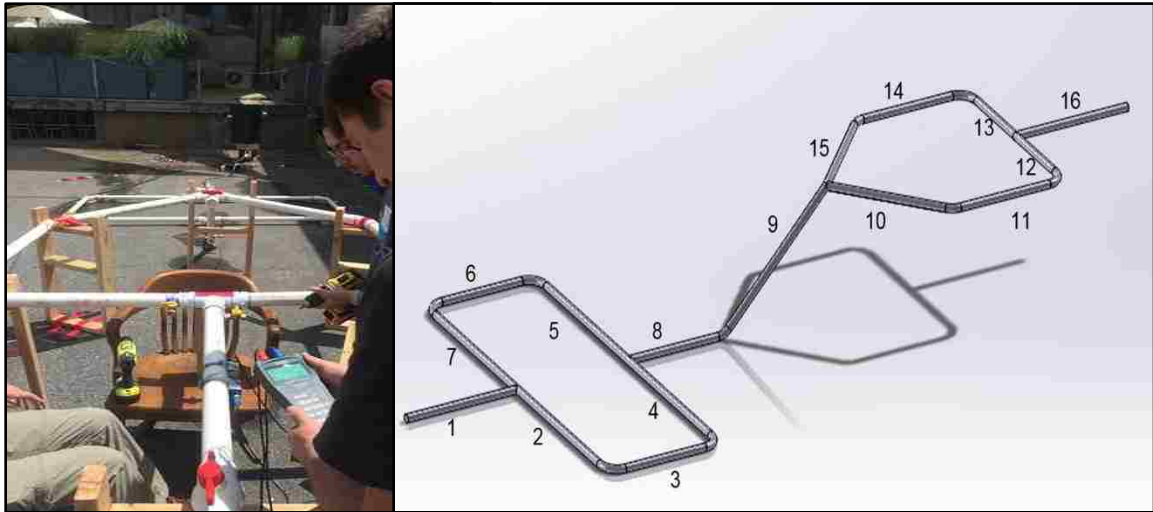
Figure 3.4: Layout of the investigated Network of 2 in. PVC Pipe
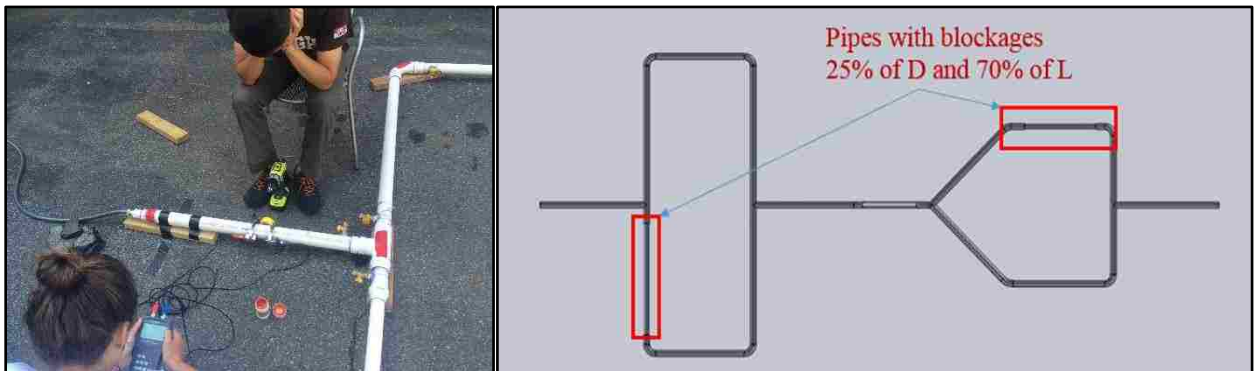
Figure 3.5: Locations of Inserted Blockages (replace the 2in. pipe with 1.5in.)

To preserve simplicity in the network, the second design was modeled as a branched network at ground level with a tiny variation in nodal elevations. The first design (i.e., looped network) included only one inlet and one outlet, however the new design contained one inlet and four outlets to decrease the nodal pressure inside the system and to provide a control on pressure values. Figure 3.6 presents the new system without any blockages (i.e. $\alpha = 100\%$). The new design covered a rectangular area of dimensions 7ft $\times$ 17 ft. Methods similar to those used in the previous design were implemented to insert

blockages and reuse water. Two 1 inch pipes were used as replacements of pipes 3 and 6 to simulate the blockages as shown in Figure 3.7.
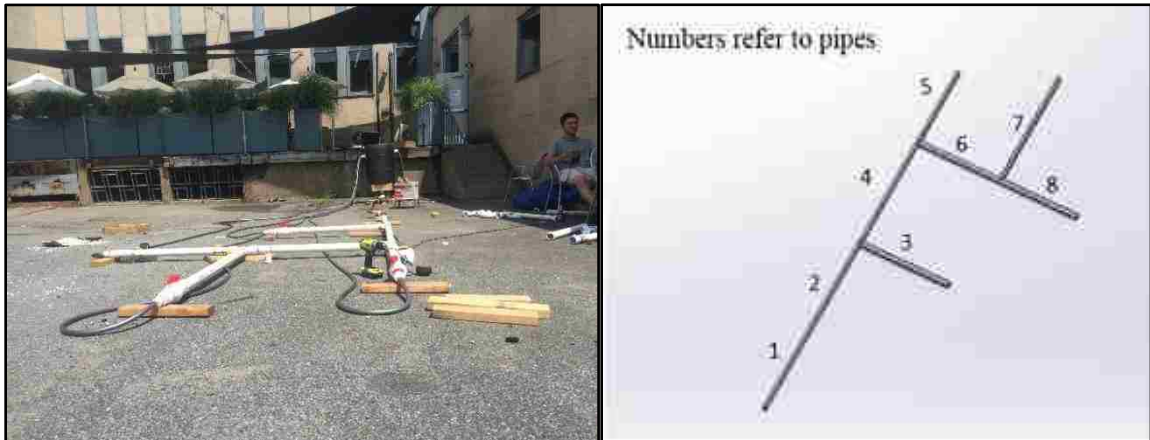
Figure 3.6: Layout of the investigated branched Network of 2 in. PVC Pipe
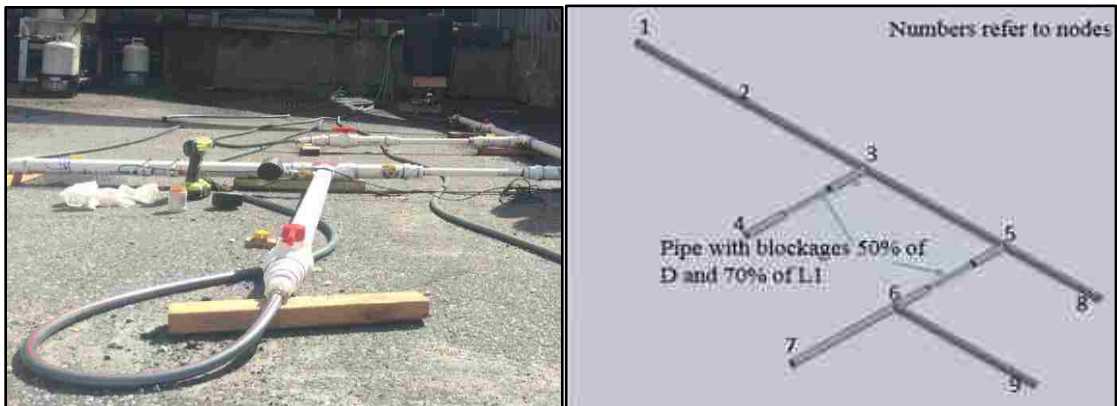
Figure 3.7: Locations of Inserted Blockages (replace the 2in. pipe with 1in.)

3.4 Data Analysis and Results

To obtain a preliminary prediction about the results, MATLAB [R2015a] and ANSYS [2016] simulations have been used to generate the results numerically. The looped system without blockages was analyzed theoretically by using both mass continuity and *Bernoulli* flow equations; the results were compared with those obtained by simulations. Table 3.1 shows the comparison of flow measurements at each pipe of such design. The

flow was modeled in its steady state, thus the flow was assumed constant in the inlet and outlet of the system (continuity law). In other words, at every intersection, the sum of inlet flow rates equaled the sum of outlet flow rates as presented in the one-dimensional continuity equation:

$$Q = V_1 A_1 = V_2 A_2$$

Where:

Q: flow rate

V_1, V_2 : Average flow velocity before and after intersection

A_1, A_2 : Effective cross area in the pipe before and after intersection

The first step of solving the above formula requires the inlet flow or velocity to be defined. In this experimental work the inlet flow value was obtained by recording the time it took to fill up a small bucket with known volume. After pipes flow is known, it is possible to find out the nodal pressure heads from *Bernoulli's* equation, which is:

$$h_1 + \frac{v_1^2}{2g} = h_2 + \frac{v_2^2}{2g} + H_L$$

Where:

h_1, h_2: Pressure heads at node 1 and 2 respectively

v_1, v_2: Average velocity

g: Gravitational acceleration

H_L: Head loss

Also, in the simulation programs (i.e., MATLAB and ANSYS) the measurements of the flow and pressure head as inlet inputs were required. In other words, the initial pressure head and/or flow measurements are required to be defined as boundary conditions.

Therefore, the theoretical values of the inlet and outlet that were calculated from previous step by using the mass continuity and *Bernoulli* equations were used as inputs to obtain the simulated values via MATLAB [2015] and ANSYS FLUENT [2016]. The ANSYS simulation results are shown in Figure 3.8.

Pipe	The Flow m^3/sec				Velocity (m/s)		
	Theoretical flow	MATLAB simulation	ANSYS simulation	Area	Theo.	MATLAB	ANSYS
1	0.00058	0.000585	0.000587	0.00203	0.28631	0.2887745	0.29
2	0.00029	0.000293	0.000302	0.00203	0.14315	0.144634	0.149
3	0.00029	0.000293	0.000302	0.00203	0.14315	0.144634	0.149
4	0.00029	0.000293	0.000302	0.00203	0.14315	0.144634	0.149
5	0.00029	0.000287	0.000302	0.00203	0.14315	0.1416723	0.149
6	0.00029	0.000296	0.000302	0.00203	0.14315	0.1461149	0.149
7	0.00029	0.000295	0.000302	0.00203	0.14315	0.1456213	0.149
8	0.00058	0.000585	0.000587	0.00203	0.28631	0.2887745	0.29
9	0.00058	0.000585	0.000587	0.00203	0.28631	0.2887745	0.29
10	0.00029	0.000293	0.000302	0.00203	0.14315	0.144634	0.149
11	0.00029	0.000293	0.000302	0.00203	0.14315	0.144634	0.149
12	0.00029	0.000293	0.000302	0.00203	0.14315	0.144634	0.149
13	0.00029	0.00029	0.000302	0.00203	0.14315	0.1431532	0.149
14	0.00029	0.000292	0.000302	0.00203	0.14315	0.1441404	0.149
15	0.00029	0.000295	0.000302	0.00203	0.14315	0.1456213	0.149
16	0.00058	0.000585	0.000587	0.00203	0.28631	0.2887745	0.29

Table 3.1: Comparison of Theoretical and Simulated Data Using the MATLAB Code and ANSYS

It can be noticed that the results of pipe flows obtained from the theoretical computations and simulations for 2 inch pipes were consistent.
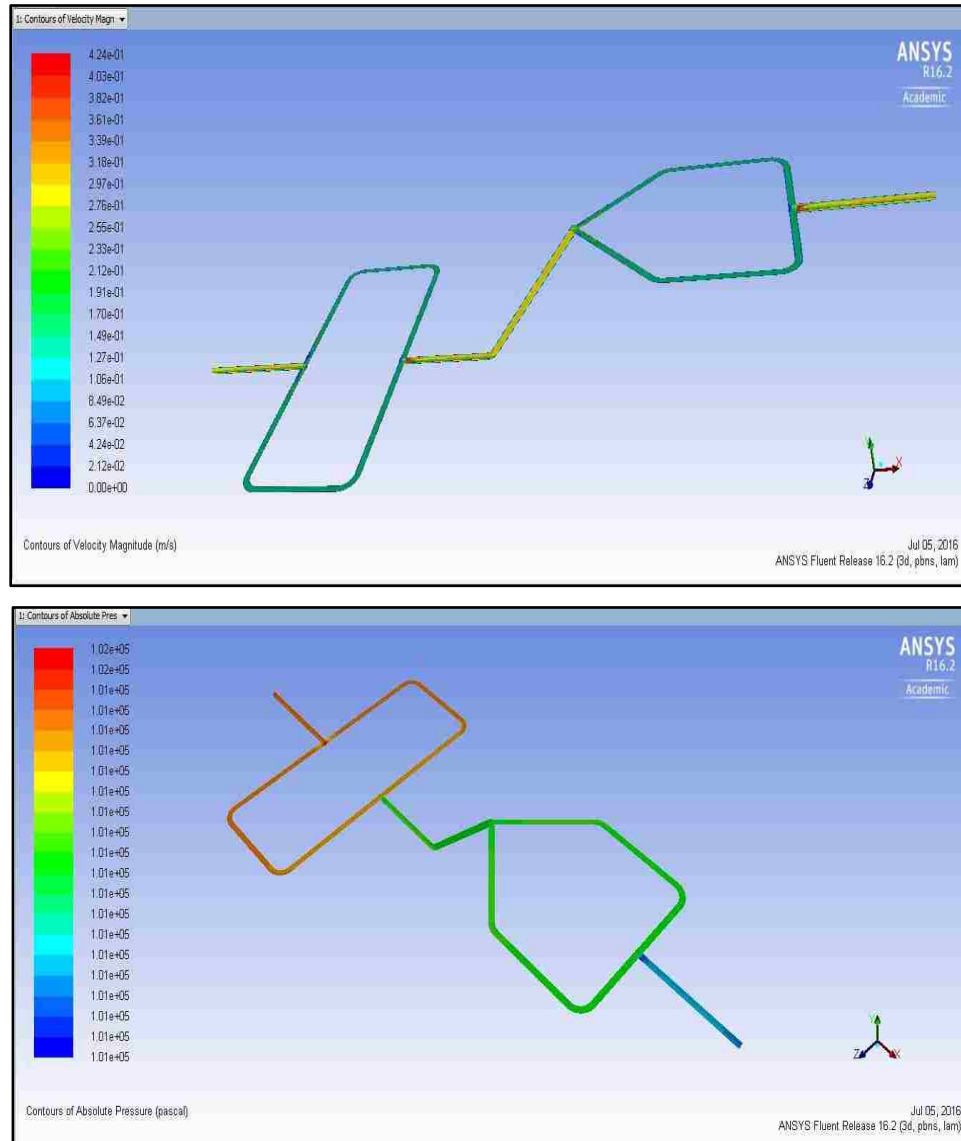
Figure 3.8: ANSYS Simulation of Velocity and Pressure heads for Looped No-Blockage Setup

To monitor the stability and efficiency of the proposed technique in such design, the system was analyzed numerically by superimposing a 5% noise to the flow and pressure head values computed numerically via FEM. For system inspected without any blockage, it was expected for the "residual diameter factor" to equal 1 (indicating a completely clean pipe). In this scenario, flow measurements at all pipes were collected, except for pipe 9, and all nodal pressure head measurements were gathered. The average temperature for all

pipes was 22º C. The PVC pipe roughness was 0.0015 m. Moreover, an equivalent pressure of 14.63m was imposed at node 1, and to keep the flow continuity throughout the network, it was imposed discharge of $587.10^{-6} \, m^3/s$ at the last node. Finally, GAs were setup to perform the optimization using 100 individuals per generation and a maximum of 200 generations.

The proposed technique successfully identified the system as it was anticipated, with a small discrepancy in the results. These approximation were expected due to the nature of the code (it computed several parameters approximately, and it included FEM, which is an approximate model). Also, the 5% imposed noise may be larger than a realistic value for such design. Figure 3.9 presents the simulated looped network of 2 inch PVC pipe as generated by the MATLAB model. The results of the identification via GAs are illustrated in Figure 3.10. The output of the proposed methodology, which is the "residual diameter factor", α is described in Table 3.2 with the most relevant error percentage.
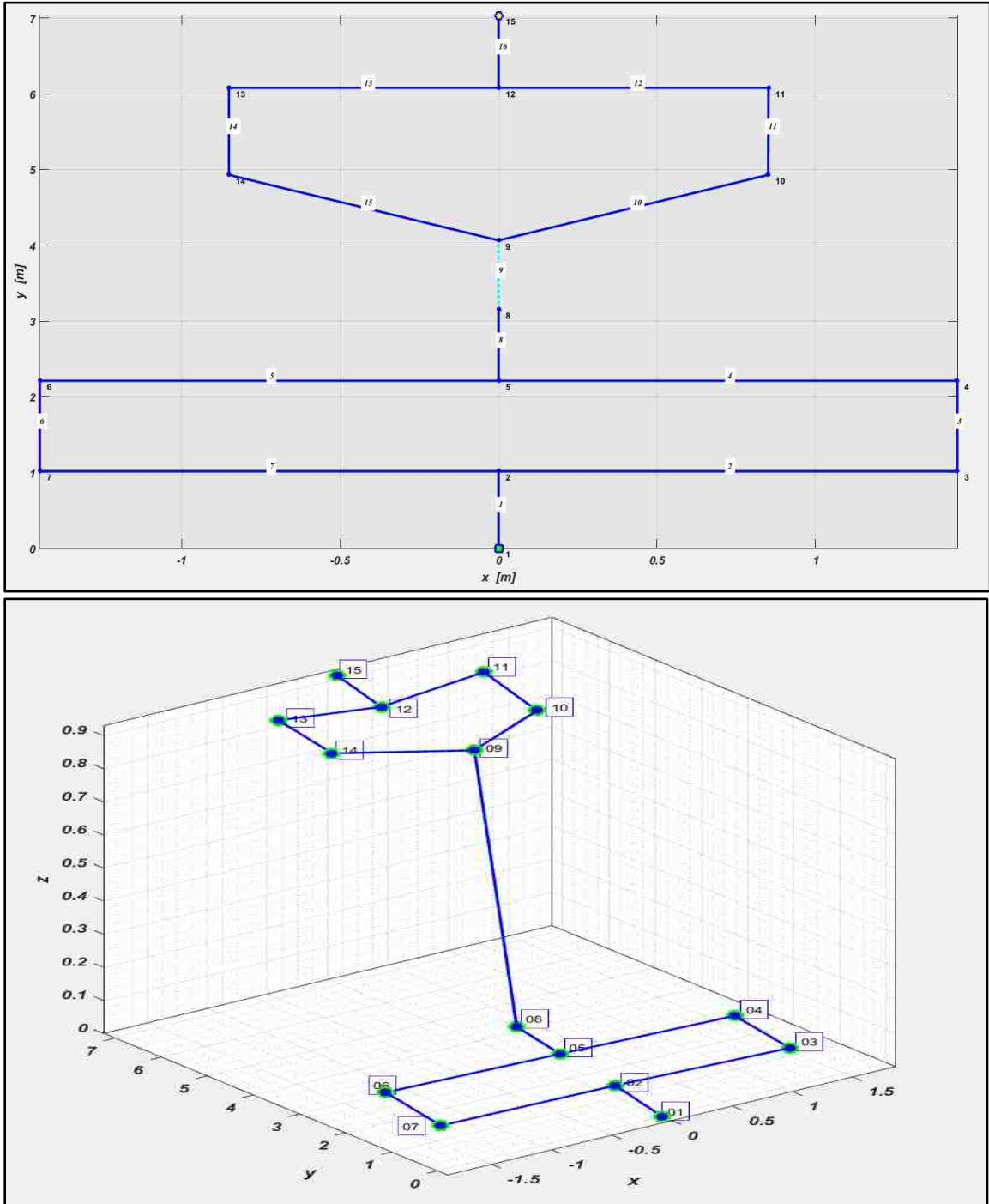
Figure 3.9: Layout of the simulated network by MATLAB program

51
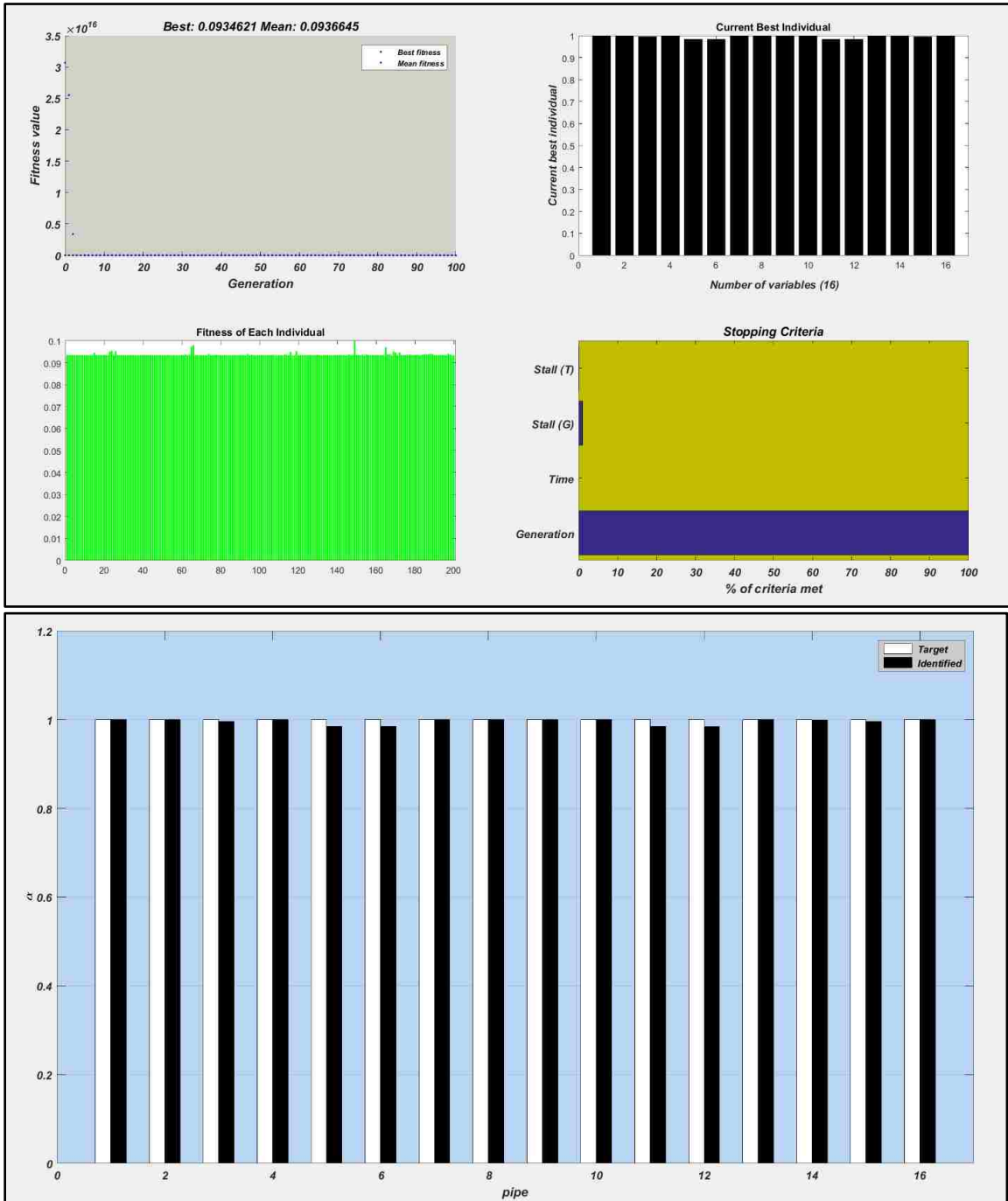
Figure 3.10: Identification procedure of non-blocked system solved by GAs

Results of the identification			
Pipe	alpha real	alpha identified	error %
1	1	1	0
2	1	1	0
3	1	0.9962	0.38
4	1	1	0
5	1	0.9845	1.55
6	1	0.9845	1.55
7	1	1	0
8	1	1	0
9	1	1	0
10	1	1	0
11	1	0.9845	1.55
12	1	0.9844	1.56
13	1	1	0
14	1	0.9988	0.12
15	1	0.9961	0.39
16	1	1	0

Table 3.2: System Results Identification

After acquiring a better insight of such model from the numerical results, the measurements of the flow and the pressure heads were taken experimentally by using the flowmeter and the pressure gauge. Analytical values of pressure head and flow rate, obtained through FEM, were compared to the empirical measurements as shown in Table 3.3.

Pipe	MATLAB simulation	Experimental Meas.	error %
1	0.000585	0.00057	2.564
2	0.000293	0.000294	-0.341
3	0.000293	0.00029	1.024
4	0.000293	0.000299	-2.048
5	0.000287	0.000299	-4.181
6	0.000296	0.000296	0
7	0.000295	0.000301	-2.034
8	0.000585	0.000582	0.513
9	0.000585	missing	missing
10	0.000293	0.000285	2.73
11	0.000293	0.000285	2.73
12	0.000293	0.000288	1.706
13	0.00029	0.00032	-10.345
14	0.000292	0.000312	-6.849
15	0.000295	0.00032	-8.475
16	0.000585	0.000571	2.393

Nodes	MATLAB simulation	Experimental Meas.	error%
1	14.627	14.627	0
2	14.586	14.656	0.478
3	14.598	14.708	0.748
4	14.568	14.73	1.1
5	14.554	14.611	0.39
6	14.545	14.676	0.893
7	14.578	14.83	1.699
8	14.521	14.681	1.09
9	13.733	14.039	2.18
10	13.735	13.975	1.717
11	13.684	13.851	1.206
12	13.713	13.848	0.975
13	13.68	13.744	0.466
14	13.715	13.974	1.853
15	13.668	13.838	1.229

Table 3.3: Comparison of Empirical and MATLAB Simulated Measurements of flow and pressure heads

The comparison of the theoretical analysis of pipe flows and nodal pressure heads with the experimental measurements shows a good match (almost consistent) in the results. The small error percentage shown in Table 3.3 can be attributed to the efficiency of the instruments and their sensitivity to the environmental changes. Indeed, in any experimental work, it is expected to have such small discrepancy between the theoretical and experimental measurements. The computed measures were derived via FEM and then a noise of 5% was imposed on these measurements to simulate the empirical values. It is important and practical to investigate several types of networks by considering different values of noise to come up with a general conclusion about noise effects, which will be explained in Chapter 5.

The code was adjusted to implement two cases of analysis. The first case was discussed in the previous example, where the measurements were simulated experimentally by adding a 5% noise to the numerical measurements computed via FEM. In the second case, the real data (i.e., experimental measurements) of flow and pressure heads were used directly. Thus, there was no need to impose any artificial noise. The same example above has been used to implement the second case. The same identification procedure used in the first case was repeated again. The results of blockage identification are presented in Figure 3.11, and the values of "residual diameter factor" for each pipe are described in Table 3.4.
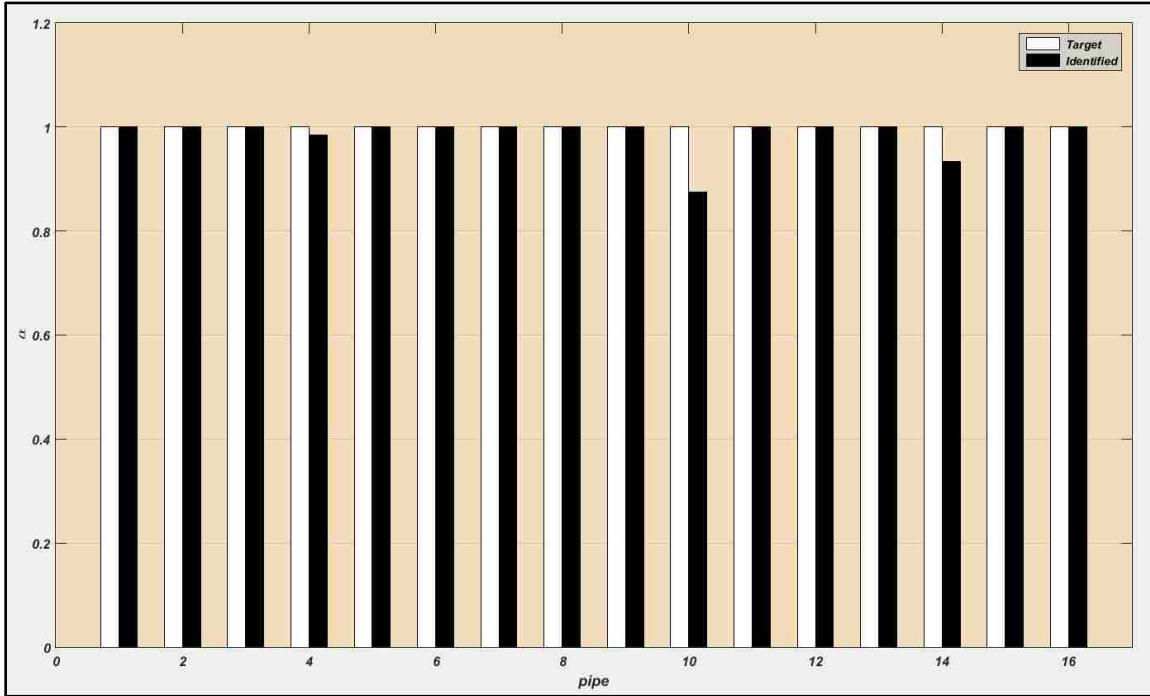
Figure 3.11: Results of the blockage identification procedure

Results of the identification			
Pipe	alpha real	alpha identified	error %
1	1	1	0
2	1	1	0
3	1	1	0
4	1	0.984	1.6
5	1	1	0
6	1	1	0
7	1	1	0
8	1	1	0
9	1	1	0
10	1	0.875	12.5
11	1	1	0
12	1	1	0
13	1	1	0
14	1	0.934	6.6
15	1	1	0
16	1	1	0

Table 3.4: System Results Identification

Four trials of measurements have been taken for each setup to check the accuracy of the instruments. The measurements of pipe flows and nodal pressure heads varied from trail to trail. Therefore, some discrepancy in the results was expected. Table 3.4 illustrates that the value of alpha fluctuated between 88-100%. The results show that pipe 10 and pipe 14 have the lowest values of alpha, being 0.875 and 0.934 respectively. This can be attributed to the wye and 90º angle intersections that change the fluid motion sharply, which in turn affects the reading of the subsequent pipes.

The same network is used by reducing the diameter of pipes 2 and 14 in a certain length to 1.5 inch, as shown formerly in Figure 3.5. These pipes are modeled with uniform blockage, which is a 25% reduction of the original diameter for 70% of the pipe length. Since the design was looped with several junctions, it was anticipated the flow rate would be higher in the pipes without blockages than in those with blockages. The nodal pressure head, on the other hand, was expected to be highest at the node closest to the blockage and drop significantly after the blockage. Due to the inability of collecting nodal pressure head exactly at the node, the measurements were taken directly by the end of the pipe (i.e., approximately 2-3 inch from the node), and that might have affected the accuracy of the results. Table 3.5 presents the measured quantities of pipe flows and pressure heads in a partially blocked pipeline system.

System with blockages		System with blockages	
Pipe	Flow (m^3/sec)	Node	Pressure head, h (m)
		1	14.627
1	0.000564	2	14.578
2	0.000226	3	14.987
3	0.0002655	4	14.787
4	0.0002685	5	14.702
5	0.0003305	6	14.537
6	0.0003335	7	14.728
7	0.00033	8	14.412
8	0.000548	9	14.038
9	-	10	14.0134
10	0.00031	11	14.216
11	0.000321	12	13.516
12	0.000312	13	13.785
13	0.000307	14	14.013
14	0.000256	15	13.269
15	0.000309		
16	0.000598		

Table 3.5: Pipes flow and Pressure heads measurements in obstructed system

The results of blockage identification were not very accurate, as shown in Figure 3.12. In fact, the proposed technique depends on the objective function that minimizes discrepancy in the measurements to detect the pipes that are blocked. However, by comparing the results when the pipes are completely clean (Table 3.3) with the results when the blockages exist (Table 3.5), it can be seen that there is not a big difference in the measurements, as presented in Table 3.6. Thus, in such model, it is difficult to identify the exact location of blockage without false positives. The 25% reduction in diameter, on the other hand, was not enough to create a significant change in the measurements. Also, most of the nodes have little pressure difference before and after the blockage and the same applies to discharge measurements, which introduce difficulty for the blockages to be

captured without error. The boundary conditions (the imposed pressure and flow) as well have a significant impact on the efficiency and accuracy. The technique could not specify exactly which pipe had the blockage. Instead, it could define the region that included the pipe(s) that was clogged.
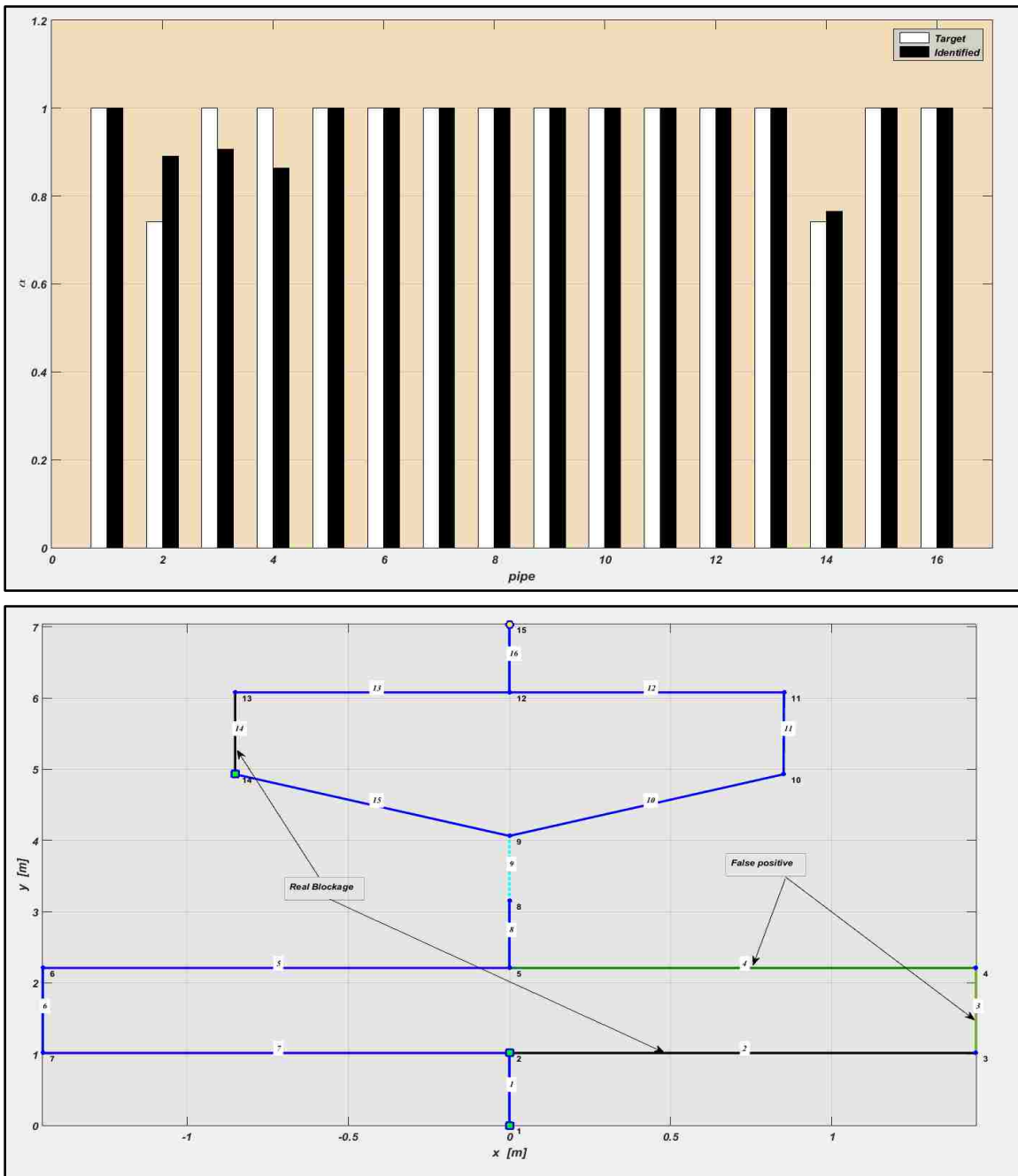
Figure 3.12: Blockage identification results

59

Pipe	Pipes Flow without Blockage and with Blockage		Difference %
1	0.00057	0.000564	1.053
2	0.000294	0.000226	23.13
3	0.00029	0.0002655	8.449
4	0.000299	0.0002685	10.201
5	0.000299	0.0003305	-10.536
6	0.000296	0.0003335	-12.669
7	0.000301	0.00033	-9.635
8	0.000582	0.000548	5.842
9	missing	-	N/A
10	0.000285	0.00031	-8.772
11	0.000285	0.000321	-12.632
12	0.000288	0.000312	-8.334
13	0.00032	0.000307	4.063
14	0.000312	0.0002555	18.109
15	0.00032	0.0003085	3.594
16	0.000571	0.0005975	-4.641

Node	Nodal Pressure head without Blockage and with Blockage		Difference %
1	14.627	14.627	0
2	14.656	14.578	0.533
3	14.708	14.987	-1.897
4	14.73	14.787	-0.387
5	14.611	14.702	-0.623
6	14.676	14.537	0.948
7	14.83	14.728	0.688
8	14.681	14.412	1.833
9	14.039	14.038	0.008
10	13.975	14.0134	-0.275
11	13.851	14.216	-2.636
12	13.848	13.516	2.398
13	13.744	13.785	-0.299
14	13.974	14.013	-0.28
15	13.838	13.269	4.112

Table 3.6: Comparison of flow and pressure heads measurements for a system with and without blockages

The proposed technique identified the blockage in both pipes with an absolute error of 21% and 1.26% respectively. This trial yielded significant errors and false positives in other pipes, specifically pipes 3 and 4. It was expected to get some errors in pipes 3 and 4 since the blockage in pipe 2 affected the flow passing through the subsequent pipes. It should be noticed from Table 3.6, the difference percentage of a system with and without occlusion was not tangible. As a result, the proposed technique could not detect the blockage of such model in a precise way.

To obtain a better explanation about the *nodal pressure head measurements*, a second design was tested, as shown previously in Figure 3.6. Since the new design consisted of four outlets, it was expected to realize a significant drop in the measurements of pressure heads, as explained in Table 3.7. Also, because this was a simple model with few intersections, the empirical measurements were expected to be more precise and to achieve flow continuity inside the pipes. The system was analyzed without blockages. The results show that the technique was able to define the quantities of residual diameters with a remarkable accuracy (almost identical). Table 3.8 presents the values of residual diameter factor for such model, and results of blockage identification are described graphically in Figure 3.13.

Node	Pressure head, h (m)
1	2.636
2	2.602
3	2.555
4	2.577
5	2.463
6	2.464
7	2.489
8	2.454
9	2.437

Table 3.7: Pressure heads measurements of new model
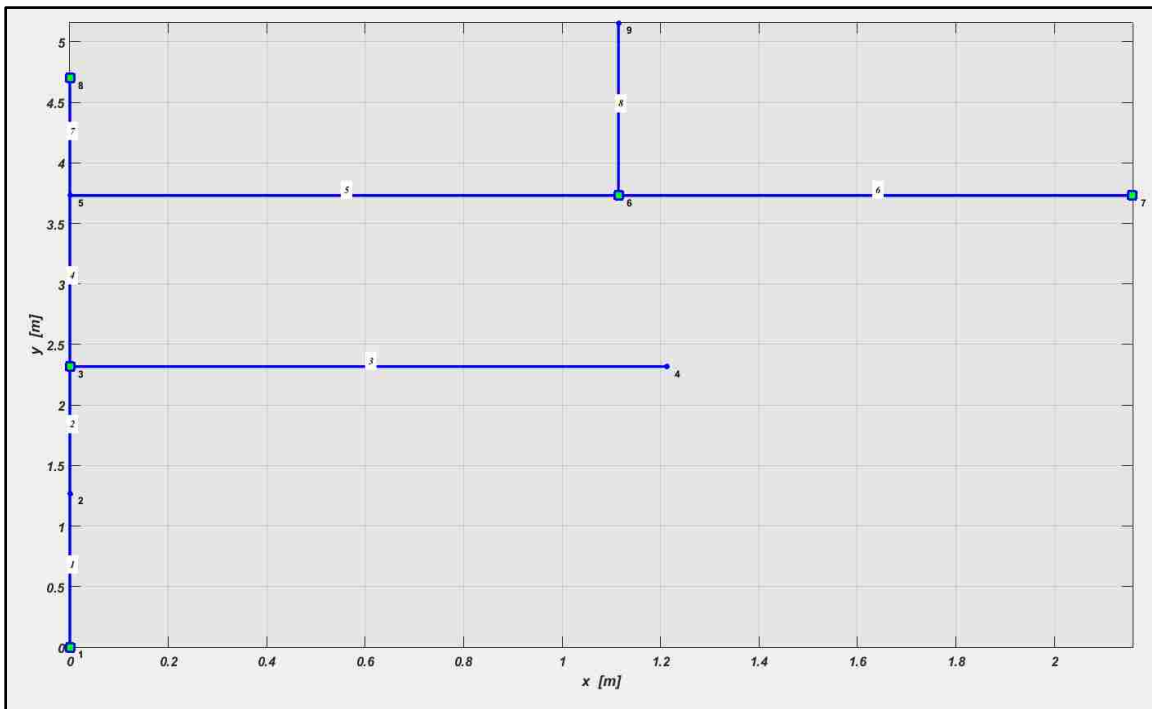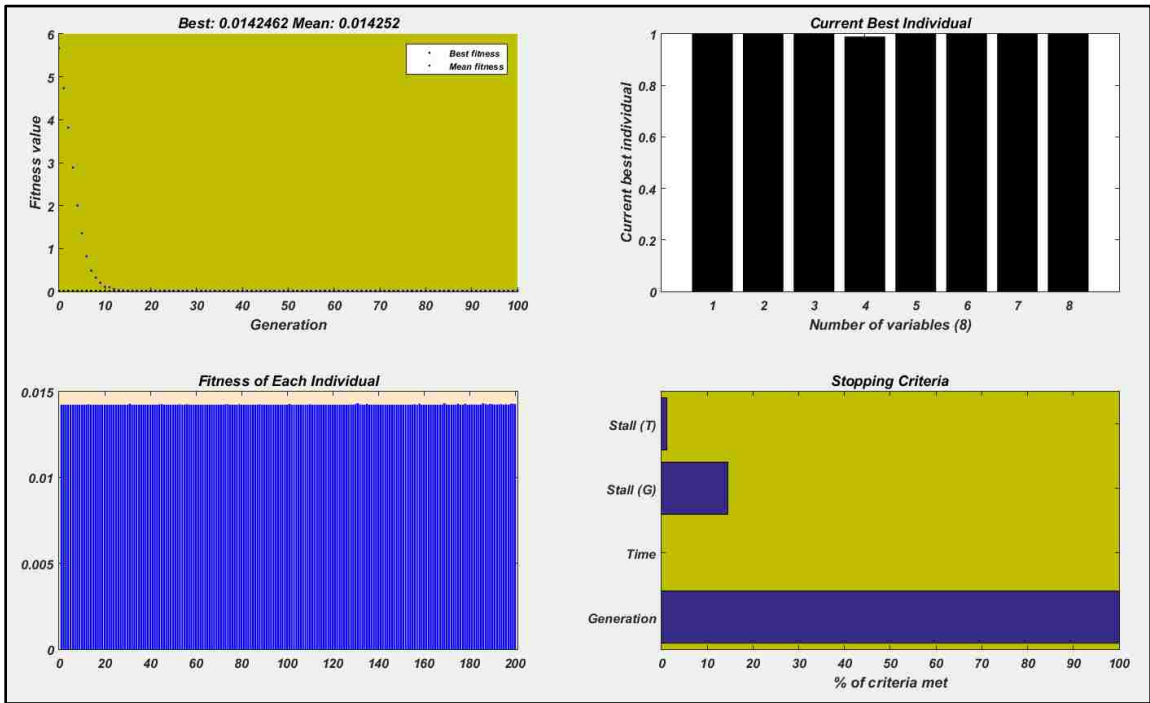
Figure 3.13: Network Layout and Identification procedure for Branched No-Blockage Setup

Results of the identification			
Pipe	alpha real	alpha identified	error %
1	1	1	0
2	1	1	0
3	1	1	0
4	1	0.989	1.1
5	1	1	0
6	1	1	0
7	1	1	0
8	1	1	0

Table 3.8: System Results Identification

The results indicate a very good accuracy in this application. It can be concluded that the proposed technique can work better with branched network rather than looped network.

The analysis has been repeated again with the same network but replacing pipes 3 and 6 with a PVC pipe of diameter 1 inch. These pipes are modeled with uniform blockage, which is 50% reduction of the original diameter over 70% of the length of the pipe. Since the design was branched with a few intersections, it was expected a good result would be attained, in comparison with the result of the first design. The nodal pressure head, on the other hand, was expected to be highest at the node closest to the blockage and drop significantly after the blockage. Also in this case, due to the inability of collecting nodal pressure heads exactly at the nodes, the measurements were taken directly by the end of the pipe (i.e., approximately 2-3 inch from the node), and that might lead to inaccuracy in the results. In addition, in this model, it was assumed that the measurements of pressure heads for nodes 2 and 4 were not available, as shown in Figure 3.14. Table 3.9 presents the measured quantities of the nodal pressure heads in a partially blocked pipeline system. The measured values of pressure head at the outlets were considered as control points (i.e., the required imposed pressure as an input in this methodology) to perform the simulation of blockage identification. The results of the blockage identification are presented in Figure 3.15.
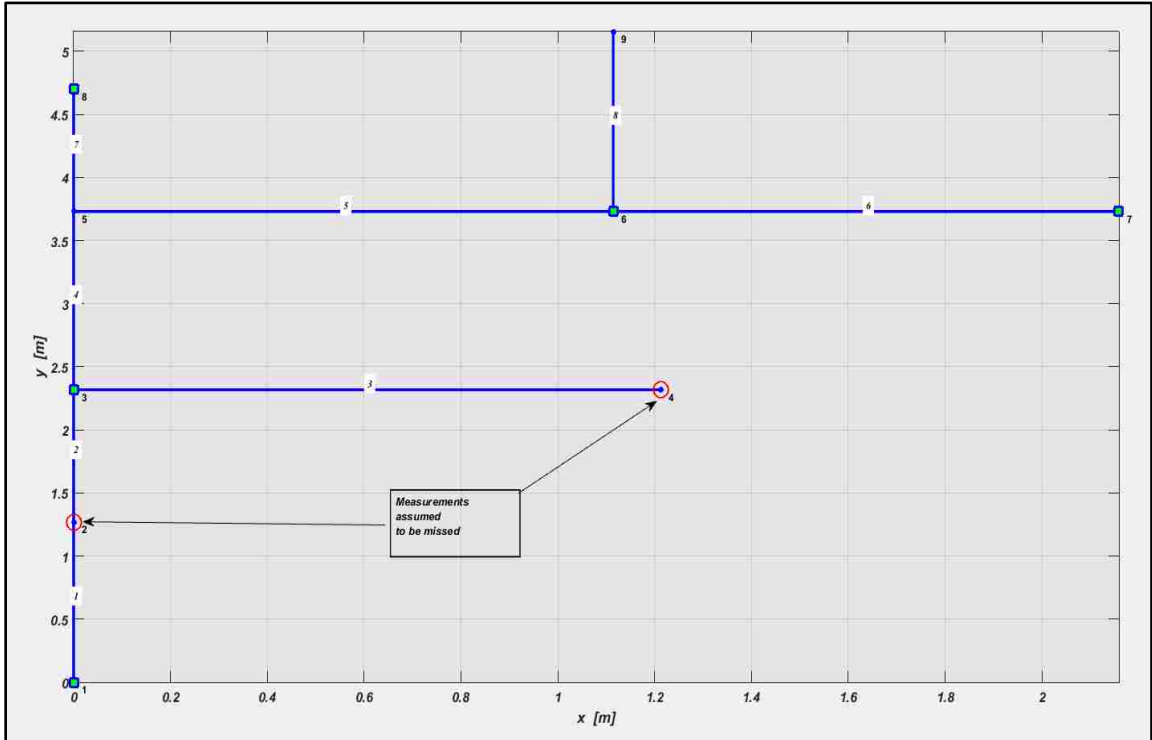
Figure 3.14: Layout of the simulated network by MATLAB program with missing measurements

System with blockages	
Node	**Pressure head, h (m)**
1	2.751
2	2.715
3	2.663
4	2.686
5	2.642
6	2.559
7	2.578
8	2.659
9	2.515

Table 3.9: Pressure heads measurements of blocked network
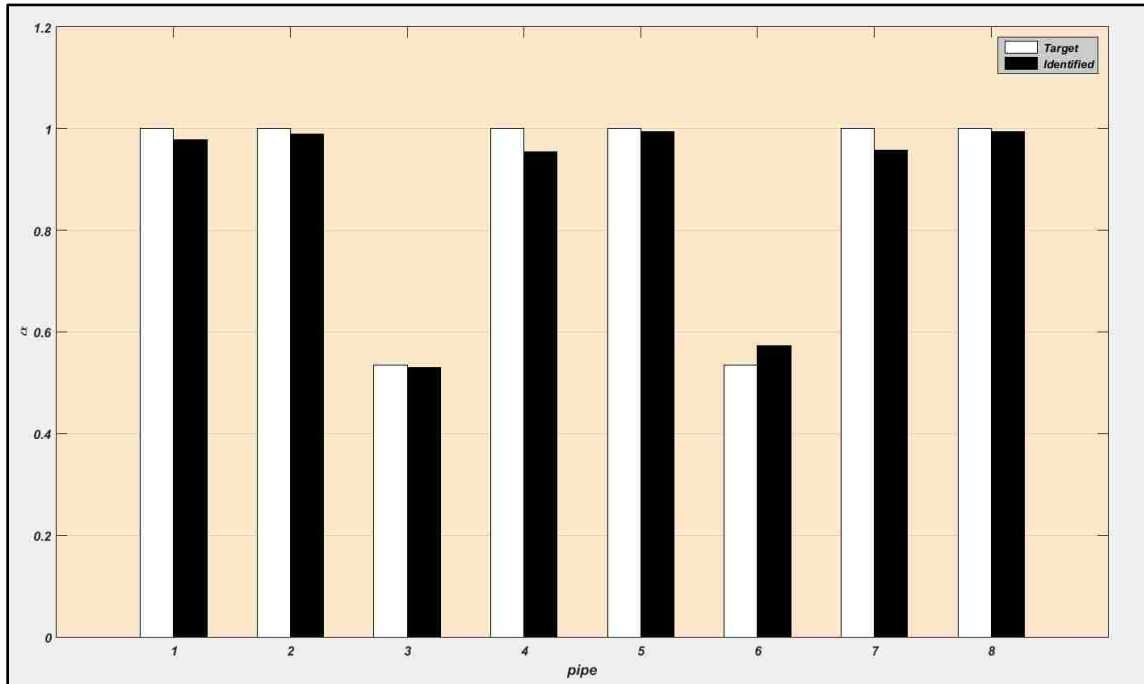
Figure 3.15: Results of blockage identification

The results of the identification procedure show a better accuracy in this design

compared to the first one. Nevertheless, there is still a small discrepancy in the results of

residual diameter for pipes adjacent to the pipe that is blocked. The proposed technique proves a better accuracy in the case of branched network rather than looped network, even though there is still little difference in the measurements when the system was tested with and without blockages. The suggested methodology was able to detect the occlusions with a very small discrepancy in results of residual diameter. This issue can be eliminated by modifying some parameters in the proposed technique, which will be discussed in detail in the next Chapter.

3.5 Discussion and Analysis the Discrepancy in the Experimental Results

As stated earlier, this chapter aims to validate the proposed technique experimentally with a reasonable degree of accuracy in the results. In the set of experiments, it was obvious that the suggested technique was able to capture the pipe that had blockage with a small discrepancy in the results. It has been proven that the technique operated with remarkable accuracy in the case of branched network, better than with looped network. However, the reason behind the discrepancy in the results can be associated also with the setup of the experiment itself. The conditions of the material used and the connections between parts of the structure can have a direct impact to alter the results. Since the interior of the pipes was not perfectly smooth, the roughness was taken into consideration to compute the friction it caused. However, during the setup, some modifications to the pipes made the interior "rougher" and hard to quantify. For example, there were holes drilled into the pipes for the use of the pressure gauge. In addition, inserted adapters used to attach the pressure meter to the pipe created protrusions on the interior, which changed the expected pressure values. The connections between the pipes increased the friction as well. Generally, whenever pipes are joined (i.e., intersection points), there is

a brief change in the inner diameter (there is always a gap inside between a pipe and a connector or an adapter). This causes extra turbulence and more friction. In the end, the real friction in the network was larger than the simulated values that were calculated numerically by *Chen's* formula (explained in detail in Chapter 4). Indeed, *Chen's* formula itself is an approximate method. As a result, the pressure head loss was more than expected.

As it is known in fluid dynamic, whenever there is a change in direction of the pipeline network or/and intersections, it is expected to have minor losses of pressure head, in addition to major losses. Attempts were made to account for this, however the minor loss was too minimal to close the gap between the empirical and numerical pressure heads measurements.

Another reason, which is not taken into consideration was the stability of the fluid's flow. The water flow within the network maintains a quasi-equilibrium state, as opposed to the equilibrium state assumed in the design of the experiments. Due to constraints of the budget, only one pressure gauge and one flow meter were available to conduct the experiments. The pressure at each node and the flow rate at each pipeline section were measured one at a time. However, the pressure and flow rate provided by the pump fluctuated slightly, thus rendering the readings relatively inconsistent. This error brought an uncertainty into the data, which might intensify or alleviate other errors.

For the looped setup specifically, the empirical pressure head values were slightly higher than those generated numerically. In reality, it was rather contradictory to have such a result, while multiple factors led to lower pressure heads (larger pressure head losses) than expected. According to the *Darcy Weisbach* formula, four factors were considered as possible reasons behind this discrepancy: the friction factor f_r, the pipe length L, the

original diameter of pipes D, and the flow rate Q. To have smaller pressure head losses than those simulated by the MATLAB code, there must be a smaller friction factor, a smaller pipe length, a larger original diameter, or a smaller flow rate. The pipe length and the diameter have been discarded from being a possible reason, since they are fundamental parameters that need to be defined as input. Also, pipes flow measurements were consistent throughout the study. Thus, we concluded that the friction factor must have been the parameter to alter the results. A detailed study will be conducted in the next Chapter to provide a better understanding about f_r effects in such technique.

The uncertainty in the results can be explained as follows: when the measurements were taken in the case of the first design (i.e., looped network without blockage), the original pump failed. It was soon replaced by a new pump of the same model. However, the pump's failure during the third trial resulted in the pressure head values being much lower than those from the first two trials. The new pump on the other hand, provided slightly higher pressure, which is depicted in the fourth trial. In fact, the first two trials have an average variance of $0.31m^2$, whereas the first three trials have an average variance of 0.51 m^2, and the four trials combined have an average variance of 0.47 m^2. This shows that the failure of the original pump increased the uncertainty in the measurements through the third trial, and the new pump reduced the uncertainty, nonetheless, it provided a little high pressure.

The proposed technique could successfully identify the blockage in the looped network but with false positives. More likely, the error occurred as a result of the small size of the network. It was mentioned formerly that the proposed technique utilizes an objective function that captures the discrepancy in measurements and simulated data to

69

identify blockages. Hence, the identification procedure depends on both pressure and flow rate to determine the blockages through the used objective function, and 'labels' a pipe as potentially blocked whenever the measurements are inconsistent. Theoretically, in a long straight pipe with a relatively small diameter, the flow rate is constant, while the pressure drops significantly from start to finish. As the pipe length increases, the pressure losses increase as well, and the pressure reading will drop notably in the next point. In the experimental work, short pipes (i.e., max. 3ft in length) were used, which made the blockage identification difficult to be recognized accurately. When the pipes are short, there is minimal drop in pressure; thus the differences between the pressure drops in pipes with and without blockages are almost unnoticeable, as it was seen in the looped network. Such small differences made the technique unable to detect the exact location of blockage, therefore, it just determined every pipe where there was a potential blockage (pipes 2, 3, 4, and 14).

Moreover, it is possible that the uncertainty in the measurements comes from inaccuracy of the instruments, and background noise. The flowmeter has an accuracy of 1% of reading, and the pressure gauge 0.25% full scale terminal point. This small inaccuracy of the equipment should be in the allowable range of the proposed technique requirements; otherwise, it will have a significant impact on the accuracy of the results.

Finally, in this study, we used the objective function that combined the flow discrepancy function (Φ_Q) and pressure head discrepancy function (Φ_h) only. However, by looking at the objective function suggested by Bocchini et al., [2014], which was described in Chapter 2, it also included the penalty factor term (γ). This factor was introduced to improve the results quality. According to Marzani et al., [2013], the value of

γ =17 has shown a good improvement on the accuracy and robustness of such technique by testing several networks. However, this term was neglected through the experimental work to make the technique working without limitations of using a specific number (i.e., γ =17). An attempt will be examined by using different objective functions in next Chapter.

It can be concluded that, based on the empirical data, it is evident that the suggested methodology can detect blockages and their correct general location for models utilizing relatively short pipes. Even with discrepancies in pressure measurements, the technique detects blockages, but with false positives for the preceding and subsequent pipes. Therefore, the proposed method is still a valid option for detecting blockages in pipes of short length, but with less accuracy. The accuracy of long pipeline networks will be discussed with real examples in Chapter 6.

Chapter 4

CONDUCT PARAMETRIC STUDIES TO ASSESS THE

TECHNIQUE'S SENSITIVITY

Abstract

This chapter focuses on evaluating the accuracy and sensitivity of the proposed technique by examining several examples numerically. The most relevant parameters such as friction factor (fr), objective function ($J(\alpha)$) and other design criteria are taken into consideration to observe their effect on the technique's sensitivity. The substantial goal of this chapter is to define guidelines to select an appropriate mathematical model for such parameters (i.e., fr and $J(\alpha)$) and generalize it for all pipeline systems, whether complex, simple, looped or branched.

4.1 Introduction

In the previous chapter, the experimental analysis demonstrated a little discrepancy in the results. The pipe flows and nodal pressure measurements that were obtained empirically vary from one trial to another. These measurements were taken by the flowmeter and pressure gauge without calibration of the accuracy limits. The manufactures provide specifications for their equipment that defines accuracy, precision, resolution and sensitivity. During the experimental work, flow rates were taken via flowmeter with specifications of accuracy ±1% and repeatability of 0.2%. Pressure heads measurements were taken by the pressure gauge with 0.25% accuracy in reading. The accuracy and sensitivity of the measurements that were obtained by these instruments have been verified and compared with the measurements simulated via ANSYS. The results were almost identical, as presented in the previous Chapter. At the same time, the proposed technique did not specify any restrictions or specifications about the instruments that should be used.

This chapter discusses in detail the most qualifying factors, which are more likely the main reason for variation in the results. It explains how these factors can alter the accuracy and sensitivity of the suggested technique through several examples of pipeline networks. Thus, the chapter introduces an attempt to minimize the discrepancy in the results. In fact, in engineering applications, it is uncommon to obtain an exact solution. Since the proposed technique used FEM, which itself is an approximate method, such small discrepancy was expected to be noticeable from the beginning. However, it was not clear whether this discrepancy in the measurements was acceptable or not.

The proposed technique aims to identify the exact location of a blockage, which can lead to time and monetary savings. Thus, it is worth to conduct parametric studies that inspect the accuracy and sensitivity of such technique. A brief overview about the most relevant parameters examined are described below:

a- Individual pipe characteristics (i.e., length, diameter, roughness, distributed head losses and average temperature). Also, it includes characteristics of blockages (i.e., location, length and diameter.)

b- Objective function

Several functions are implemented to observe their abilities on the improvement of the results accuracy. Afterwards, the best function is determined by monitoring the accuracy of the results and comparing them to the exact values.

c- Friction factor

Since most of the flow inside the pipes is turbulent, an accurate value of the friction factor should be calculated by the *Colebrook-White* formula. However, this formula makes iterations necessary (i.e., an implicit solution is required). Hence, an approximate formula

(*Chen* formula) has been used to avoid the iterative solution. This thesis has investigated other approximate formulas to compute the friction factor and compare the results with those that are generated by the *Colebrook-White* equation. Finally, according to the network analysis results and their accuracy, an indication for which formula gives a better response is provided.

d- Boundary conditions

It is paramount to understand the stability of the system and where to impose the boundary conditions (i.e. impose pressure heads and flow). Several examples are analyzed numerically with different boundary conditions to this purpose.

e- GAs Parameters

Generally, in most of the optimization procedures that use GAs, as the generations progress, the individuals in the population approach the minimum point. Several examples with different population sizes and numbers of generations are investigated to identify the optimal numbers for any network.

4.1.1 Input Parameters of the Networks Design

The fluid networks contain interconnected pipes that form the system. These pipes can take any shape, depending on the design requirements. The pipe characteristics should be consistent with the network requirements. In other words, individual pipe characteristics (i.e., length, diameter, and roughness) should be able to satisfy the design conditions (i.e., the required pipes flow and pressure heads). Consequently, the pipe characteristics can be computed by knowing the pipe flows and nodal pressure heads of the required design.

The proposed technique is an analysis method that can identify the blockage by knowing the flow quantities and pressure heads. This means, that the suggested

methodology solves an inverse problem (i.e., pipe characteristics need to be known). In the experimental designs, depending on the available time and constraint of the budget, only 2 inch pipeline network was tested. The selected diameter has a direct impact on the accuracy of the results.

Bernoulli and *Darcy* formulas illustrate that the pipe flows are directly proportional to the pipe diameter and inversely proportional to pipe length. Technically, the scaled-down models cannot be equivalent to real cases of large networks. Thus, it is expected to have small discrepancies in results of short pipes with small diameter compared to large-scale realistic models. Also, in most of the small-scale models, the head losses (potential differences) at each node are neglected, therefore, it is difficult to observe any differences in pressure measurements from one node to another.

In this section an attempt is made to check the accuracy of the blockage identification by testing the network with different pipe lengths and diameters. It is expected for a large-scale network (i.e., large length and diameter) to obtain a more accurate result compared with a small-scale network. The comparison of the results and the most relevant conclusion are presented afterwards.

Numerical Example:

A network is designed with different elevations (each node has different elevation, z) and all pipes have a diameter of 300 mm, except for pipes 1 and 2 that have a diameter of 400 mm. The temperature range is assumed to be 22°-28°, and the roughness of each pipe is $6.1 . 10^{-4} \, m$ (i.e., pipes are copper). The network consists of 10 segments of pipe and 10 nodes and utilizes a single phase fluid (i.e., water). A piezometric head of 10 m is imposed at node 1. Flow measurements are collected in all pipes, except pipe 2, whereas the nodal

pressure heads are taken in all nodes, excluding node 5. The network data is shown in Table 4.1. The investigated scenario is implemented by inserting a blockage in pipes 3 (30% blockage over 70% L) and 9 (50% blockage over 70% L). The proposed methodology should detect $\alpha_3 = 0.7 \; and \; \alpha_9 = 0.5$, and all the other $\alpha_i = 1.0$. Also, a noise of 5% is superimposed to simulate the measurement errors.

GAs were setup to perform the optimization procedure using 200 individuals per generation and a maximum of 200 generations. Figure 4.1 shows the layout of the examined network. The results of simulation for flow rates and pressure heads are presented in Figure 4.2. The results of the blockage identification in terms of residual diameter are illustrated in Figure 4.3 graphically and in Table 4.2 numerically.

| Pipe | Connectivity | Nodal Coordinates | | | D(mm) | e (mm) | h (m) |
		X(m) (*1000)	Y(m) (*1000)	Z(m)			
1	1-2	0	4	60	400	0.61	10
2	2-3	0.1	3	40	400	0.61	-
3	3-4	0.75	3	0	300	0.61	-
4	3-5	0.9	2	-80	300	0.61	-
5	4-5	0.95	3	-100	300	0.61	-
6	5-6	1.25	4.25	-140	300	0.61	450
7	5-7	1.32	3.25	-280	300	0.61	490
8	4-8	1	0.8	-240	300	0.61	450
9	4-9	1.3	2	-300	300	0.61	-
10	4-10	1.4	1	-440	300	0.61	480

Tabel 4.1: Network data
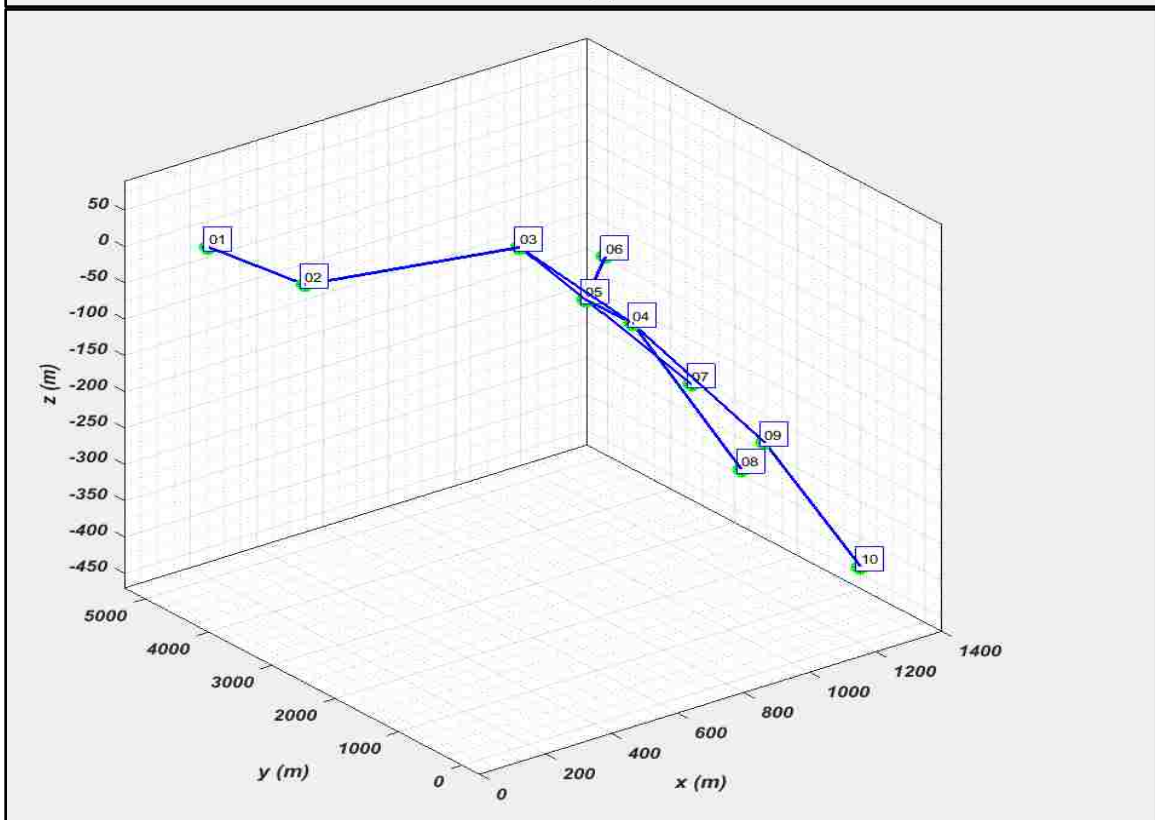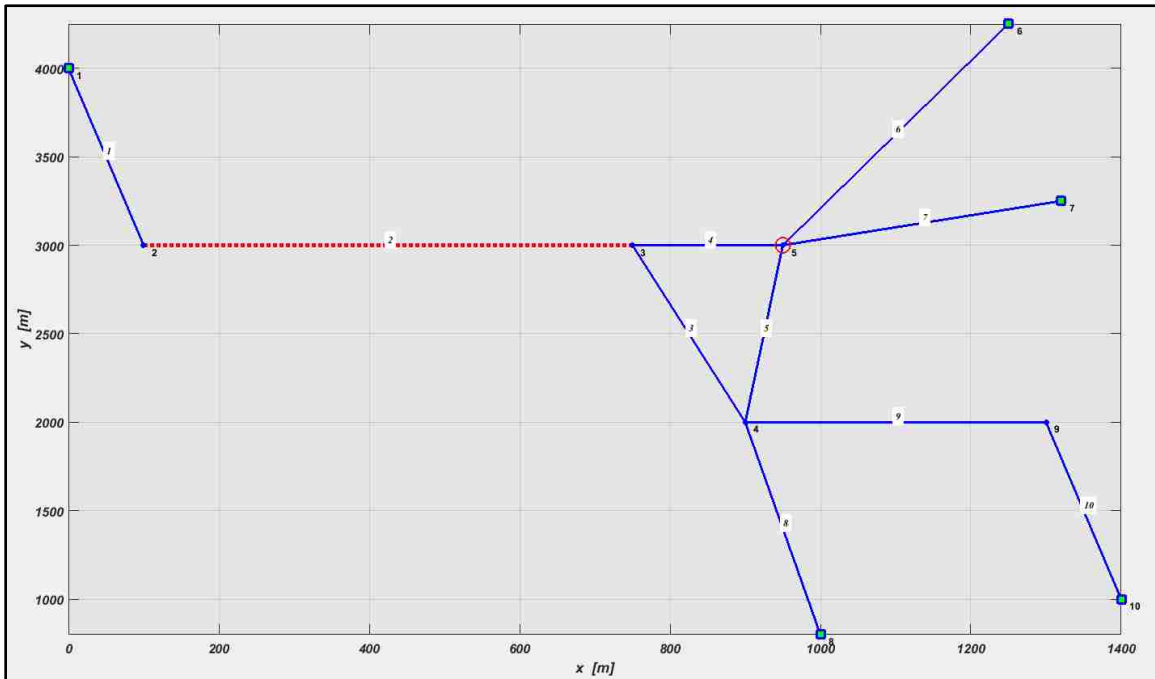
Figure 4.1: Layout of the simulated network via MATLAB

```
ALTITUDE AND PIEZOMETRIC HEAD AT NODES

         nodo          z (m)           h (m)          HGL(m)
           1             60              10              70
           2             40          83.361          123.36
           3              0          157.94          157.94
           4            -80          270.71          190.71
           5           -100          295.14          195.14
           6           -140             450             310
           7           -280             490             210
           8           -240             450             210
           9           -300          352.01          52.014
          10           -440             480              40


FLOW IN PIPES

         pipe          node i          node j         Q (m^3/s)
           1             2               1             0.54712
           2             3               2             0.5472
           3             4               3             0.092506
           4             5               3             0.45474
           5             5               4             0.073314
           6             6               5             0.33285
           7             7               5             0.1952
           8             8               4             0.13973
           9             4               9             0.12052
          10             9              10             0.12052
```

Figure 4.2: Distribution of pipes flow and Pressure heads through the Network
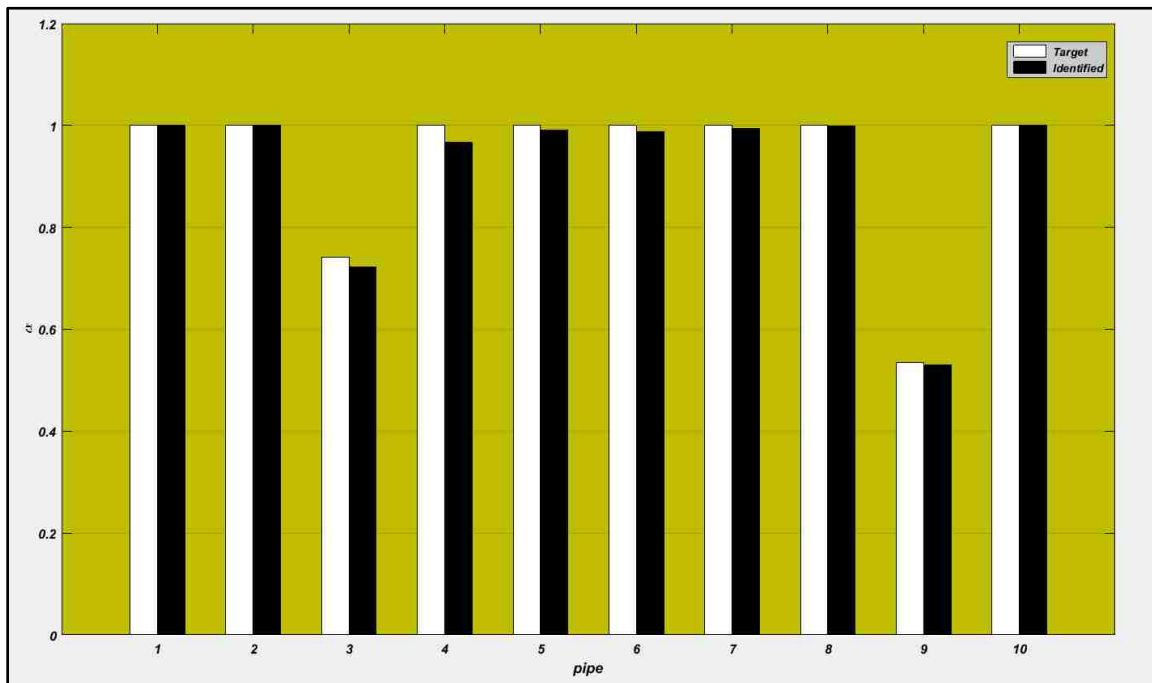
Figure 4.3: Results of the blockage identification procedure

Results of the identification			
Pipe	alpha real	alpha identified	error %
1	1	1	0
2	1	1	0
3	0.741	0.722	2.564
4	1	0.966	3.4
5	1	0.992	0.8
6	1	0.988	1.2
7	1	0.994	0.6
8	1	0.999	0.1
9	0.536	0.53	1.119
10	1	1	0

Table 4.2: The numerical computation of the blockage identification

The results demonstrate a remarkable accuracy of blockage identification. The proposed technique was able to identify the two pipes that were blocked (i.e., pipes 3 and 9) without false positives. Also, it is important to remember that the suggested methodology identifies the blockages, even if some measurements are missing (i.e., the flow at pipe 2 and the pressure head at node 5 are not available).

Moreover, since iteration is necessary in this method, and the optimization algorithm is not deterministic (the result changes slightly in each run), a statistical analysis is performed by running the proposed technique 20 times to prove the robustness of GAs. Each time a constant random noise of magnitude 5% on the computed measurements was superimposed. The statistical results in terms of mean value μ and standard deviation σ are listed in Table 4.3 for the examined network. The results indicate that the identified mean values for the blocked pipes (i.e., 0.75 and 0.55) are slightly greater than the respective target values (i.e., 0.70 and 0.50). Even though there is a small discrepancy in results, statistically the proposed technique is capable to identify all the obstructed pipes with a

very low dispersion as shown in Table 4.3. The statistical results are presented graphically in Figure 4.4 by using a Box-and-Whisker plot for each pipe. It can be seen that the lowest value (outlier value) of α for pipe 3 is approximately 0.70, whereas it equals to 0.722 in Figure 4.3. As mentioned, this is because the results of identification are slightly different from one trial to another. The data in the figure show that the procedure tends (on average) to slightly overestimate the residual diameter. It can be noticed that the suggested methodology provides very good accuracy in blockage identification for such network (i.e., a large-scale pipeline network).

Statistical Identification Results									
Pipe	1	2	3	4	5	6	7	8	9	10
μ	0.99	0.99	0.75	0.99	0.95	0.98	0.99	0.99	0.54	0.99
σ %	0.722	1.267	2.416	1.601	4.903	0.859	1.542	1.266	1.009	5.511

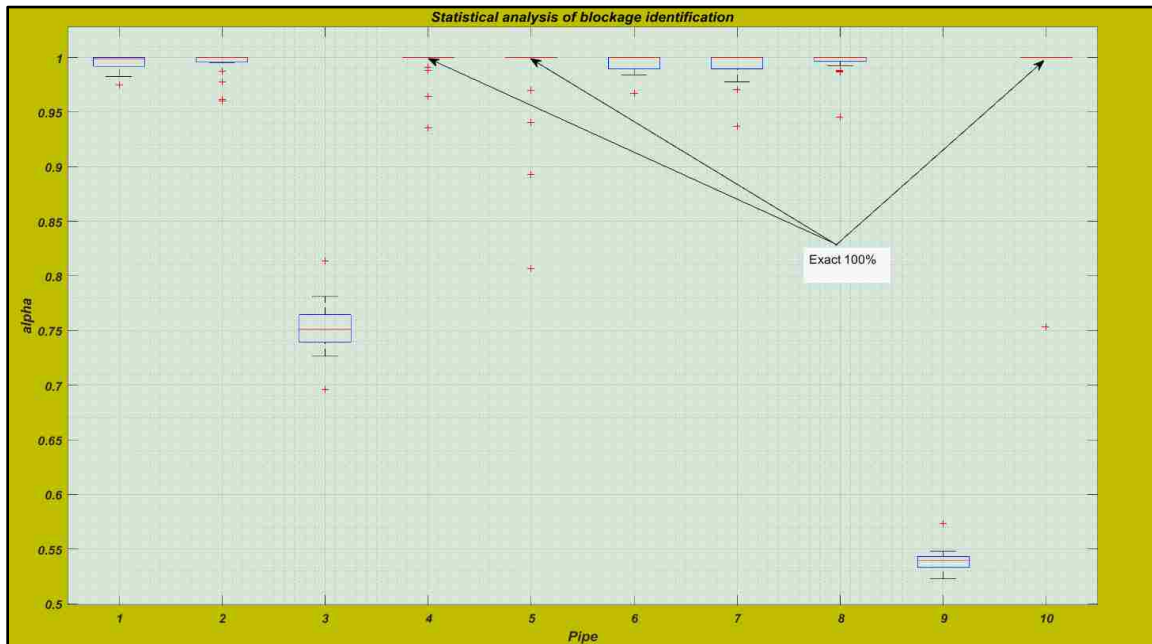*Table 4.3: Results of the statistical identification*

Figure 4.4: Results of the statistical analysis

The same example above is analyzed again but scaled down by 1:1000 (i.e., short pipes and small diameters). The aim of this example is to clarify how the accuracy in the results is affected when the pipe with a short length and a small diameter is used. In fluid dynamics, it is well-known that as the length of the pipe gets shorter, the minor and major losses of pressure head become almost negligible. Also, it was proved experimentally that in the short-scale network, the measurements of nodal pressure head were almost the same, no matter whether the system was blocked or not.

As stated earlier, the proposed technique relies on minimizing the objective function that captures the discrepancy between the measures and computed data of flow and pressure head. However, in the small-scale system, the drops in nodal pressure head were not significant to be helpful in blockage identification. Therefore, the optimization procedure depended only on the pipe flows to detect the pipes that were blocked. The measurements of the discharge alone are not enough to identify the blockage within reasonable accuracy. Furthermore, according to the one-dimensional mass continuity formula, the small diameter leads to reduced the flow inside this pipe. Thus, it is expected to have small discrepancy in the result of blockage identification. Figure 4.5 shows the layout of the scaled-down network. The results of the scaled-down network flow rate are compared with the results of the large-scale network flow rate in Table 4.4. The results of blockage identification in terms of residual diameters are illustrated in Figure 4.6. The results indicate false positives in other pipes, especially pipes 8 and 10. Indeed, it is expected to have such inaccurate result in these pipes that are located next to the blocked pipe, since the blockage in the target pipes affects the flow passing through the preceding pipes.
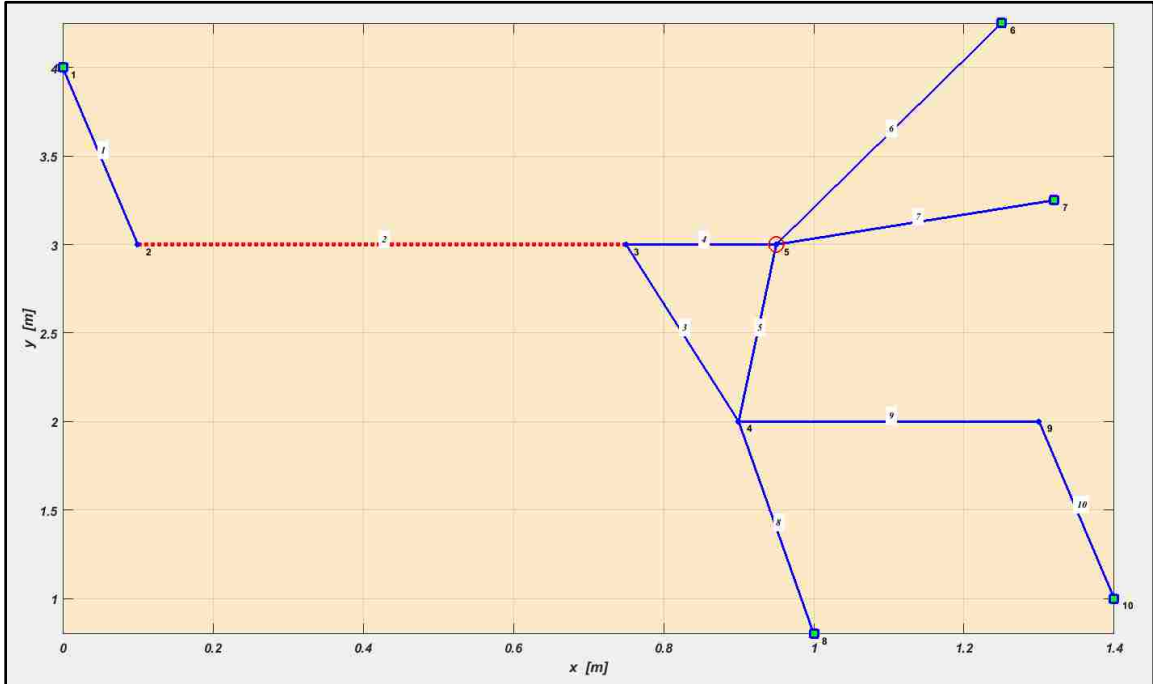
Figure 4.5: Layout of the simulated scaled-down network through MATLAB

Pipes flow of scaled-down network $(m^3/$ sec$)$	Pipes flow of Large scale network $(m^3/$ sec$)$
3.644e-09	0.547
3.645e-09	0.547
9.598e-10	0.093
2.684e-09	0.455
1.075e-09	0.073
4.003e-09	0.333
2.423e-10	0.195
1.380e-10	0.139
2.226e-11	0.121
2.232e-11	0.121

Table 4.4: The comparison of pipes flow in scaled-down and large-scale network
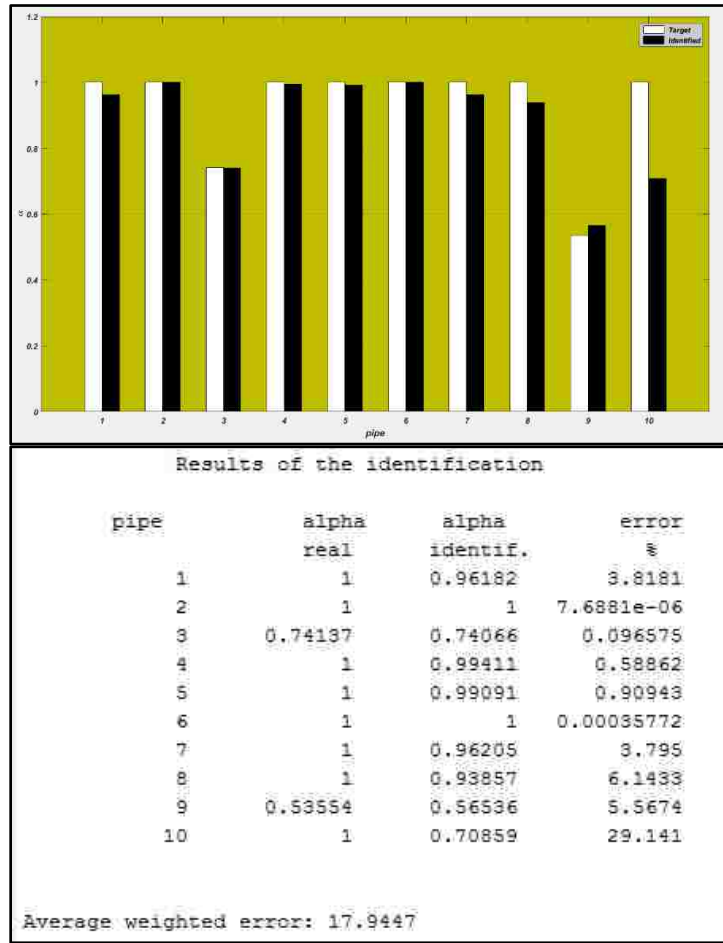
Figure 4.6: Results of the blockage identification procedure

It can be seen from Table 4.4 that the pipe flows is very small in the case of a small-scale network, compared with a large-scale system. These small values introduce difficulty for the proposed technique to process the exact location of the blockage. Hence, for such methodology to detect exactly where the blockage is, it is imperative for the drops in pressure due to blockages to be significant. However, the drops in pressure in a short length network are almost negligible, resulting in inaccurate α values. For the small-scale pipe model, this problem is more important due to the relationship among pipe length, diameter, and changes in pressure. In a small-scale model the pressure changes are very small. This makes for the blockage identification heavily dependent on the flow values.

Instead, in large-scale/real world systems, both the length and the diameter of a pipe are much larger, which leads to more significant pressure losses when a blockage is present. As explained, the ratio between length and diameter of the pipe is quite important. The larger this ratio, the more accurate results can be obtained, as seen in previous examples. The proposed technique identified pipe 10 with a 30% blockage, but in fact it was entirely clean. Figure 4.6 indicates 29% error in the result of pipe 10, which is a significant error for such applications. The analysis was repeated 20 times to portray the variation in the residual diameter results. Figure 4.7 shows the comparison of the statistical analysis of a scaled-down network, a large-scale network (the analysis represented via a Box plot), and the exact target values in terms of the mean. Overall, the analysis of the large-scale network shows a suitable degree of accuracy compared to the analysis of the scaled-down network. The ratio of the pipe diameter to its length has a large effects on pipe flows, pressure heads and on the accuracy of the blockage identification. The data in Figure 4.7 show that the procedure identifies the pipes that are blocked, slightly overestimating the residual diameter; and it provides a false positives in the results of other pipes that are linked to the obstructed pipe. Such results are expected in a scaled-down network.
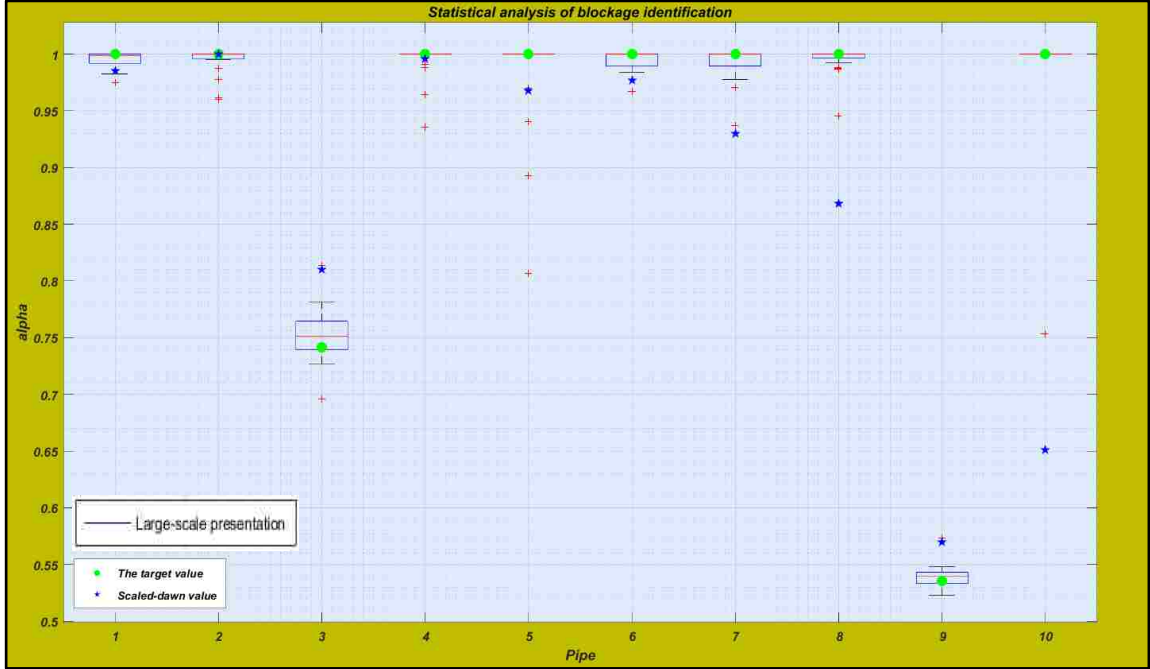
Figure 4.7: Results of the statistical analysis comparison

4.1.2 Objective Function

All previous examples were analyzed by using the following function:

$$J(\alpha) = \Phi_h + \Phi_Q$$

This formula does not include the penalty factor (γ) term, compared to the formula that was proposed in Chapter 2 by Bocchini et al., [2014]. The penalty factor was introduced to improve the quality of the results and to control the stability and speed of convergence. However, the elimination of this term in the former examples was intended to make the selected objective function more general.

To gain a deep understanding of how the γ term affects the accuracy, this section examines different objective functions with and without γ. Primarily, five objective functions were considered, to come up with conclusions about the penalty factor advantages and disadvantages in the proposed technique. The five fitness functions are:

$$J_1(\alpha) = \log(\Phi_h) + \log(\Phi_Q) - \frac{\gamma}{n}\sum_{p=1}^{n}\alpha_p$$

$$J_2(\alpha) = -\left[\log(\Phi_h) + \log(\Phi_Q) - \frac{\gamma}{n}\sum_{p=1}^{n}\alpha_p\right]^2$$

$$J_3(\alpha) = \Phi_h$$

$$J_4(\alpha) = \Phi_Q$$

$$J_5(\alpha) = \Phi_h + \Phi_Q$$

Numerical example:

The study of these five objective functions is conducted by designing a system with all pipes having a diameter equal to 400 mm, except pipe 1, which has a diameter of 500 mm. The layout is the same of the network illustrated in Figure 4.8. The temperature range is assumed to be $22°$-$28°$, and the roughness of each pipe is $5.10^{-4}m$. The network consists of 14 segments of pipe and 14 nodes and utilizes a single phase fluid (i.e., water). A piezometric head of 10 m is imposed at node 1. Flow measurements are collected in all pipes, except pipes 4 and 10, whereas the nodal pressure heads are taken in all nodes, excluding nodes 6 and 11. The network data are shown in Table 4.5. The investigated scenario is implemented by inserting a blockage in pipes 5 (50% blockage over 50% L) and 7 (30% blockage over 70% L). The proposed methodology should detect $\alpha_5 = 0.5 \ and \ \alpha_7 = 0.7$, and all other $\alpha_i = 1.0$. Also, a noise of magnitude 5% is superimposed to simulate the measurement errors.

It is expected that the best fitness function will decrease monotonically toward the correct value. The results of the analysis presented in Figure 4.9 show that the behavior of $J_2(\alpha)$ was the best. The results proved that the γ term in the first and second objective

functions was useful to improve the results accuracy in some pipes for such a system. Additionally, Marzani et al. verified that the value of $\gamma=17$ showed an optimal robustness and accuracy with respect to many network topologies. Thus, in many networks, γ is important parameter that needs to be tuned to improve the accuracy convergence and remove the false positives. However, this is not always the case. Even with the elimination of γ term from the rest of the suggested objective functions, the results presented an acceptable accuracy in some pipes of such network. Thus, the γ term did not help substantially in finding the exact value of the blockage, but it led to the expected behavior (monotonically decreasing function) of the objective function. Surprisingly, the fourth selected objective function, which only depended on the flow measurements provided a reasonable degree of accuracy in such system, as shown graphically. It can be concluded that with accurate flow measurements, more precise results can be obtained. More likely the superimposed noise has an essential contribution to the accuracy of the simulated pipe flows and the overall efficiency of the suggested method. The noise effects will be discussed in the next Chapter.
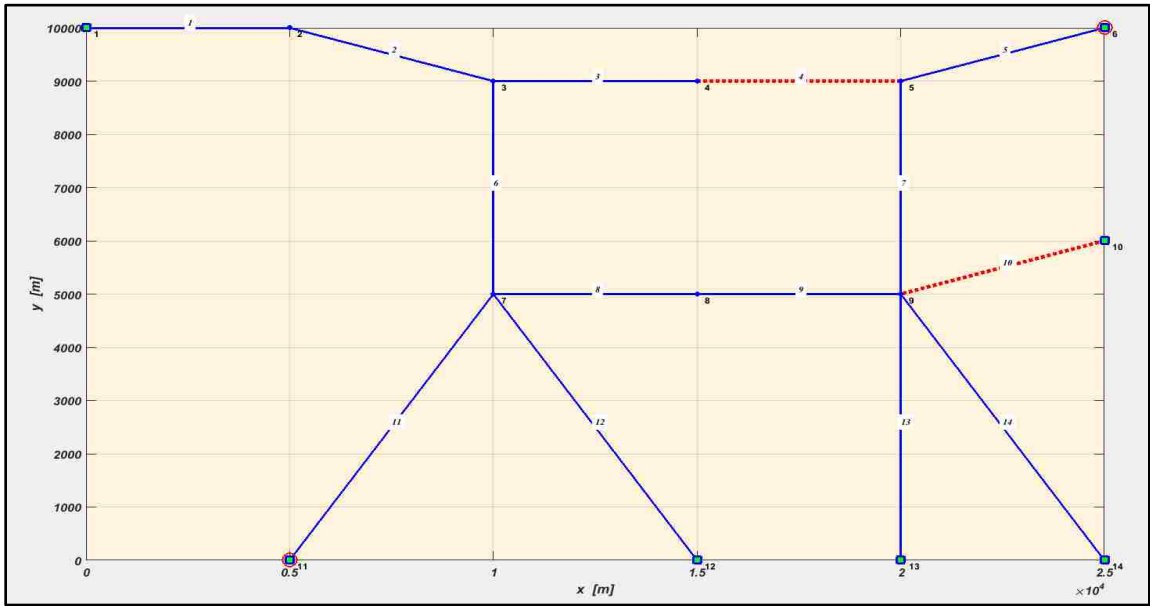
Figure 4.8: Layout of the examined network

Pipe	Connectivity	Nodal Coordinates			D(mm)	e (mm)	h (m)
		X(m) (*1000)	Y(m) (*1000)	Z(m)			
1	1-2	0	10	60	500	0.5	10
2	2-3	5	10	40	400	0.5	-
3	3-4	10	9	20	400	0.5	-
4	4-5	15	9	-10	400	0.5	-
5	5-6	20	9	30	400	0.5	-
6	3-7	25	10	40	400	0.5	180
7	5-9	10	5	10	400	0.5	-
8	7-8	15	5	-20	400	0.5	-
9	8-9	20	5	20	400	0.5	-
10	9-10	25	6	30	400	0.5	190
11	7-11	5	0	-50	400	0.5	270
12	7-12	15	0	-40	400	0.5	260
13	9-13	20	0	-60	400	0.5	280
14	9-14	25	0	-100	400	0.5	320

Table 4.5: Network data

89

Figure 4.9: Presentation of the five selected objective functions

4.1.3 Friction Factor (fr)

The proposed methodology is based on the *Darcy-Weisbach* equation. This formula is one of the main building blocks in such technique. It links the head losses due to friction with the fluid flow, which are the main parameters in the suggested procedure. Thus, the accuracy of the blockage identification can be associated with the computation of fr. In fluid dynamics, the well-known precise formula to calcula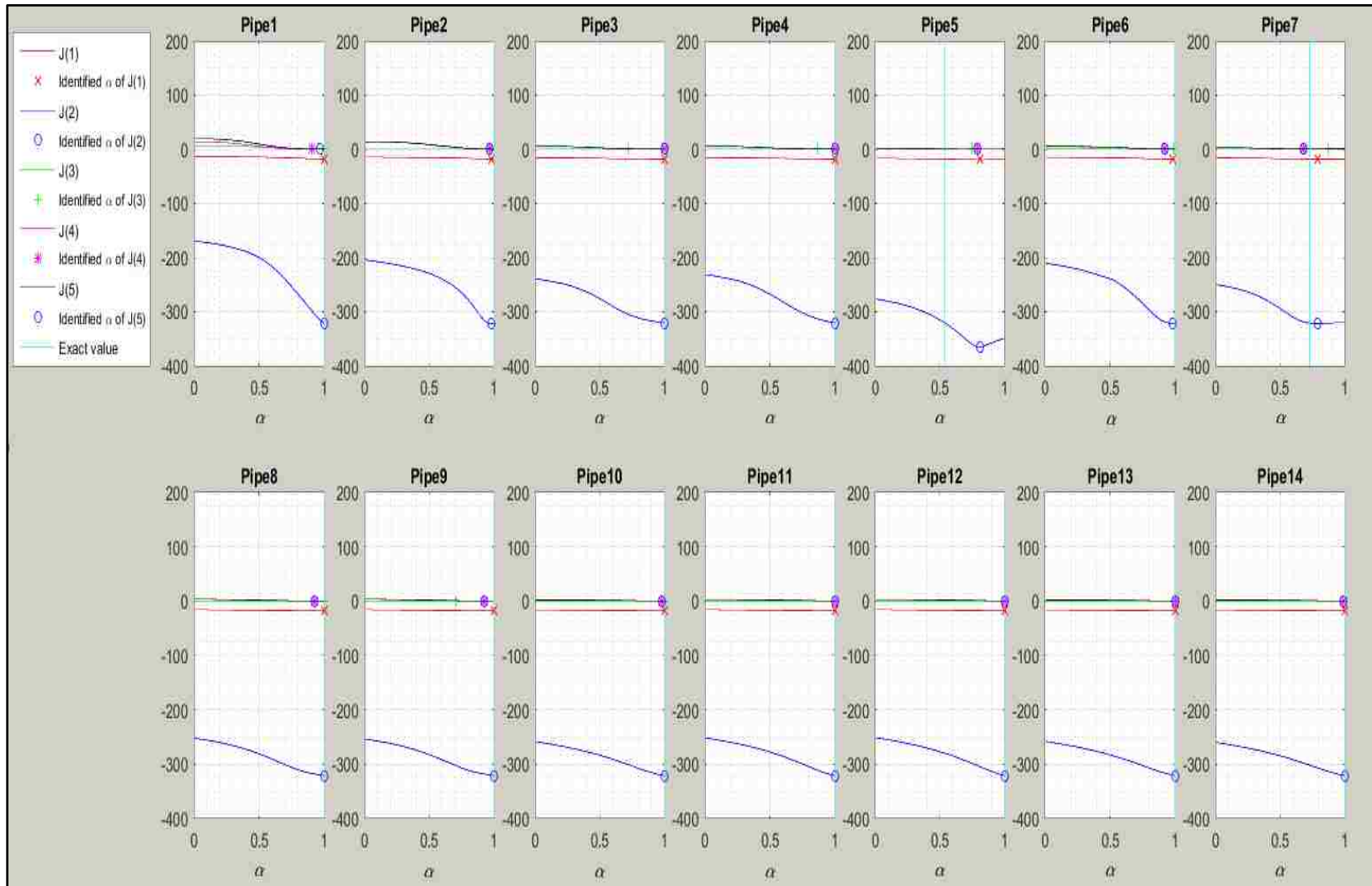te fr when the flow is turbulent is the *Colebrook-White* equation. This formula is preferred in many engineering applications because it covers the whole range of Reynolds numbers and relative roughness. However, this expression, as shown below, is an implicit scheme that makes an iterative solution necessary.

$$\frac{1}{\sqrt{fr}} = -2log\left[\frac{e/D}{3.7} + \frac{2.51}{Re.\sqrt{fr}}\right]$$

The application of the *Colebrook-White* equation with complex networks or a large-scale systems is time consuming and requires several steps of iteration. Therefore, explicit approximate methods were developed by researchers. All these methods were able to compute fr explicitly in a complex structure with minimal errors. It is interesting to verify which of these explicit formulas can provide fr with high accuracy.

During the experimental work mentioned in Chapter 3, the *Chen* equation was used as an explicit form to compute fr in the proposed technique. This section discusses four equations (including *Chen* equation) that deviate from *Colebrook- White* equation to observe their effects on the proposed methodology. The same experimental example of the looped network without blockage is repeated to check which approximate formula provides a higher accuracy in flow measurements, compared to real measurements. The flow

measurements that were simulated through ANSYS as shown previously in Table 3.1 are considered to present the exact data. To indicate whether the flow in each pipe is laminar or turbulent, Reynolds number (Re) is computed for each pipe as explained in Table 4.6. The results show that the minimum Re is greater than 2100, which is the limit between laminar and turbulent flow, thus all pipes have a turbulent flow.

fr and the simulated flow quantities were calculated by using each explicit equation, as listed below. The error percentage in the simulated pipe flows quantities of the first five pipes is reported in Table 4.7. Also, since the proposed method requires an iterative solution, and it is not deterministic, the blockage identification procedure of the first 10 pipes is repeated 30 times for each explicit formula. The mean of the results is compared with the exact values, as demonstrated by using a Box-and-Whisker plot in Figure 4.10.

$$\frac{1}{\sqrt{fr}} = -2.\log\left[\frac{e}{3.7065.D} - \frac{5.0452}{Re}.\log\left(\frac{1}{2.8257}.\left(\frac{e}{D}\right)^{1.1098} + \frac{5.8506}{Re^{0.8981}}\right)\right] \quad \text{Chen equation}$$

$$fr = \frac{0.308642}{\left[\log\left(\left(\frac{e}{3.7.D}\right)^{1.11} + \frac{6.9}{Re}\right)\right]^2} \qquad \text{Haaland equation}$$

$$fr = \frac{0.25}{\left[\log\left(\frac{e}{3.7.D} + \frac{5.74}{Re^{0.9}}\right)\right]^2} \qquad \text{Swamme-Jain equation}$$

$$fr = \frac{0.2479 - 0.0000947.(7 - \log Re)^4}{\left[\log\left(\frac{e}{3.615.D} + \frac{7.366}{Re^{0.9142}}\right)\right]^2} \qquad \text{Papaevangelou et al. equation}$$

Pipe	1	2	3	4	5	6	7	8	9	10	11	12	13	14	15	16
Exact Velocity (m/s)	0.29	0.149	0.149	0.149	0.149	0.149	0.149	0.29	0.29	0.149	0.149	0.149	0.149	0.149	0.149	0.29
Diameter (m)	0.051	0.051	0.051	0.051	0.051	0.051	0.051	0.051	0.051	0.051	0.051	0.051	0.051	0.051	0.051	0.051
Dynamic viscosity (kg/(m.s))	0.00096	0.00096	0.00096	0.00096	0.00096	0.00096	0.00096	0.00096	0.00096	0.00096	0.00096	0.00096	0.00096	0.00096	0.00096	0.00096
Density (kg/m^3)	996	996	996	996	996	996	996	996	996	996	996	996	996	996	996	996
Re	15425	7925.24	7925.24	7925.24	7925.24	7925.24	7925.24	15425	15425	7925.24	7925.24	7925.24	7925.24	7925.24	7925.24	15425

Table 4.6: Reynolds number computations for non-blockage looped network

	Pipe	1	2	3	4	5
Error %	Chen Equation	$2.183.10^{-6}$	2.814	2.814	2.814	2.814
	Haaland Equation	$2.354.10^{-6}$	2.814	2.814	2.814	2.815
	Swamme-Jain equation	$5.373.10^{-6}$	2.814	2.814	2.814	2.815
	Papaevangelou et al. equation	$1.776.10^{-6}$	2.814	2.814	2.814	2.815

Table 4.7: Error percentage in each explicit equation

It can be seen from Table 4.7 that all the equations provide the same error percentage in terms of the simulated flow quantities. The maximum error in the results is almost 3%, which is considered to be an acceptable error in fluid flow computations. The differences in pipe flows were not that significant from one equation to another, therefore, it was not obvious which equation led to higher accuracy results.

The statistical analysis show that the results of the identification procedure due to the fr obtained by *Haaland* and *Swamme* formulas appeared with high dispersion, compared to the *Chen* and *Papaevangelou* equations. That can be related to the appearance of the terms, Re and e/D twice in the *Chen* equation, and also Re appears twice in the *Papaevangelou* equation. These terms reduced the dispersion of the values. Despite the high dispersion, the error percentage in term of the mean value was not very significant.

93

Thus, it is possible to use the *Haaland* or *Swamme* equations to obtain an acceptable degree of accuracy. It is preferred to use the *Chen* or *Papaevangelou* formulas with a sophisticated large-scale network to provide higher accuracy. It can be concluded that the selected formula to compute fr does not greatly affect the accuracy and sensitivity of the proposed technique. In other words, the errors presented by such formulas are not significant from one equation to another.

Another numerical proof was given by Papaevangelou et al., [2010]. In the study, fr computed by each one of the equations stated above, and the results were compared with values of fr obtained through the *Colebrook-White* equation. Papaevangelou et al. in their research considered 10 values of the ratio e/D and 19 values of Re. For each set of data $(e/D, Re)$, the researchers calculated the relative error as the following:

$$error = \frac{fr_{Colebrook-White}}{fr_{equation}} - 1$$

The results verified that the relative error exceeded 1% when the *Haaland* relation was used, whereas the error approached up to 3% in use of the *Swamme-Jain* equation. The *Chen* equation included complex terms and dual appearance of both e/D and Re, but it bounded the errors from -0.22% to +0.47%. *Papaevangelou* et al., on the other hand, developed a simple expression to minimize the error to less than 0.8% [Papaevangelou et al., 2010]. The same conclusion was drawn earlier, according to the Box-and-Whisker plot, which portrayed a good accuracy of the *Chen* and *Papaevangelou* equations.
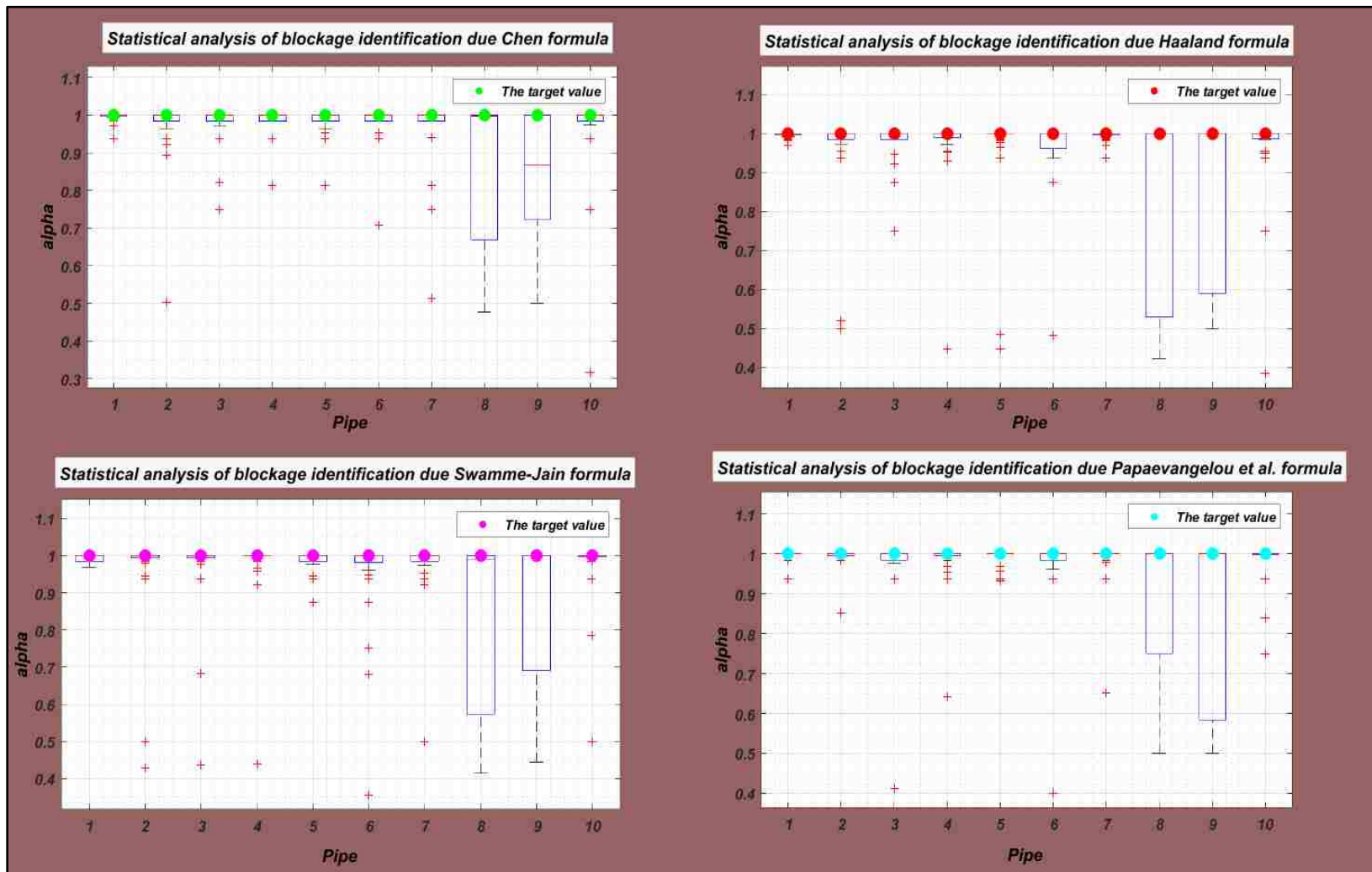
Figure 4.10: Results of the statistical analysis for each of the explicit equations

4.1.4 Assigning the Boundary Conditions

Obviously, the boundary conditions play an important role in the model. In particular, boundary conditions are essential to obtain "unique" solutions. Boundary conditions in this methodology can be flow rate and/or pressure head. These conditions are necessary to connect the simulated system with what it interfaces. Boundary conditions define the inputs of the model and without them the solutions cannot be found. The proposed technique requires boundary conditions in their steady-state. This means that the flow rates or pressure heads assigned as a boundary condition should stay constant throughout the simulation, whether the pipes are blocked or not.

Boundary conditions can be subjected to the problem requirements, fluid behavior and number of the inlets and outlets. To acquire suitable accuracy in solutions, it is necessary to be aware of the information that is required of the boundary condition, and locate the boundaries where the information of the pipes flow or pressure heads are known. These points are considered a reference to simulate other quantities through FEM in the suggested technique. Therefore, lacking information in defining boundary conditions can have a significant impact on the results of blockage identification.

Realistically, it has been seen from previous examples that with poorly defined boundary conditions (i.e., missed one or two outlets without defining the pressure heads) the results of the identified residual diameters are poor.

The same example described in Section 4.1.2 is repeated by considering two cases as shown in Figure 4.11; 1) When boundary conditions are imposed at nodes 1, 6, 10, 11, 12, 13 and 14 (i.e., all inlet points and the outlet), and 2) When boundary conditions are imposed only at nodes 1, 10, 11, 12 and 14 The results of blockage identification are

illustrated graphically in Figure 4.12. The solution of identification indicated that the proposed technique was able to identify the exact location of blockages when the pressure head at all the inlets and outlet were assigned as inputs. In other words, the results of the first case, when more boundary conditions were taken into consideration, showed a higher accuracy compared to the second case. As it can be seen, the results of the second case demonstrated a bad accuracy of blockage identification. Additionally, the proposed technique displayed a "*Results may be inaccurate*" warning message during the run because the problem was ill-defined. It can be deduced that the blockage identification required at least all the inlet and outlet points in the network to be assigned as boundary conditions to achieve accurate results.
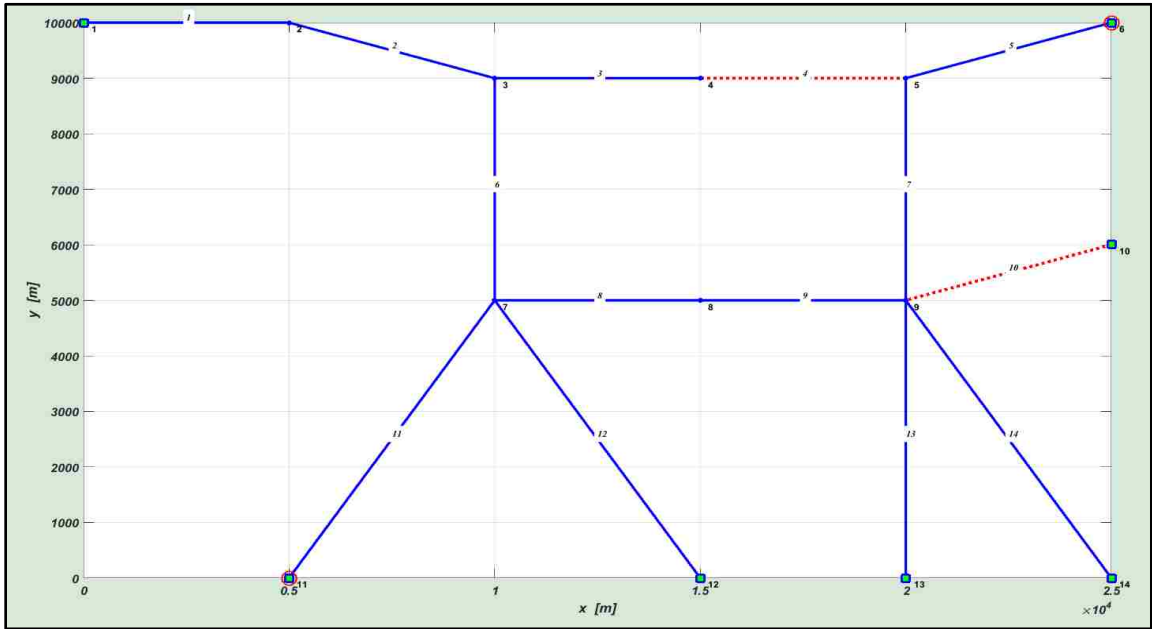
(1)
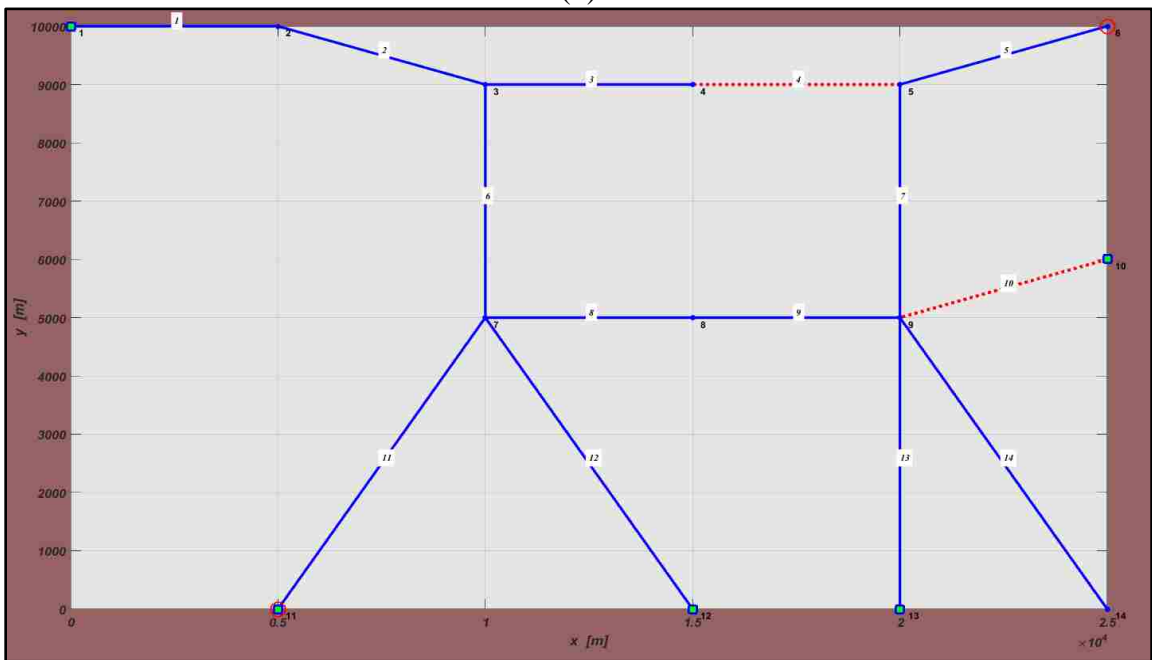
(2)

Figure 4.11: Network layout: 1) Pressure heads imposed at nodes 1, 6, 10, 11, 12, 13 and 14
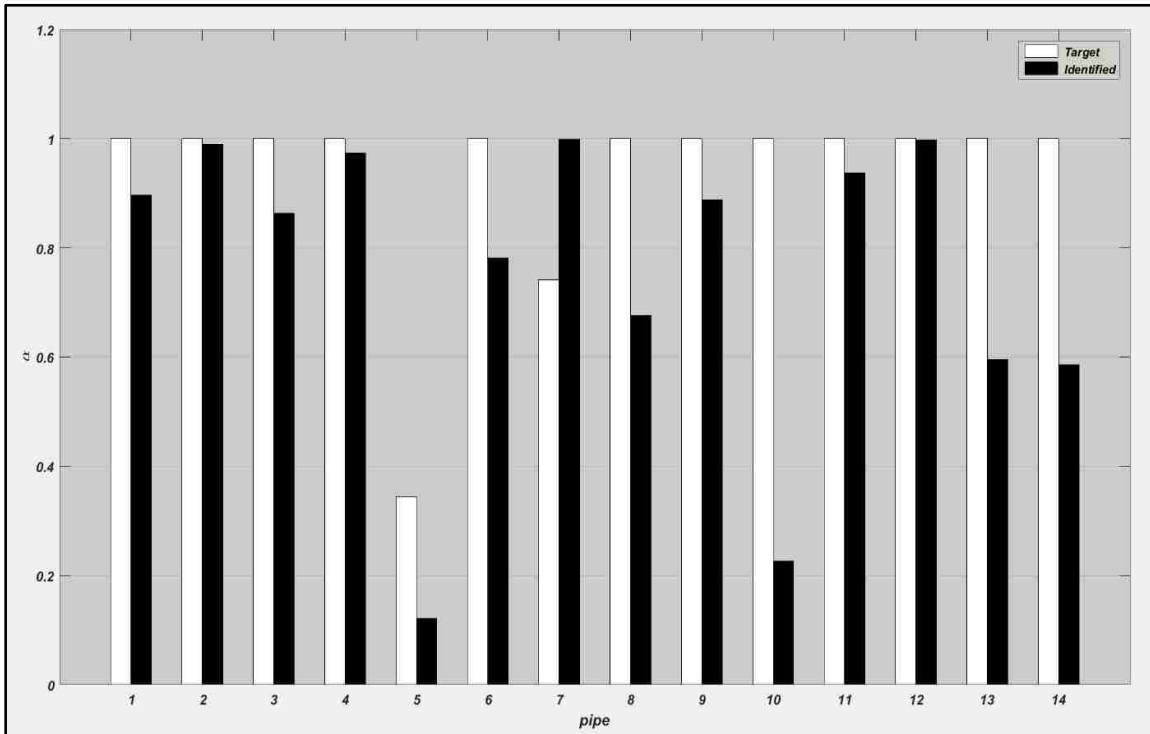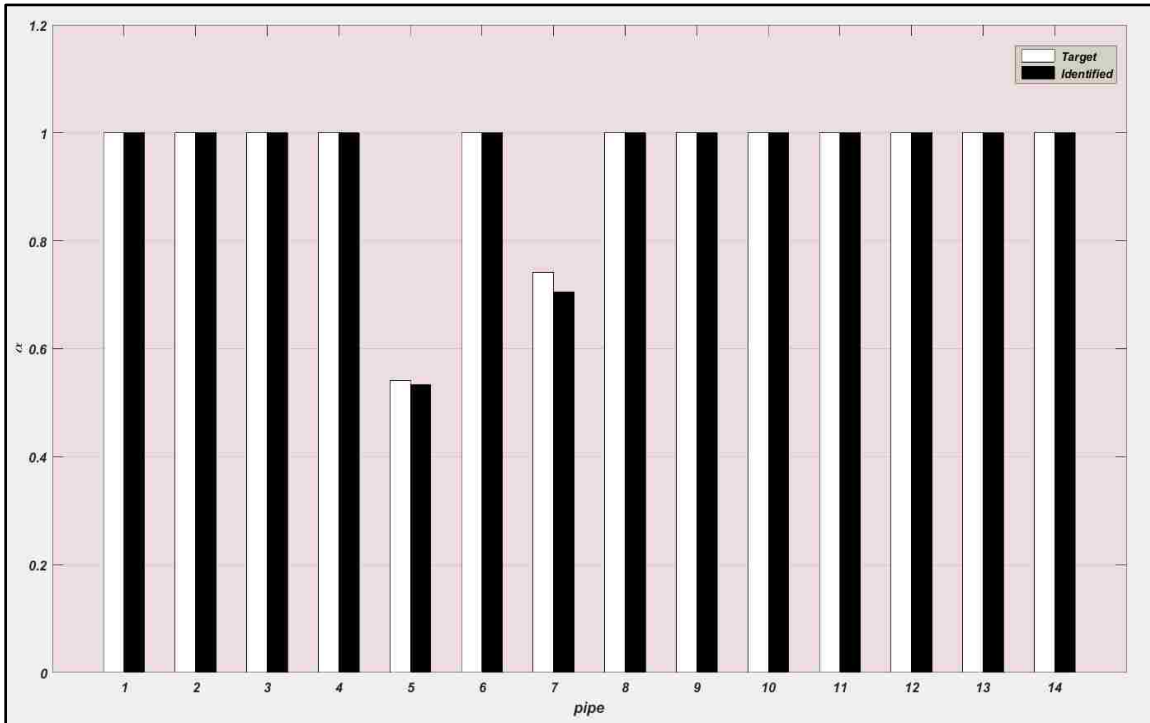*2) Pressure heads imposed at nodes 1, 10, 11, 12, and 13*

Figure 4.12: Results of the blockage identification procedure in the first and second case

4.1.5 GAs parameters

It has been mentioned in Chapter 2 that GAs are heuristic techniques that perform a search based on evolutionary sets of trial solutions. The proposed technique used GAs as a tool to find the variables α with a fixed number of generations and population size. We had setup GAs by using 100 individuals per generation and a maximum of 200 generations in most of previous examples to perform the optimization. However, it was not clear which set of algorithmic parameters will lead to the best trade-off between accuracy and convergence rate. Consequently, this section deals specifically with the study and observation of the parameters of GAs by taking into consideration the first and last objective functions that were described in Section 4.1.2.

The same example that was described in Section 4.1.1 is used with different population sizes and numbers of generations. The first case of study was performed with 50 generations and 100 population size by considering two objective functions, $J_1(\alpha)$ and $J_5(\alpha)$. This case was just an attempt to prove which fitness function could provide an appropriate accuracy. Figure 4.13 shows that the first objective function with $\gamma=17$ compared with the last function $J_5(\alpha)$ led to good results (almost identical), even though the number of generations was small. The advantages due to the penalty factor in terms of stability and speed of convergence were substantial. GAs yield a slightly different result at each run, therefore the proposed technique was executed for 100 times. The second case of study performed only on $J_1(\alpha)$. The statistical analysis of the best fitness function $J_1(\alpha)$ with different sets of generations and population sizes are presented graphically in Figure 4.14 and Figure 4.15 to prove the robustness of GAs. Later, the results in terms of the mean value μ and standard deviation σ of the parameter α for each set are stated as well in Table

100

4.8. The results of comparison the average weighted error with population sizes for the looped and branched networks are presented in Figure 4.16
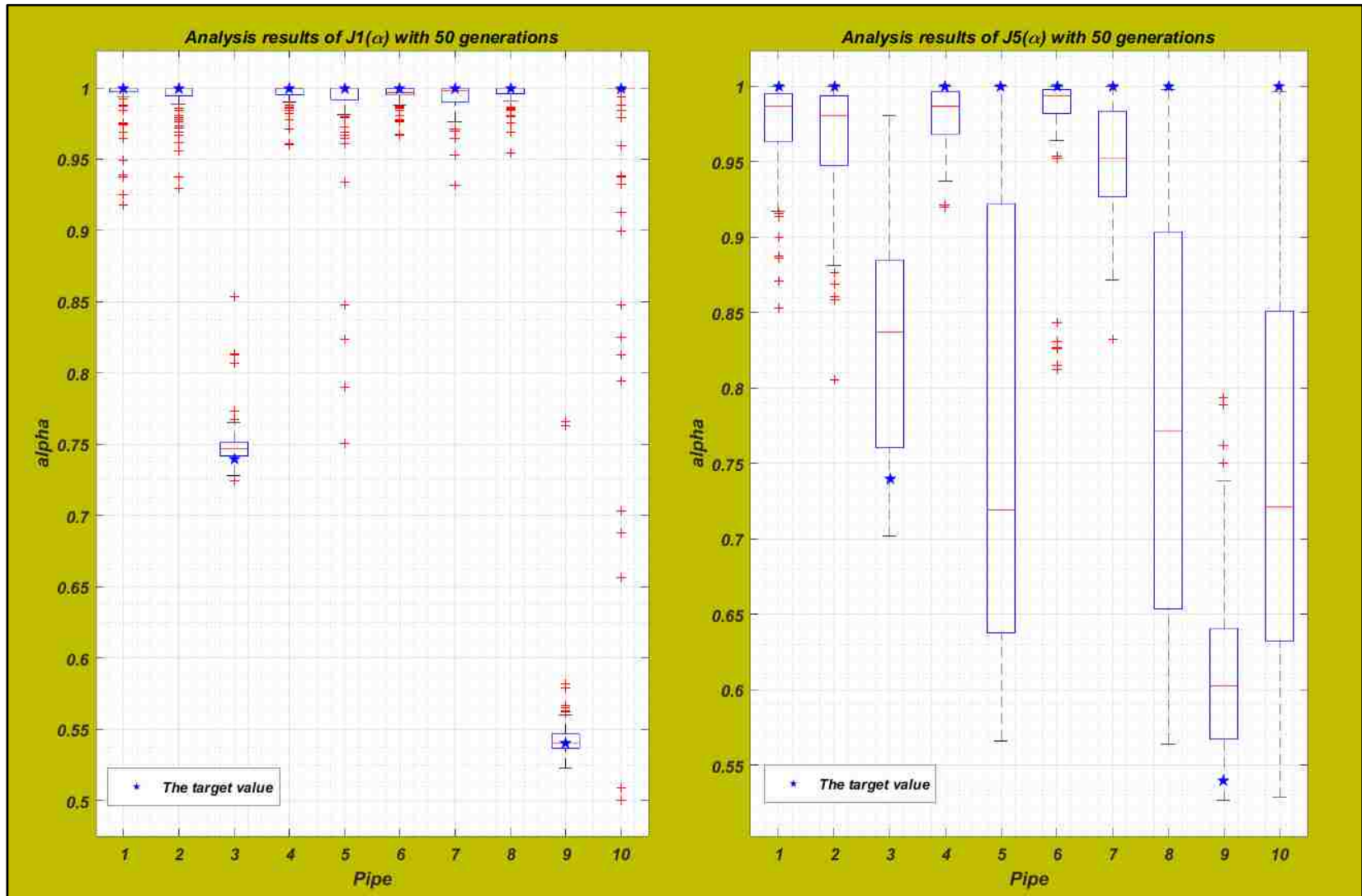
Figure 4.13: Comparison of the statistical analysis by using two different objective functions with 50 generations
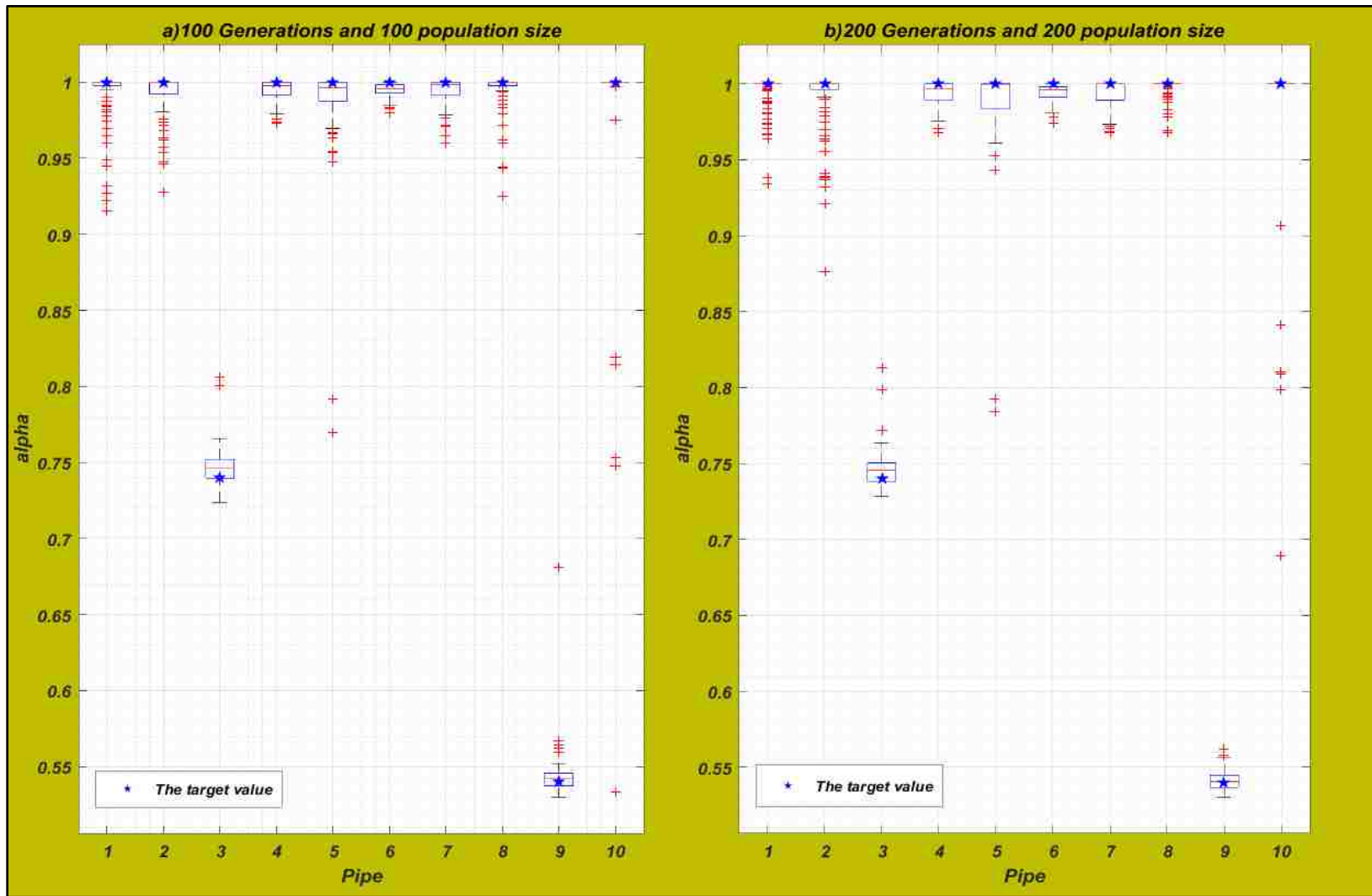
Figure 4.14: Statistical analysis of: a) 100 generations and 100 population size, and b) 200 generations and 200 population size
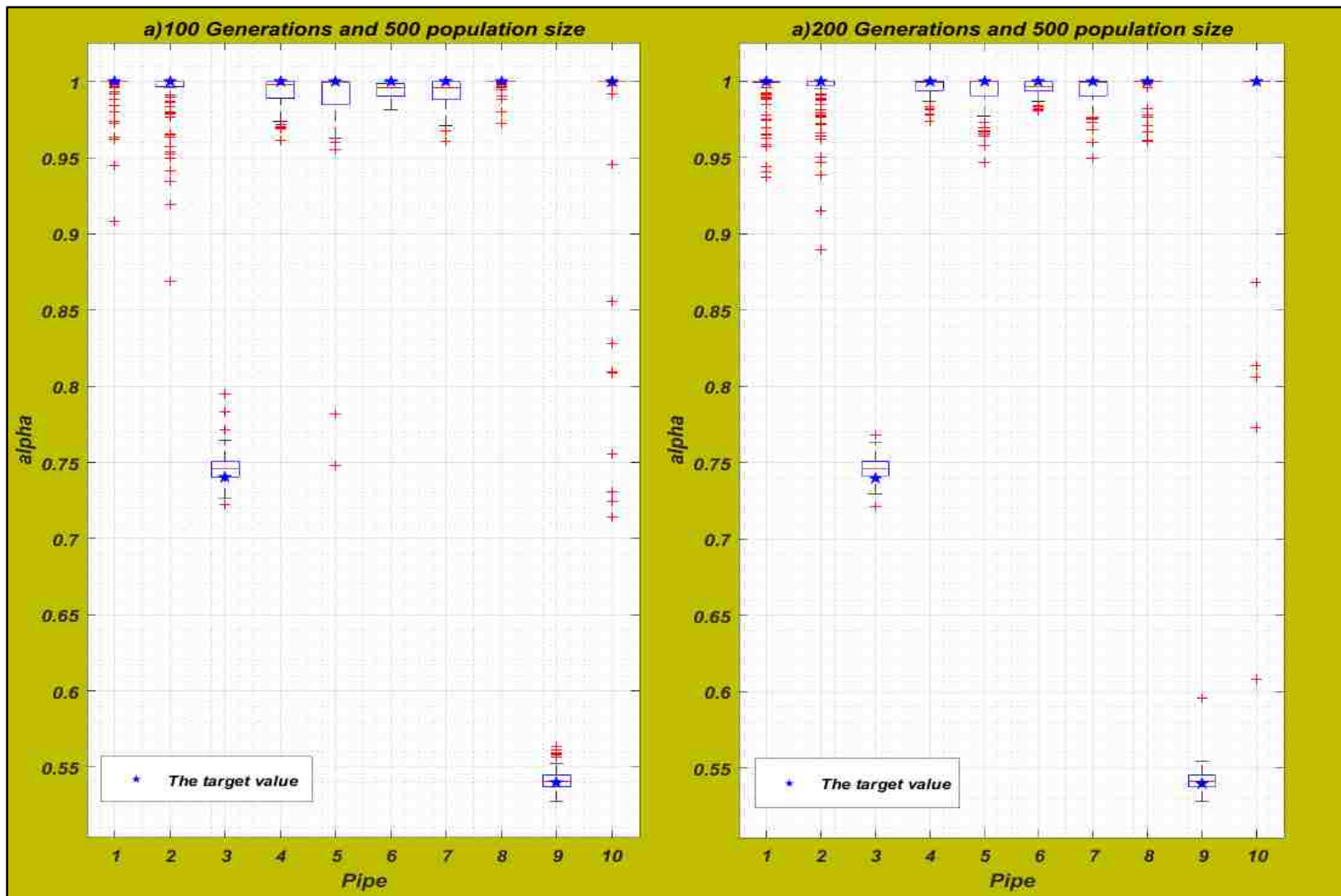
Figure 4.15: Statistical analysis of: a) 100 generations and 500 population size, and b) 200 generations and 500 population size

100 Generations and 100 Population size									
Pipe	1	2	3	4	5	6	7	8	9	10
μ	0.99	0.99	0.75	0.99	0.98	0.99	0.99	0.99	0.54	0.98
σ	0.018	0.014	0.012	0.007	0.032	0.005	0.009	0.012	0.015	0.063
200 Generations and 200 Population size									
μ	0.99	0.99	0.75	0.99	0.99	0.99	0.99	0.99	0.54	0.99
σ	0.012	0.021	0.012	0.007	0.031	0.006	0.009	0.005	0.006	0.05
200 Generations and 500 Population size									
μ	0.99	0.99	0.75	0.99	0.99	0.99	0.99	0.99	0.54	0.99
σ	0.015	0.018	0.007	0.006	0.011	0.005	0.009	0.008	0.007	0.05

Table 4.8: Results of the statistical identification
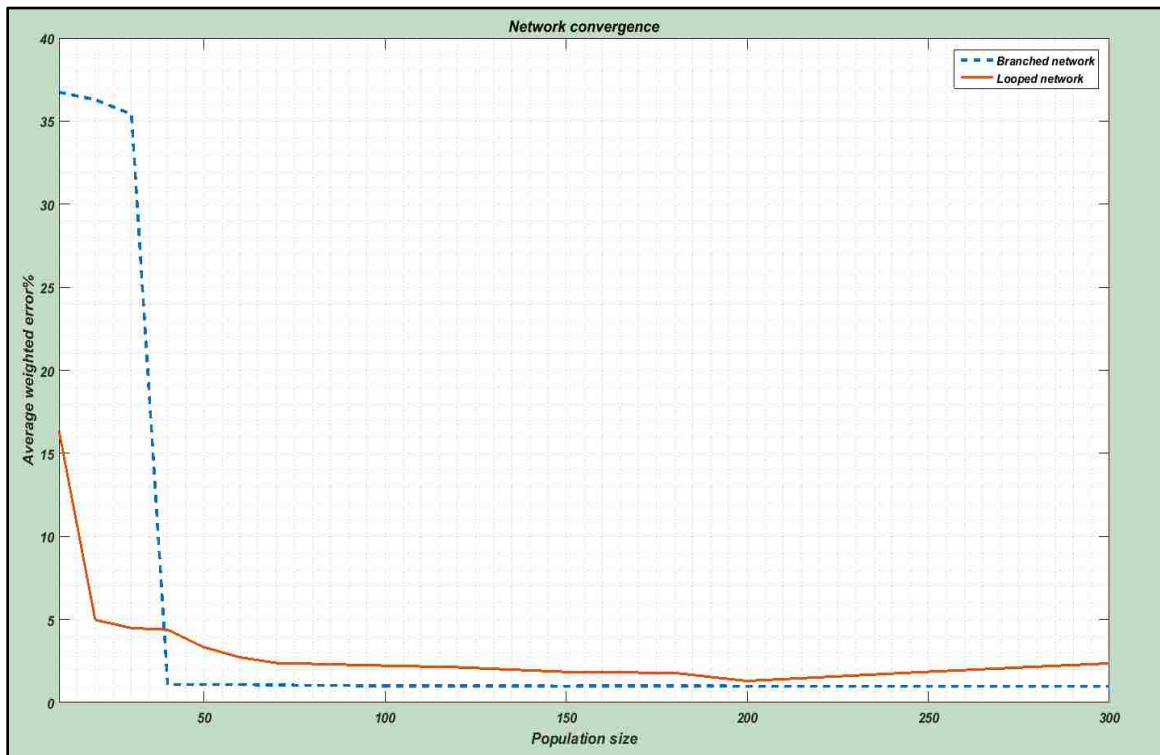
Figure 4.16: Comparison of the average weighted error and population size for looped and branched network

The results showed that the increase in the number of generations and size of the population led to remarkable accuracy, but it required a lot of time. It can be noticed from the box plots and Figure 4.16 that as the number of generations and population size increased, a better degree of convergence in accuracy was met. Also, Table 4.8 shows that with an increase of generations and population numbers, the results tended to the exact target values with a very low dispersion (see the highlighted values). In conclusion, the selected objective function, the structure of the considered network, the number of generations and the population size played a great role in the accuracy and sensitivity of the proposed technique. The suggested methodology was able to identify the two obstructed pipes without false positives and with notable accuracy in the examined network.

CHAPTER 5

ANALYSIS OF THE EFFICIENCY AND THE LIMITATION OF

THE METHODOLOGY

Abstract

This chapter aims to evaluate the efficiency and applicability of the proposed methodology. A thorough study is conducted by analyzing several examples numerically. Three categories are taken into consideration to assess the effectiveness of the suggested technique; 1) the effects of the superimposed noise by adding disturbances to the measurements, 2) the missing measurements of the pipe flow and pressure head, 3) moving the pressure head measurements to the end of the pipes instead of the nodes. Results of analysis and the most relevant conclusions are outlined.

5.1 Introduction

This chapter involves three different sections of analysis to evaluate the efficiency and versatility of the proposed methodology. The first section deals with the simulated measurements of pipe flow and nodal pressure head. As mentioned earlier, in the absence of the real field data or for validity purposes, a uniform noise is considered to simulate the measurement errors. All the numerical applications described so far in this research, simulated the "empirical" measurements by imposing 5% noise on the simulated measures. In reality, noise changes from time to time, depending on the surrounding circumstances and that will lead to alter measurements slightly or significantly. For that reason, the first section of this chapter considers different values of noises. Additional disturbances are added to the measurement to provide a better understanding about the behavior and efficiency of the technique.

The second section conducts a detailed study about the collected measurements availability and importance in the entire system. The technique can be utilized even in the

case of missing measurements. However, this will affect the accuracy and efficiency of the blockage identification. It is necessary to understand the behavior of the system and which pipes have a significant impact (more weight) on the technique's effectiveness. In other words, one should understand the flow and the location of the important measurements that need to be defined.

The third section discusses a specific case when the pressure head measurements are taken at the end of pipes, instead of the nodes. In this case the successive pipes will have different pressure head measurements at their common node. A numerical study is conducted to assess the proposed technique performance in such model.

5.2 Sensitivity to Noise

In the absence of real field data, pseudo-experimental data are used. Those data are generated by adding a random noise to the theoretical values of flow and pressure head that are computed through FEM. Previously, uniform noise levels of 5% were used, which are considered to be conservative values for field measurements. Technically, the uncertainty in the instruments vary from one industry to another. Thus, the superimposed noise of 5%, might not be enough to cover these uncertainties in the experimental data. In this section, for a given scenario of blockages, it is considered a further "disruption" to be included during the simulation of the measurements. The same example described in Section 4.1.1of Chapter 4 is repeated by considering different levels of noise. The inspected scenario is characterized by obstruction of pipes 3 (60% blockage over 70% L) and 9 (50% blockage over 70% L). This study discusses several cases by increasing the noise levels, and at the same time observing the efficiency of the proposed technique. For each case, the

identification procedure is performed 30 times. The examined noise levels that have been considered are as following:

- Superimposed 10% noise level on pressure head measurements + 5% on flow

- Superimposed 10% noise level on the pipe flow measurements+ 5% on pressure heads

- Superimposed 10% noise level on both flow and pressure head measurements

- Superimposed 15% noise level on both flow and pressure head measurements

- Superimposed 10% noise level on pipe flow and 15% on pressure head measurements

The statistical analyses for all cases mentioned above are presented graphically via a Box-and-Whisker plot in the following figures. Also, the standard deviation σ for all pipes in each scenario of superimposed additional disturbance is reported in Table 5.1. The numerical analysis proved that the proposed technique was able to identify the blockage with a reasonable degree of accuracy by adding noise levels up to 10% as shown in Figures 5.2, 5.3 and 5.4. In the last two cases, however, when the noise reached up to 15%, the results showed high dispersion, as presented in Figures 5.5 and 5.6. Overall, it can be concluded that the methodology is able to identify the exact value of the obstructions if the range of superimposed noise is between 5% and 10% in total. Figure 5.7 shows the average weighted error in terms of residual diameter for each examined case. It can be seen clearly that the last two cases (i.e., noise $\geq$ 15%) give the highest error. Thus, the efficiency of the proposed technique is limited with 10% superimposed noise, which is considered to be realistic values for field measurements.

Figure 5.1: The statistical analyses with superimposed 5% noise levels on measurements

Figure 5.2: The statistical analyses by adding 10% noise levels to the pressure head measurements

Figure 5.3: The statistical analyses by adding 10% noise levels to the flow measurements

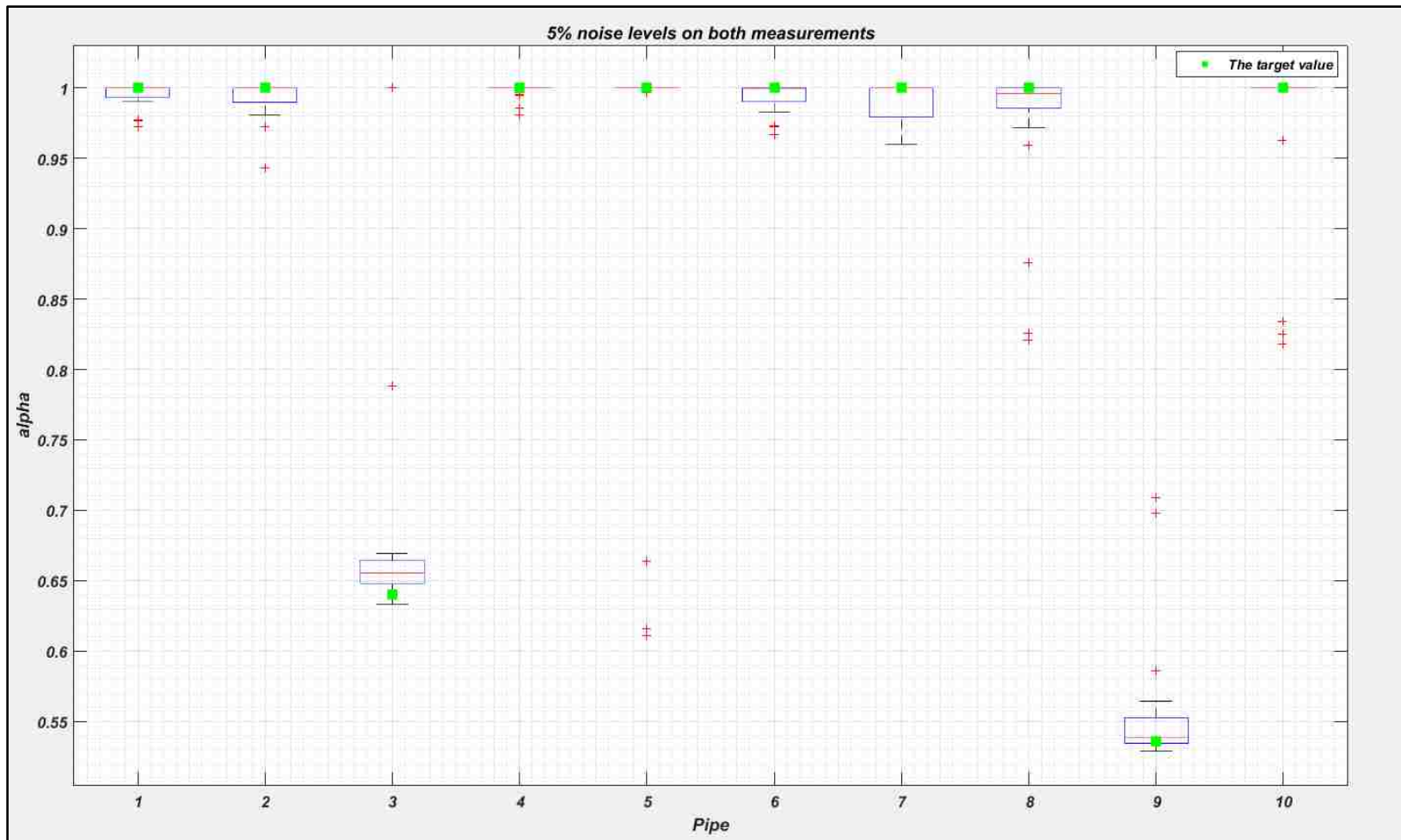*Figure 5.4: The statistical analyses by adding 10% noise levels to the measurements*

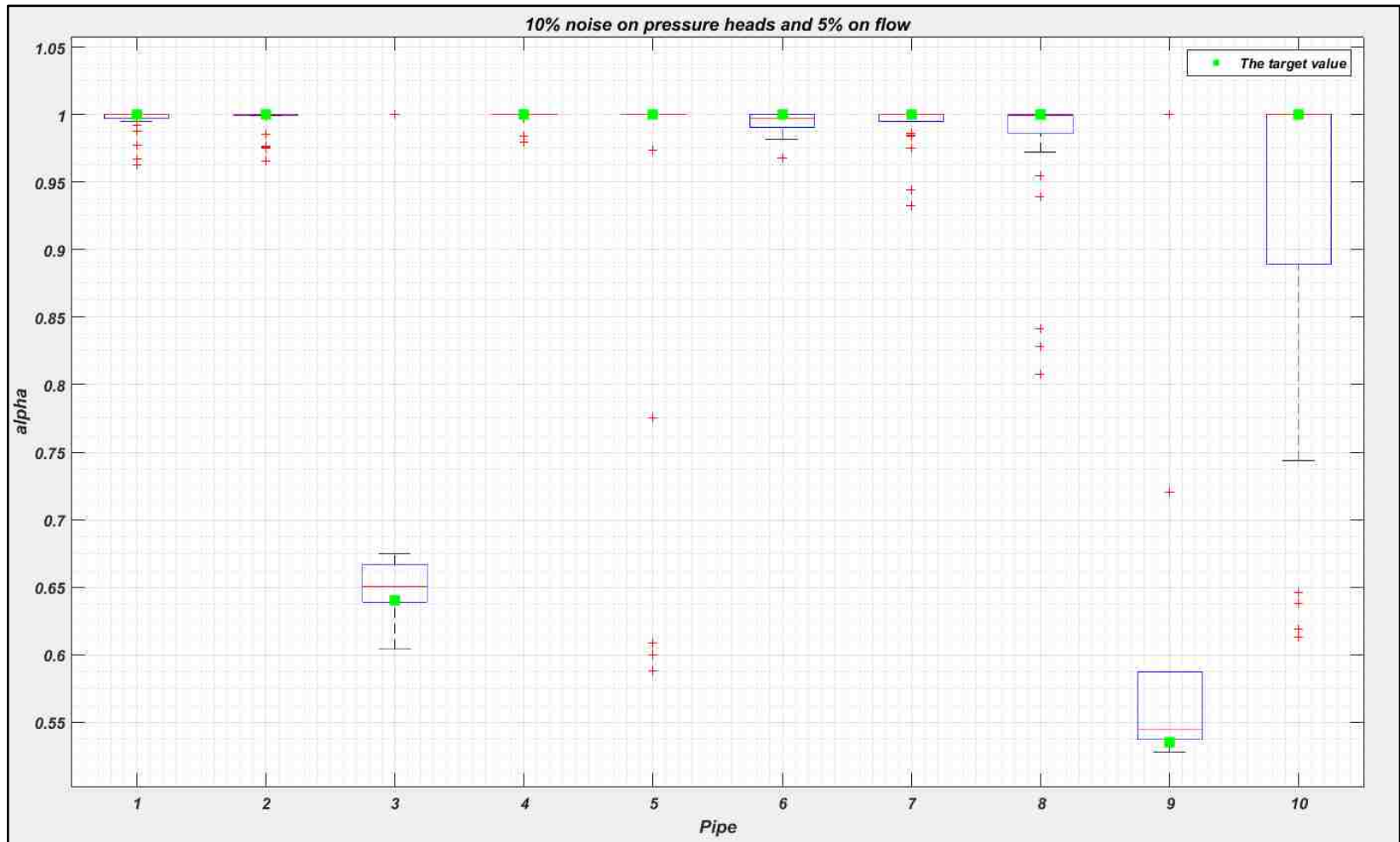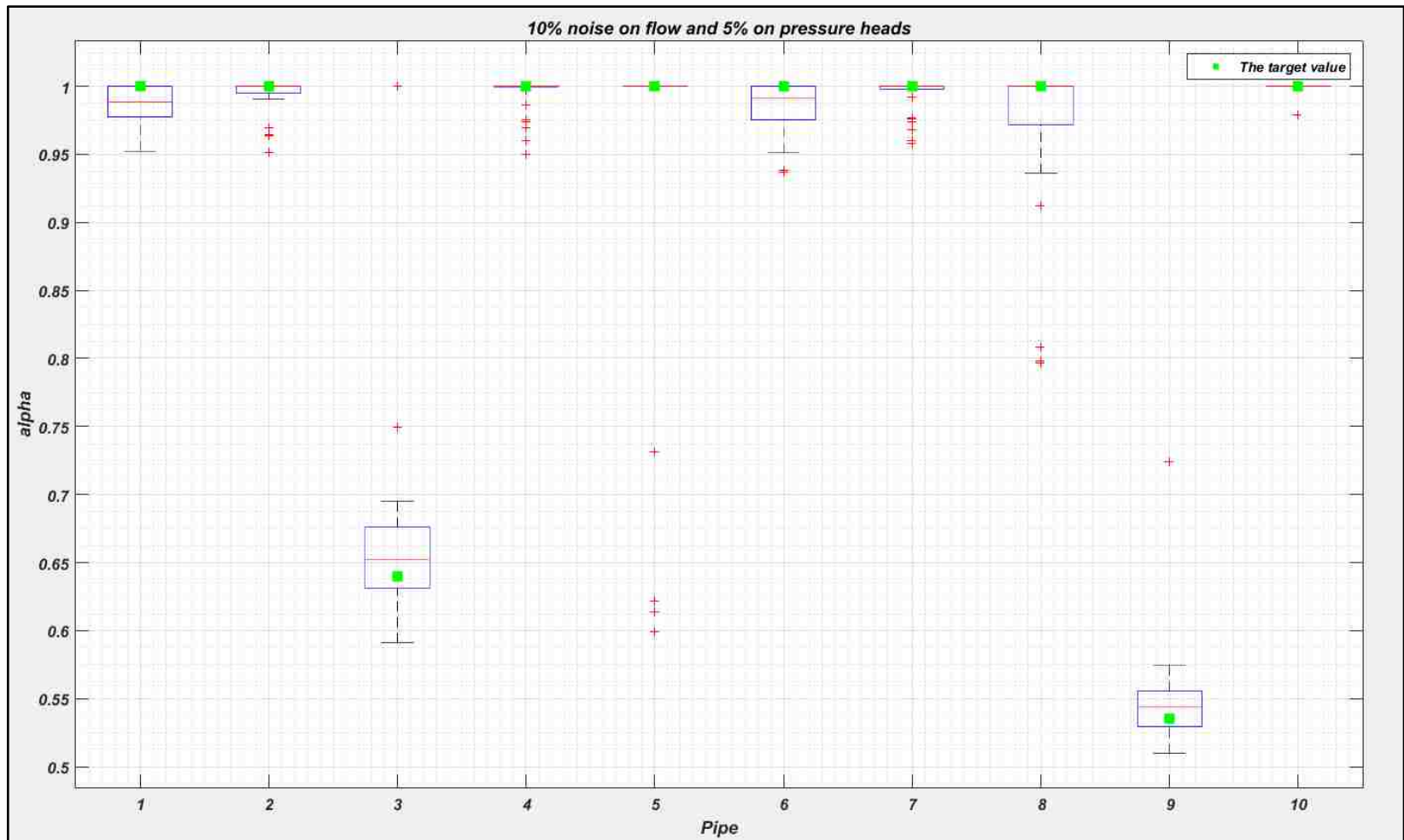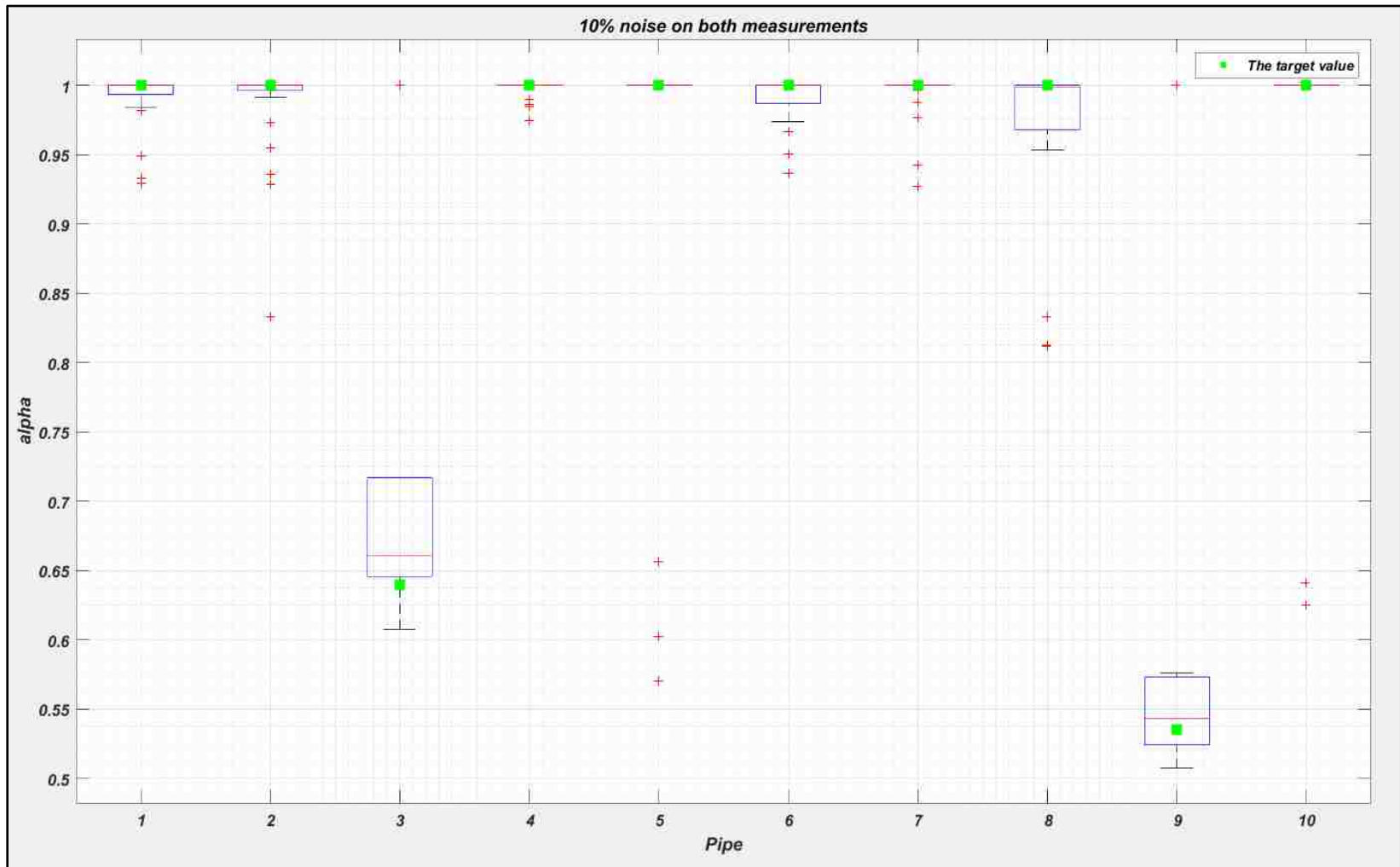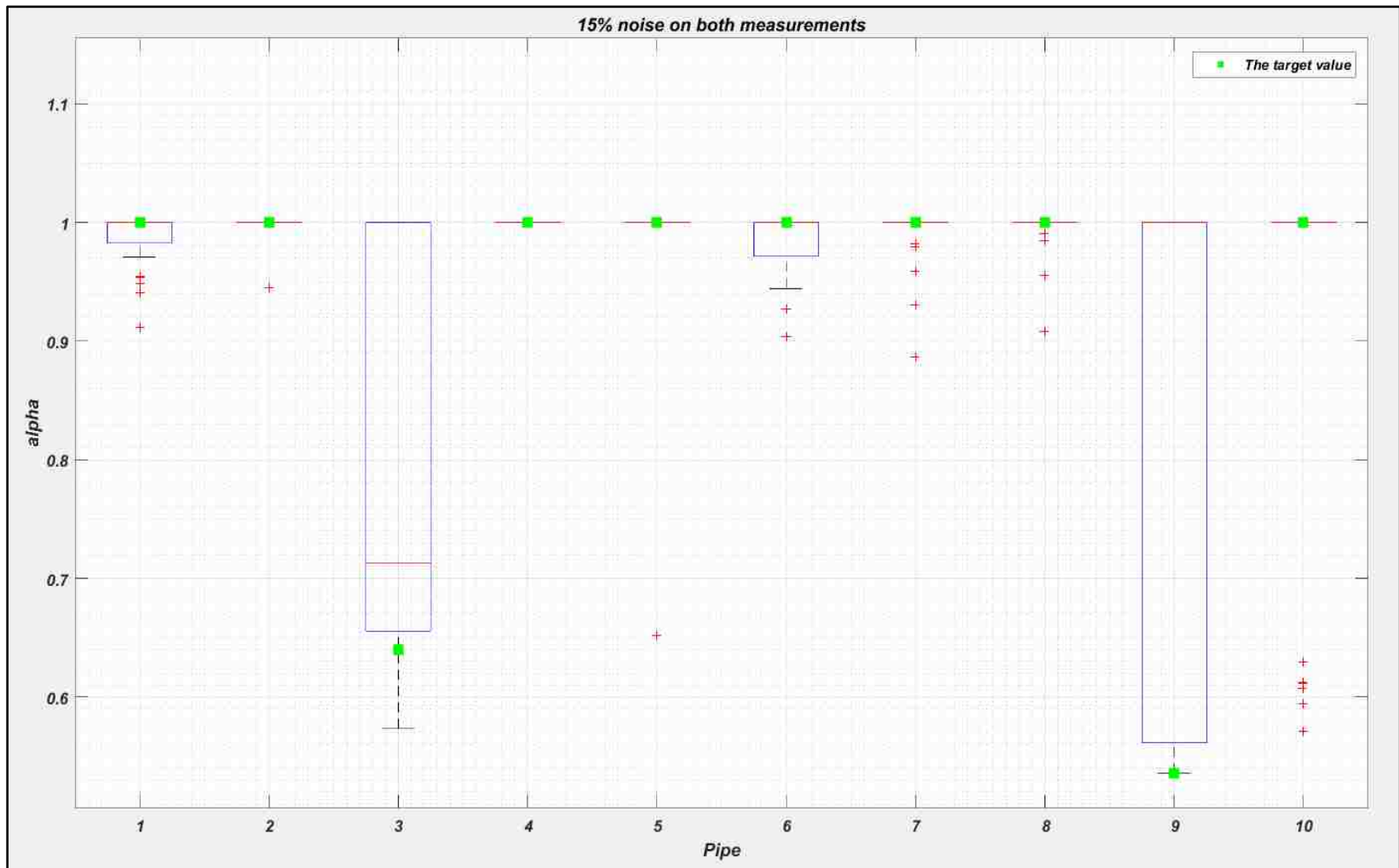*Figure 5.5: The statistical analyses by adding 15% noise levels to the measurements*
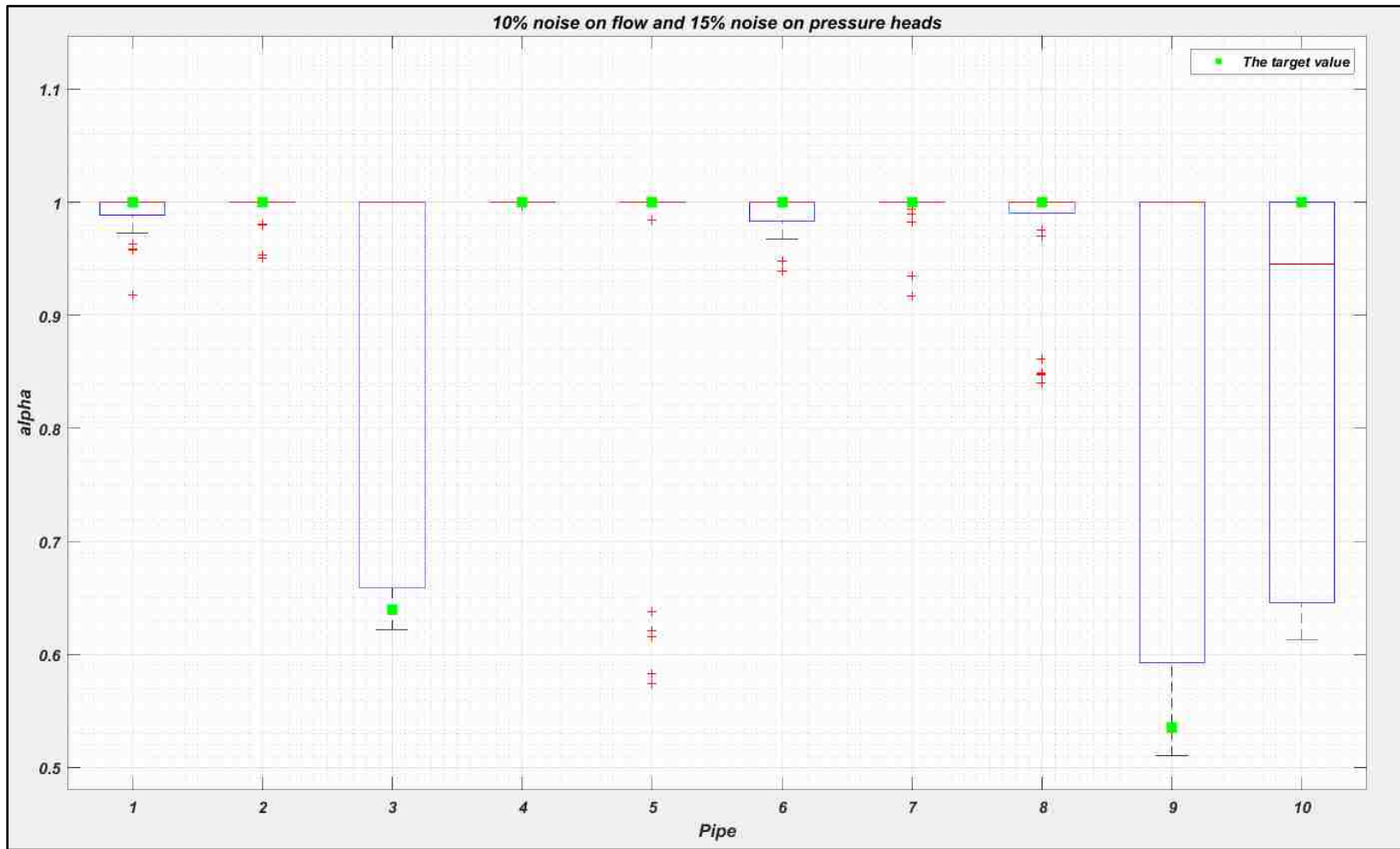
Figure 5.6: The statistical analyses by adding 10% noise levels to the flow measurements and 15% to the pressure head measurements

	5% uniform noise levels									
Pipe	1	2	3	4	5	6	7	8	9	10
$\sigma\%$	0.76	1.21	12.09	0.45	11.31	0.93	1.32	4.83	4.26	5.32
	10% noise levels on pressure heads and 5% on flow measurements									
$\sigma\%$	0.97	0.95	13.44	0.47	12.64	0.75	1.62	5.30	18.51	14.50
	10% noise levels on flow and 5% on pressure heads on measurements									
$\sigma\%$	1.50	1.32	12.47	1.36	12.55	1.89	1.31	6.10	3.70	0.39
	10% noise levels added on both measurements									
$\sigma\%$	1.92	3.46	14.89	0.59	11.96	1.57	1.69	5.43	18.86	9.30
	15% noise levels added on both measurements									
$\sigma\%$	2.32	1.00	17.29	0	6.35	2.72	2.47	1.85	22.10	16.12
	10% noise levels added on the flow measurements and 15% on the pressure heads									
$\sigma\%$	1.88	1.29	17.20	0.072	14.93	1.68	1.89	5.68	20.51	17.10

Table 5.1: Results of statistical analyses for different noise scenarios

Figure 5.7: Comparison of average weighted error of examined scenarios

5.3 The Unavailable Flow and Pressure Head Measurements

As stated earlier, the proposed technique is able to identify the blockage even with a limited number of measurements. In other words, the methodology can cope with some missing measurements of the pipe flow and nodal pressure head. In general, the more measures are available, the more accurate and reliable results can be reached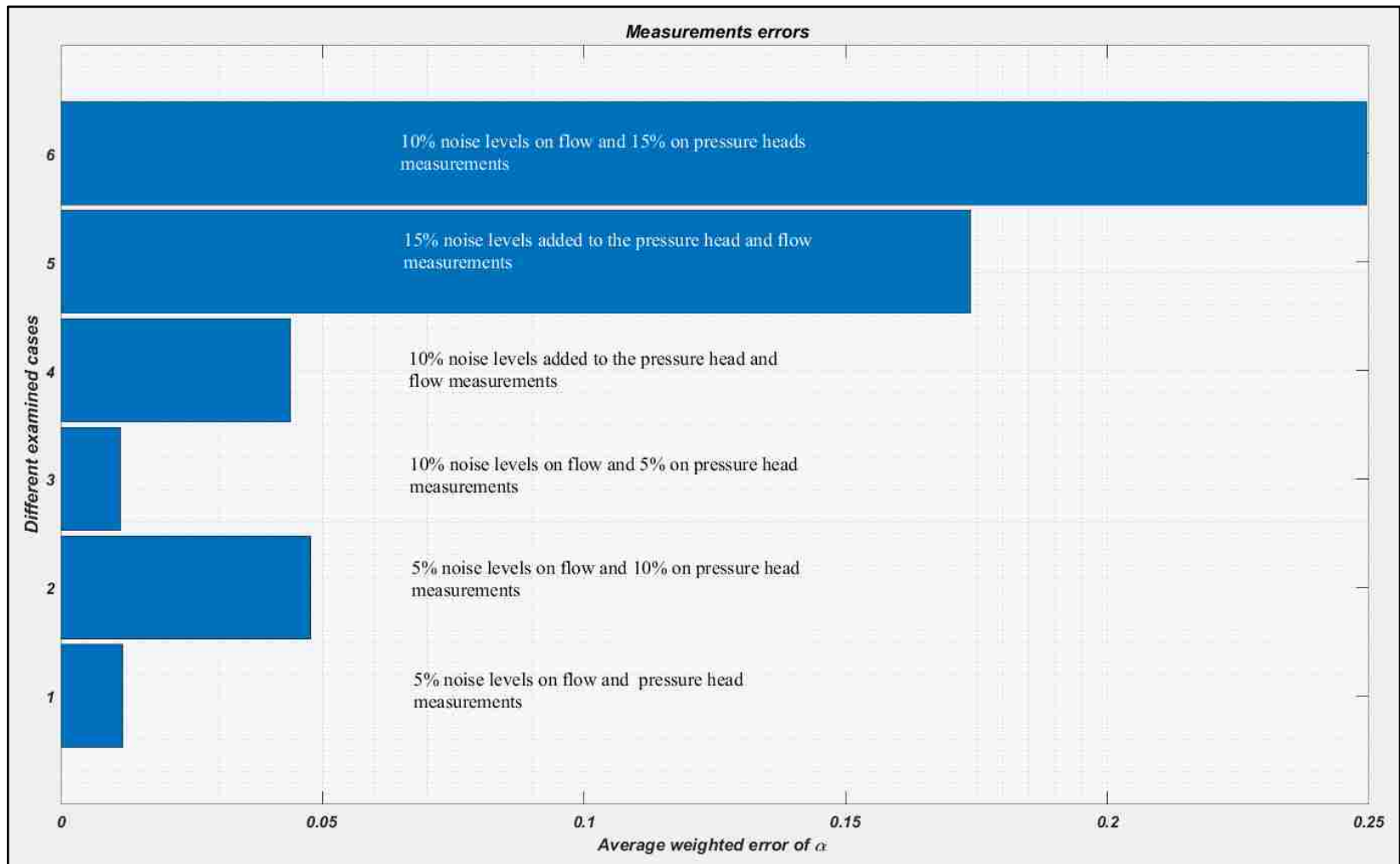. Also, the importance and needs of the available measurements are different from one scenario of blockage to another. Thus, it is necessary to understand how each pipe affects the other pipe flows. One needs to capture the correlation in the whole system, and to figure out how strongly or weakly the presence of blockage in a specific pipe can influence on other pipes behavior. When one understands this, it becomes an easy task to recognize in which pipes and nodes the measurements are required. So far in all the previous examples, it was assumed that some measurements in the network were randomly unavailable. To evaluate the importance of the measurements, the same numerical example described in Section 4.1.1of Chapter 4 is used here. In this context, the measures of flow and pressure which appear to be more sensitive to a given obstruction can be emphasized through simple recursive direct analyses. Numerically, we computed the percentage change in the volumetric flow rate of the network for a given blocked pipe, and how it can be correlated with other pipes via the following formula:

$$\Delta Q_i = \left| \frac{Q_i^B - Q_i}{Q_i} \right| * 100 \qquad i = 1, 2, \ldots \ldots \ldots pipes\ number$$

Where Q_i are the pipe flows in the clean network (i.e., without any blockage), whereas Q_i^B are the pipe flows computed by considering only one pipe blocked. Several values of α are taken into the consideration for each pipe (i.e., $\alpha = 0.8, 0.7, 0.6\ and\ 0.5$). The results are

shown in Figure 5.8. Similarly, the same procedure has been repeated with nodal pressure heads by using this formula:

$$\Delta h_n = \left| \frac{h_n^B - h_n}{h_n} \right| * 100 \qquad n = 1, 2, \ldots \ldots \ldots nodes\ number$$

Where h_n are the nodal pressure heads in the clean network (i.e., without any blockage), whereas h_n^B are the nodal pressure heads computed by considering only one pipe blocked. The results are shown in Figure 5.9. The red circles in the Figure show the imposed nodal pressure heads, which are not affected by the presence of blockages (i.e., the boundary conditions location). It can be seen from Figure 5.8 when $\alpha = 0.8$ and 0.7, the blockage in pipes 1 and 2, for example, generates variations of flows in pipes 1, 2, 7 and significant variation in pipe 3. Also, Figure 5.9 indicates that the blockage in these pipes creates a remarkable variation in the pressure head at node 2. Thus, the efficiency of the proposed technique to identify the blockage in those pipes is linked strongly to the availability of the flow measurements at pipes 1, 2, 3 and 7, along with the pressure head at node 2. The results of the blockage identification with a 30% blockage over 70% L obstruction in pipe 2 with different scenarios of missing measurements are summarized in Figure 5.10.

By looking at Figures 5.8 and 5.9, it is easy to infer which pipes are more sensitive to the presence of obstructions in the network. These analysis can provide insight for the monitoring of the entire behavior of such system. Therefore, through this analysis it is possible to know exactly which measurements of flow and pressure head should be good to monitor in order to confirm the presence of an occlusion in a certain pipe.
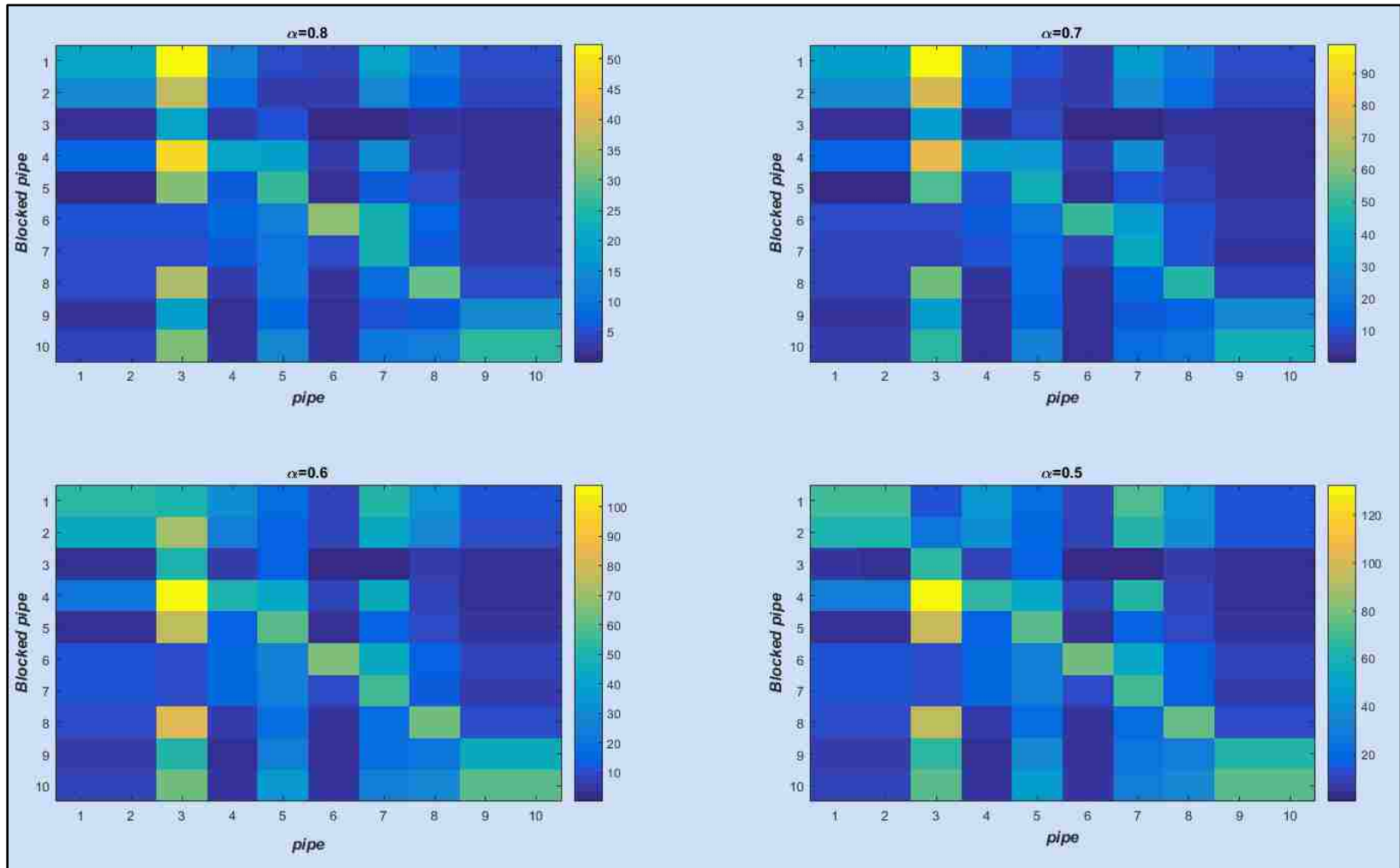
Figure 5.8: Percentage change in the volumetric flow rate in the pipes of the network for a given obstructed pipe
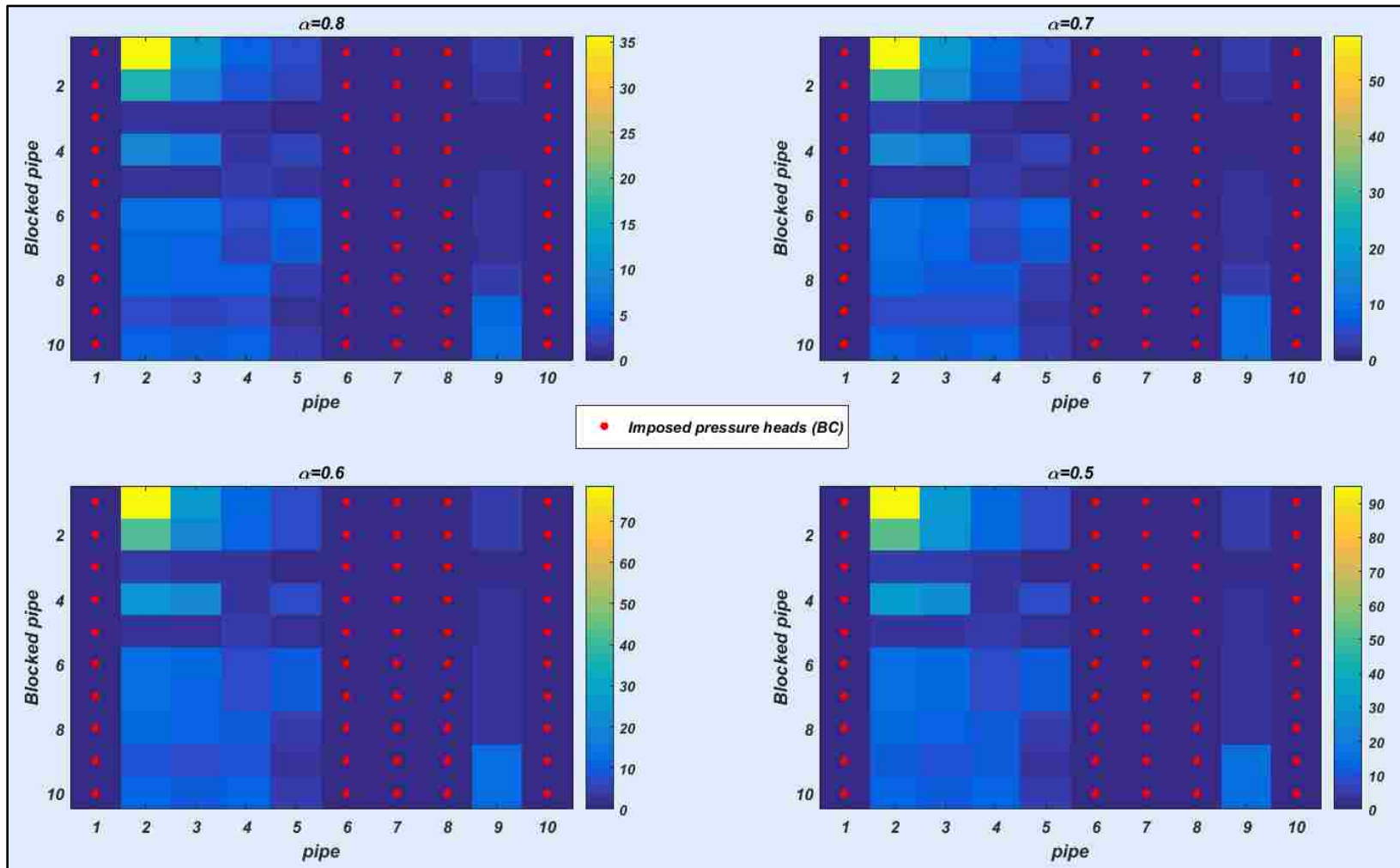
121

Figure 5.9: Percentage change in nodal pressure heads of the network for a given obstructed pipe
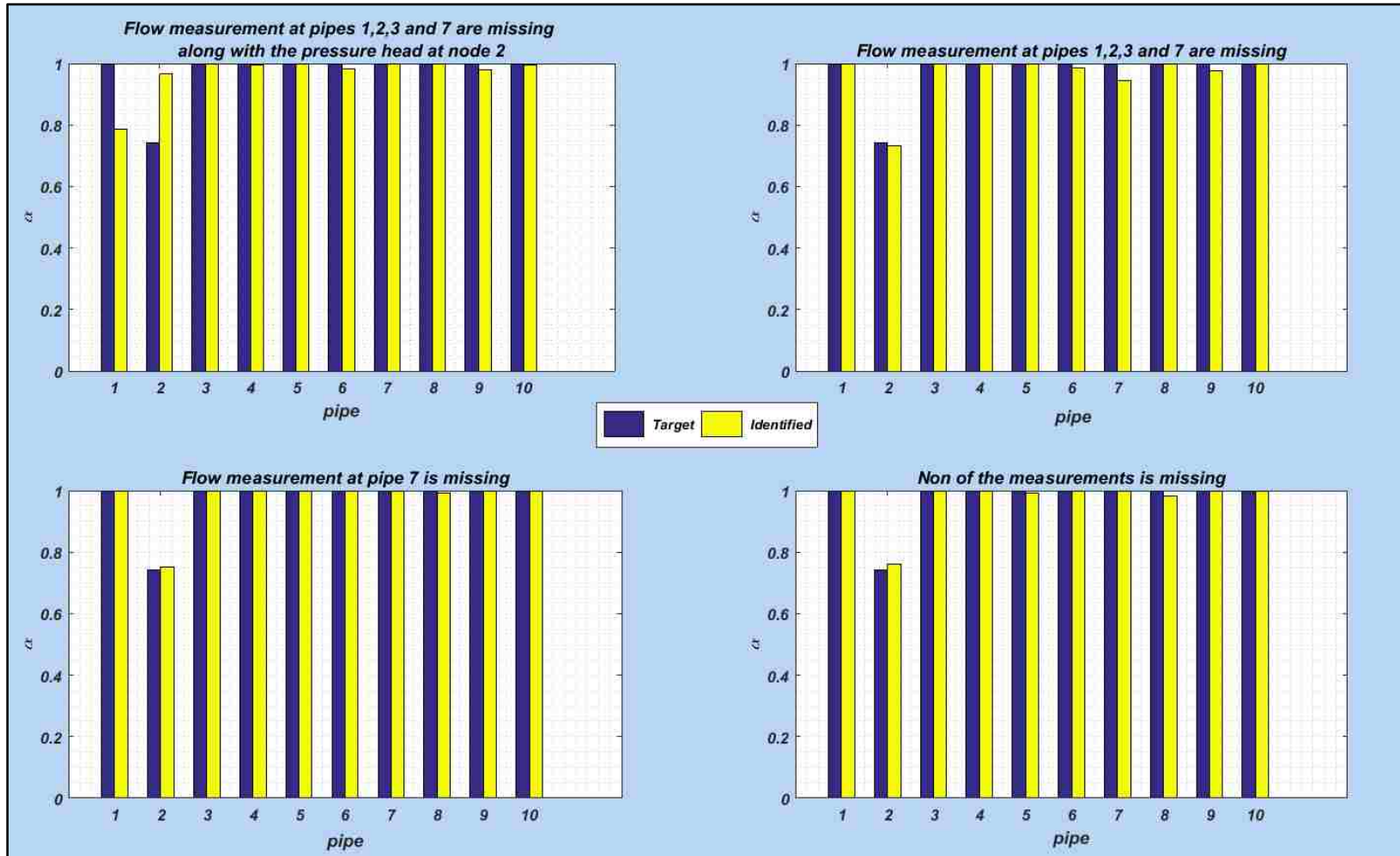
Figure 5.10: Blockage identification at pipe 2 with different scenarios of missing measurements

5.4 Suggested a Modeling Approach by Moving Pressure Head Measurements to the End of Pipe

There are different types of the pipeline networks (i.e., complex, simple, looped and branched). Each pipe is linked to another pipe via a node (junction) to build the entire network. Depending on the topology of the network, these intersections can take any shape (i.e., tee, wye or elbow in any angle) and there are different loss coefficient associated with each type. The pipeline networks can vary from few pipes to thousands of pipes. Thus, the number of intersections can vary in the same way. The presence of these intersections causes minor losses in the pressure head measurements due to change in momentum of the flow, due to friction through the system. These losses may vary depending on the type of components used in the network, material of the pipe and type of fluid flowing within the system [Vasava, 2007]. In fact, the pressure head measurements can be affected by following:

- Sudden expansion or contraction in pipeline

- Bends, elbows, tees, and other fittings

- Control valves

- Pumps and turbines

As a result, the existence of these components causes loss in the pressure measurements and therefore it will affect the accuracy of the proposed technique. As mentioned earlier, the suggested methodology depends directly on the nodal pressure heads. However, in some cases, it is difficult to measure the pressure head at the node as it was discussed Chapter 3. Through the experiments, the pressure head measurements were taken approximately 2-3 inches from the node, as illustrated in Figure 5.11; an attempt was

made by taking the average value of these measurements to minimize the generated errors. Nevertheless, the results of the blockage identification presented false positives.

This section presents a new strategy to improve the efficiency of the methodology. Each point on the pipe where the pressure head measure is taken is labeled as a "node", whereas the original connection among pipes is still considered a node but with missing measurements. In other words, we considered additional points as "pseudo-nodes" which are located at 2-3 inches from the primary node. This Section describes an attempt to improve the results of the identification procedure and the efficiency of the proposed technique when it is difficult to measure the pressure head at the node directly.

In order to discuss this issue, a simple numerical network has been simulated with a 5% noise level. The network consists of 8 PVC pipes (2 inches in diameter) and 11 nodes, as shown in Figure 5.12. Node 1 is the station where the fluid is collected and nodes 8 and 11 are pits where the fluid is introduced in the network. Piezometric heads of 10, 15 and 20 m are imposed at nodes 1, 8 and 11 respectively. The blockage scenario is characterized by the obstruction of pipes 2 (30% of 70% L) and 9 (60% of 70% L). The flow measurements are collected at all pipes, except at pipes 6 and 9, whereas the pressure head measure is missing at node 5. The pipes are connected to each other through wye section. It is difficult to measure the pressure head at this node, thus instead, the measurements of the pressure head are taken at the end of the pipes that are close to the node (about 10 cm from the node). These new points where the pressure measurements are taken are labeled as "pseudo-nodes" in the code, as shown in Figure 5.13.

During the experimental work that was presented in Chapter 3, the measurements of the pressure head were taken on the pipe itself, at points close enough to the actual node.

The nodal pressure head was found by computing the average value of the pressure head of the pipes connected to this node. However, this operation might produce error, instead of minimizing the error. By looking at the results of the pipe flow and pressure head in Figure 5.14, it can be seen that the average value of the pressure head at nodes 4, 6 and 9 equals **5.931m**, which is much larger than the pressure head at node 5, which equals **3.532m**. Thus, it can be deduced that the mean value of the pressure head measurements of the points surrounding a specific node *cannot* indicate the exact nodal pressure head. The results of moving the measurements at end of pipes in terms of identified residual diameters presented in Figure 5.15 show a very good response without any false positives.

Figure 5.11: Pressure head measurements experimentally
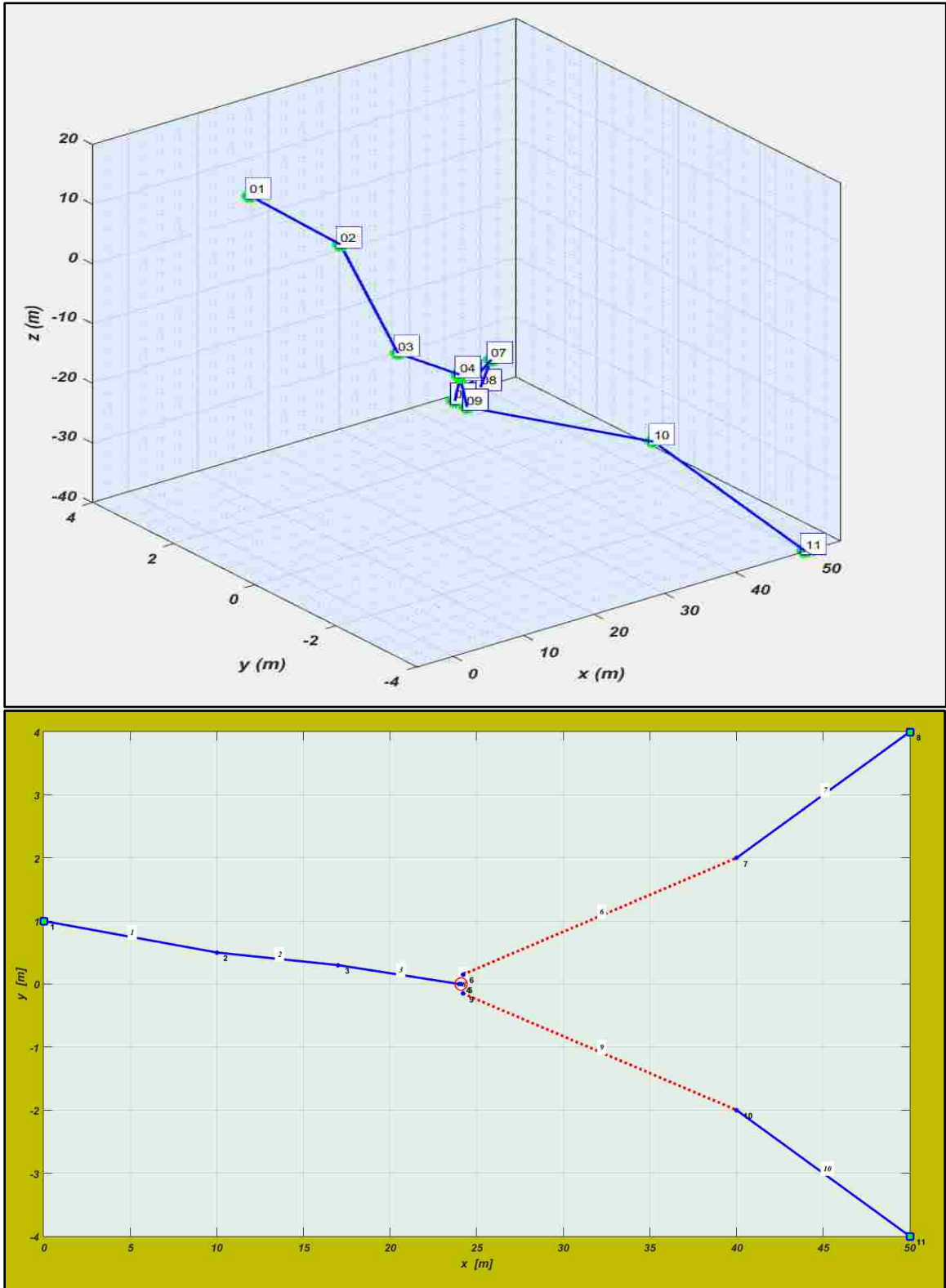
Figure 5.12: Layout of the investigated network
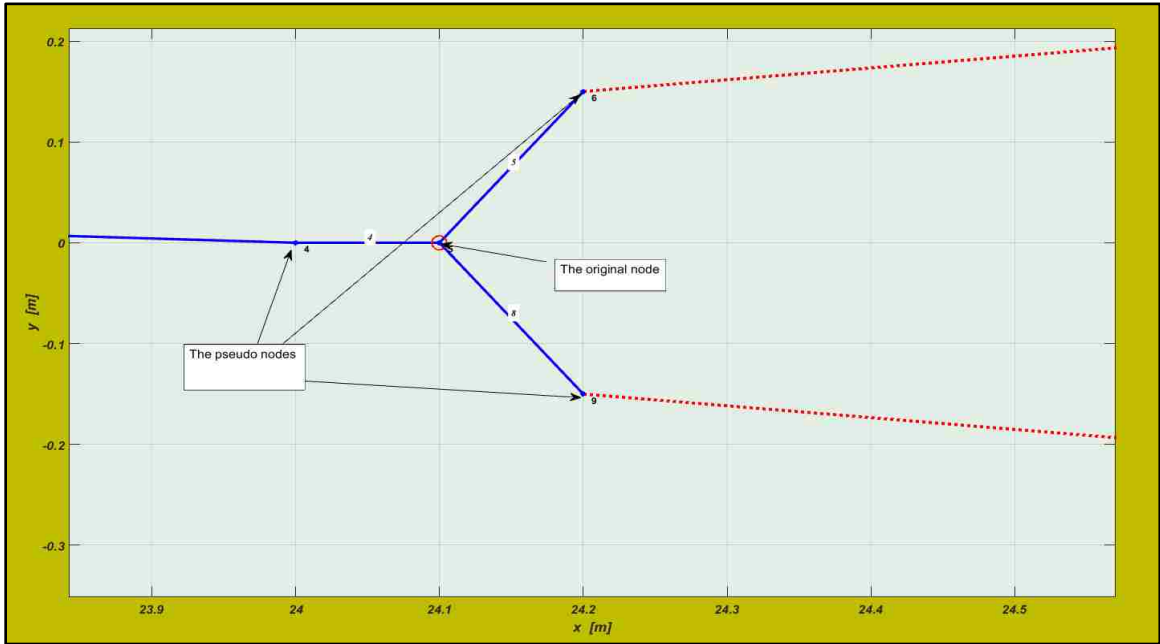
Figure 5.13: Zoomed capture to show the additional "nodes"

ALTITUDE AND PIEZOMETRIC HEAD AT NODES

nodo	z (m)	h (m)	HGL(m)
1	20	10	30
2	10	13.82	23.82
3	-10	2.014	-7.986
4	-15	3.2549	-11.745
5	-15.5	3.5323	-11.968
6	-20	6.5395	-13.461
7	-25	6.0122	-18.988
8	-40	15	-25
9	-20	7.9983	-12.002
10	-25	5.1367	-19.863
11	-40	20	-20

FLOW IN PIPES

pipe	node i	node j	Q (m^3/s)
1	1	2	0.0056521
2	2	3	0.0056521
3	3	4	0.0056521
4	4	5	0.0056521
5	5	6	0.004922
6	6	7	0.004922
7	7	8	0.004922
8	5	9	0.00073008
9	9	10	0.00073008
10	10	11	0.00073008

Figure 5.14: The simulated measurements of the flow and nodal pressure heads

128
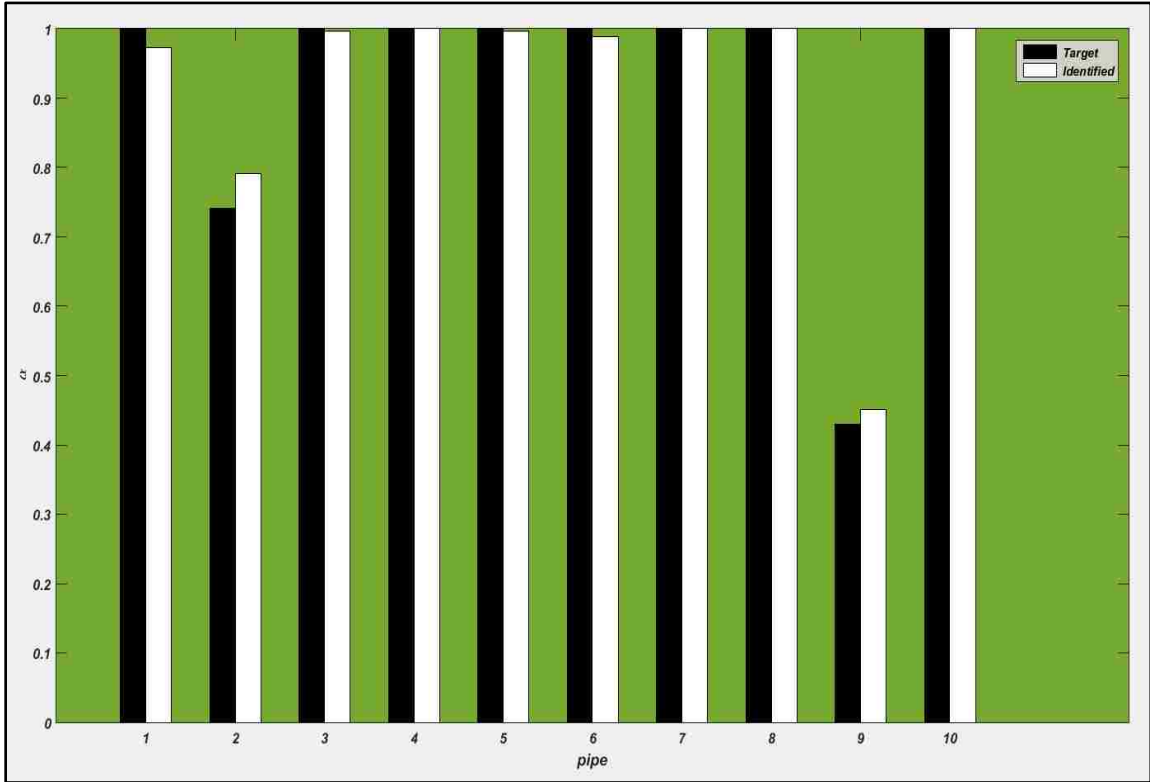
Figure 5.15: Results of the blockage identification procedure

In order to confirm that the moving of the pressure head measurements at the end of pipes instead of nodes can lead to better accuracy in blockage identification, the same network is evaluated under two cases: 1) define the end points (i.e., 4, 6, and 9) of the pipes where the pressure head measurements are taken as "pseudo-nodes"; 2) taking the average value of pressure head measurements at these points and considering it as the pressure head value at the intersection node (i.e., node 5). The proposed technique was applied again by considering that the real measures are available. The pseudo-experimental data are determined through the following formulas, which are described in details in Chapter 2. The computed data are presented in Table 5.2.

$$Q^{exp} = Q^C\left(1 + nl_Q \cdot \beta_p^Q\right) \forall p \quad and \quad h^{exp} = h^C(1 + nl_h \cdot \beta_n^h) \forall n$$

Pseudo-experimental pressure head measurements (case 1)										
Node	1	2	3	4	5	6	7	8	9	10	11
h(m)	9.35	15.23	1.95	3.35	3.63	6.63	6.35	15.10	7.86	5.47	19.31

Pseudo-experimental pressure head measurements (case 2)							
Node	1	2	3	5	7	8	10	11
h(m)	9.35	15.23	1.95	5.95	6.35	15.10	5.47	19.31

Table 5.2: Comparison of the pseudo-experimental pressure heads

Table 5.2 shows that the pressure head at node 5 in the second case, which was found by taking the average value of the pressure head at nodes 4, 6 and 9 of the first case, is much greater than the pressure head at node 5 in the first case. It is expected that the first case leads to better results compared to the second case, as shown in Figure 5.16. The more measures are available, the more accurate and reliable the results can be.
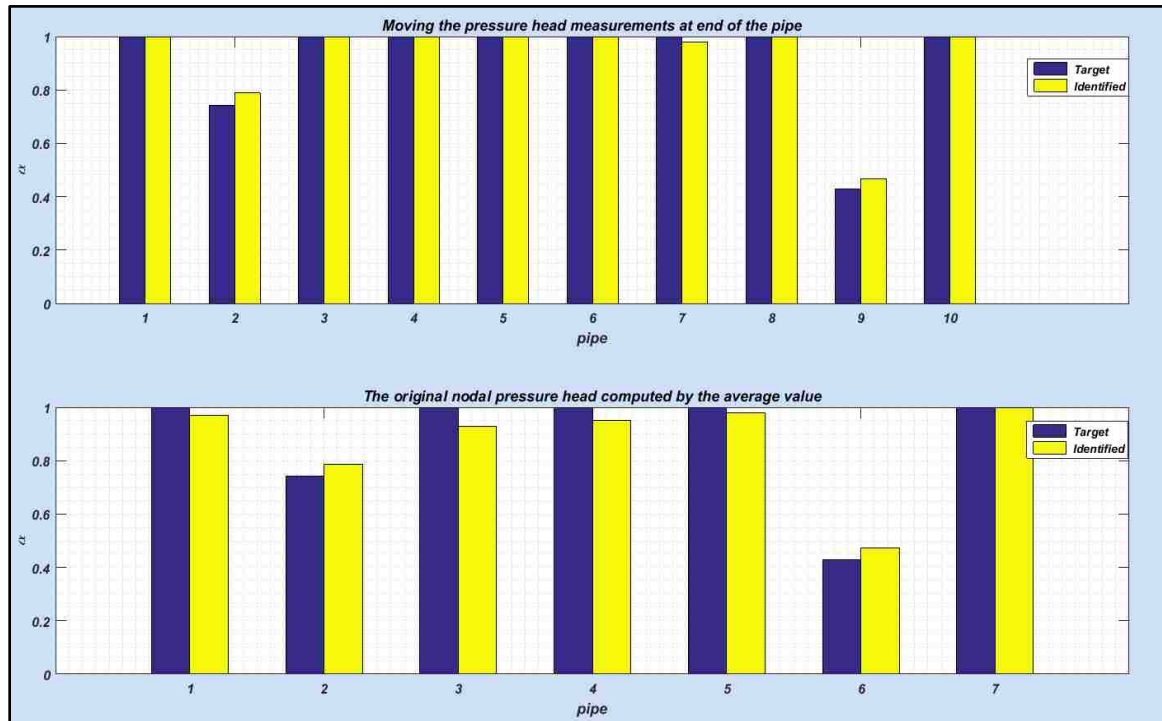

Figure 5.16: Results of blockage identification

For such simple network, it is hard to see big differences in terms of the identified residual diameters. The difference in the results will be more apparent when the large-scale network is used. In the large-scale network, the drop in pressure head measurements will be significant; therefore, the benefits of this strategy (moving the pressure head to the end of pipes, instead of nodes) that addressed above will be noticeable.

The looped network analyzed and described experimentally in Chapter 3 was analyzed again by considering the issue indicated in this section. The investigated scenario is characterized by inserting blockage in pipes 2 (25% of 70%L) and 9 (25% of 70%L). The looped network example is simulated again by labeling each point where the pressure head measure was taken as a "pseudo-node" with known measurements and marking the original node as a node with missing measurements. Since more measurements are available, it is expected to have a better accuracy in terms of blockage identification. The new network with extra nodes is presented in Figure 5.17. It can be seen that the new network has 16 further nodes in addition to the original nodes (point of intersection of the pipes).

The results of the blockage identification in such scenario are described in Figure 5.18. The new modeling approach improved the results with a remarkable accuracy and removed the false positives compared to the results in Chapter 3 for the same network, as shown in Figure 5.19. As it can be seen the examined network is complex, and it consists of many junctions (Tee, Wye and Elbows). The complexity in such network led to make the result of the blockage identification in pipe 29 not very accurate (it introduced with 10.223% error). In fact, the tee and wye intersections located before pipe 29 make the fluid behavior unstable for a certain distance in the pipes. This issue completely affects the

accuracy and efficiency of the methodology since the proposed technique requires the fluid to be steady state.

It can be concluded that the modeling approach by moving the pressure head measurements at end of pipes by introducing "pseudo-nodes" is a useful strategy to improve the results and remove the false positives when there is a difficulty in taking the measurements at the original node.
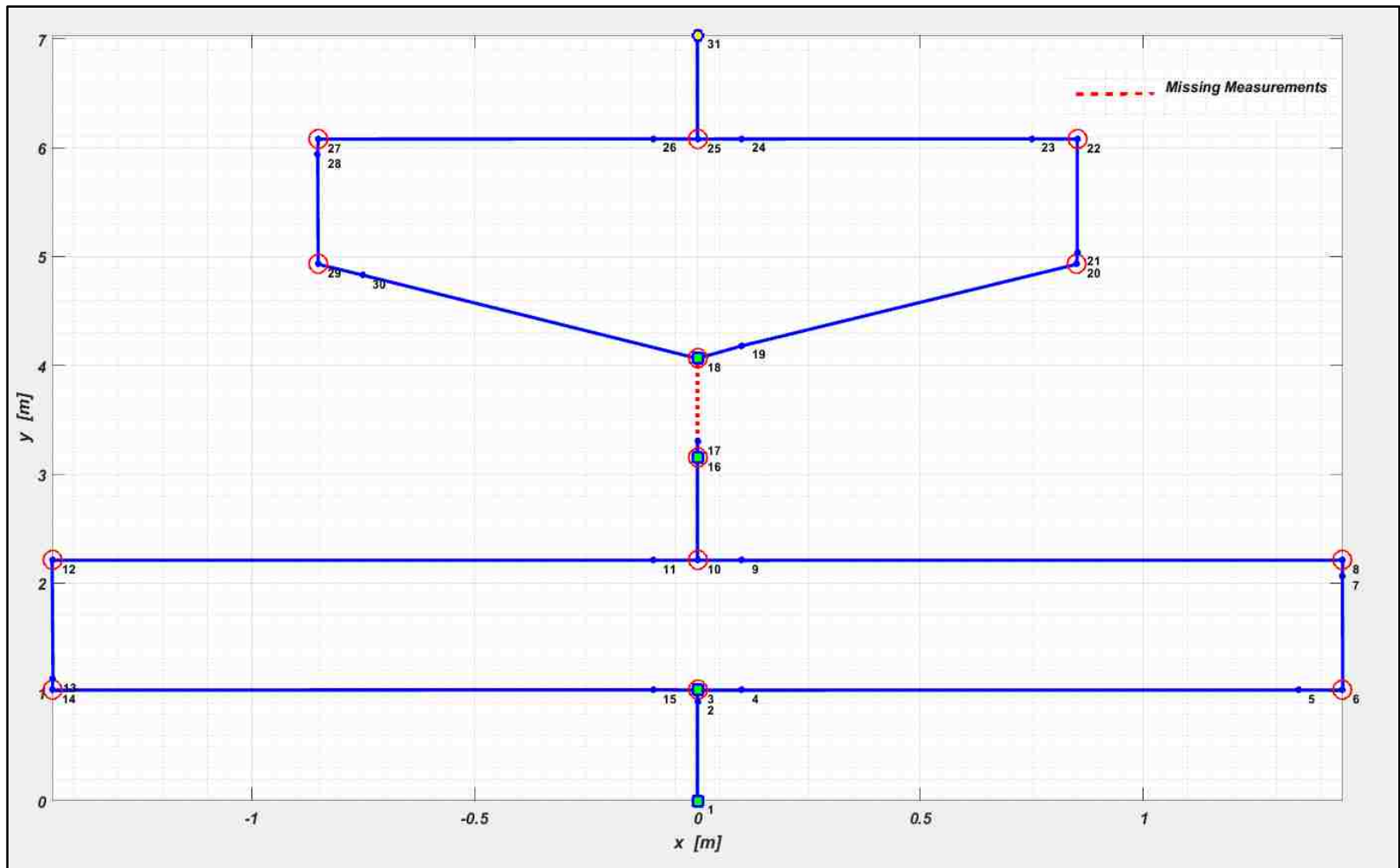
Figure 5.17: The network layout
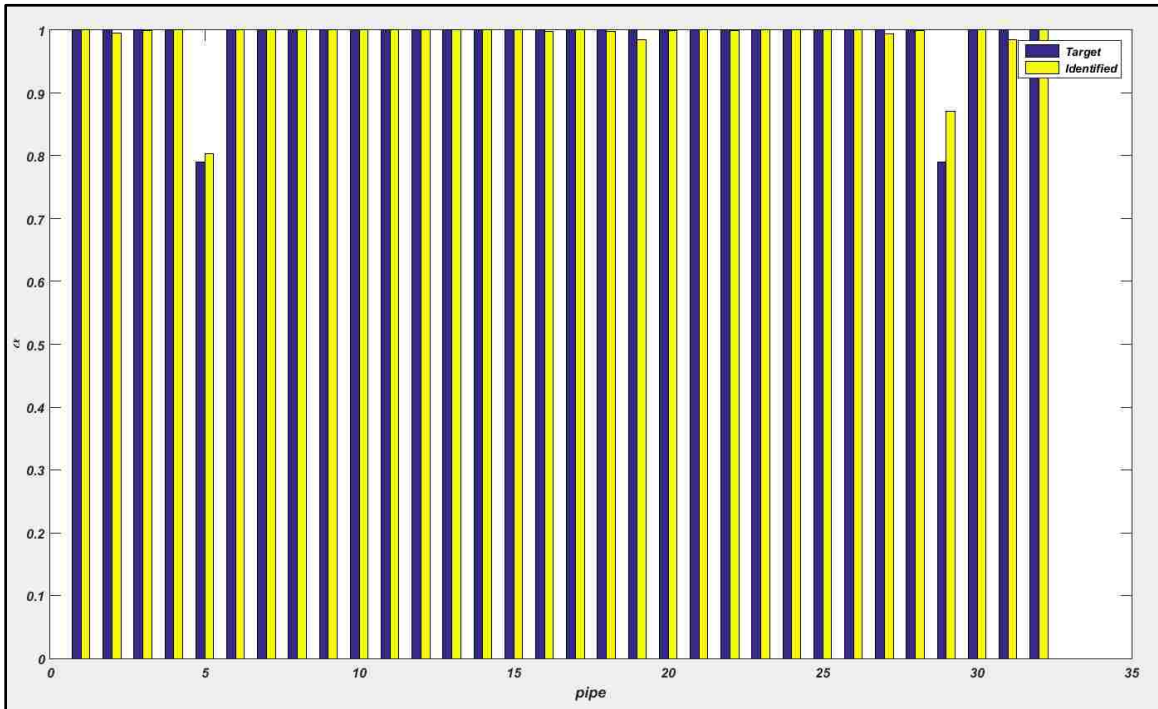
pipe	alpha real	alpha identif.	error %
1	1	1	0
2	1	0.99479	0.52147
3	1	0.99976	0.024414
4	1	1	0
5	0.79	0.80357	1.7172
6	1	1	0
7	1	1	0
8	1	1	0
9	1	1	0
10	1	1	0
11	1	1	0
12	1	1	0
13	1	1	0
14	1	1	0
15	1	1	0
16	1	0.99858	0.14191
17	1	1	0
18	1	0.99816	0.18425
19	1	0.98438	1.5625
20	1	0.99949	0.051117
21	1	1	0
22	1	0.99872	0.12779
23	1	1	0
24	1	1	9.6858e-05
25	1	1	0
26	1	1	0
27	1	0.99459	0.54131
28	1	0.99901	0.099182
29	0.79	0.87076	10.223
30	1	1	0
31	1	0.98438	1.5625
32	1	1	0

Figure 5.18: The results of blockage identification
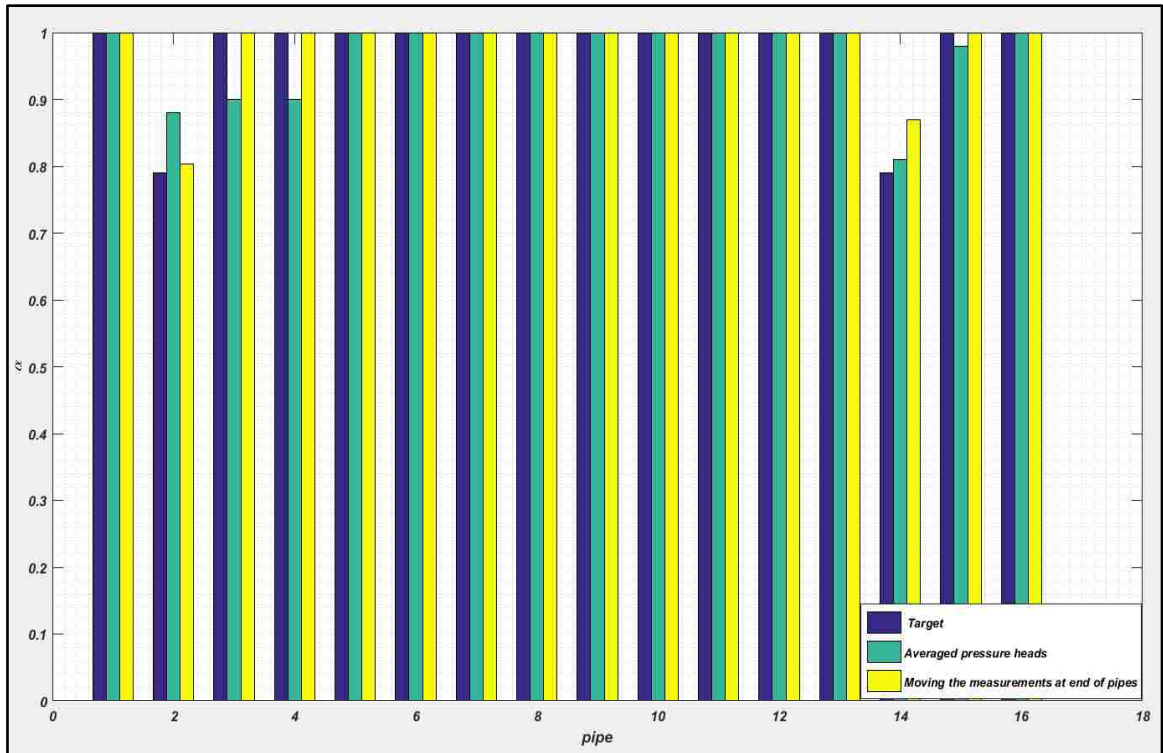
Figure 5.19: Comparison of the blockage identification results

CHAPTER 6

STUDY REAL EXAMPLES OF PIPELINE NETWORKS

Abstract

This chapter describes and analyzes two real cases of the pipeline networks. The two cases were examined by Marzani et al., [2013] and Bocchini et al., [2014] in collaboration with the sponsoring agency (the Italian National Hydrocarbon Company ENI S.p.A.). Two large-scale networks are studied by considering two different objective functions to validate the sensitivity and accuracy of the suggested methodology. A highly viscous liquid (i.e., crude oil) is used as fluid through the system to provide another proof that the proposed technique can be used with any type of fluid. The results of the analysis and the statistical data in terms of the mean and standard deviation are presented afterwards.

6.1 Introduction

To confirm the efficiency and effectiveness of the proposed technique, two real examples that were examined by Marzani et al., [2013] and Bocchini et al., [2014] are presented. Both examples contain a mixed branched-looped network, and utilize crude oil as fluid within the system. Different fitness function and blockage scenario are implemented with each example. For the identification analysis, a population of 200 individuals is used, whereas the maximum number of generations is set equal to 200. The numerical applications employ $J_1(\alpha)$ and $J_2(\alpha)$ respectively, described in Chapter 4. The γ term that is used in these functions is set equal to 17. As stated formerly, in an extensive numerical investigation, such value (i.e., γ=17) has proved to provide robustness and a good convergence ratio to the optimization procedure. Also, in order to verify the robustness of the suggested methodology, the identification procedure is performed 30 times for each example, with a superimposed constant noise of 5% in each trial. The results of the identification, the statistical data in terms of the mean and standard deviation are presented in each numerical example. The most relevant discussions and conclusions are demonstrated subsequently.

6.2 Numerical Applications

6.2.1 Description of the First Case Study

The proposed technique is applied to the artificial network shown in Figure 6.1. The network comprises 14 pipes and 14 nodes. The crude oil is extracted from the reservoirs located at nodes 6, 10, 11, 12, 13 and 14, where the pressure is imposed. The pressure head is also imposed at node 1, where the crude oil is collected. The necessary

input data of the investigated network are reported in Table 6.1. The examined scenario is characterized by inserting blockage in pipes 3 (20% blockage over 50% L), 10 (20% blockage over 60% L), 11 (30% blockage over 70% L) and 13 (30% blockage over 80% L). Flow data is collected at all pipes except pipes 5 and 14, whereas the nodal pressure head is measured at all nodes except 6 and 11.

The results in terms of identified residual diameters are illustrated in Figure 6.2. The error percentage for such system is explained in Table 6.2. The results show that the technique was able to detect all the 4 obstructed pipes without false positives and with remarkable accuracy. Also, the statistical analysis in terms of mean value μ and standard deviation σ of parameter α are illustrated in Table 6.3, and graphically are presented in Figure 6.3 by using a Box-and-Whisker plot. As it can be seen, even though the mean values for the blocked pipes are slightly greater than the exact target values, the proposed technique is able to identify the 4 obstructed pipes with a very low dispersion.
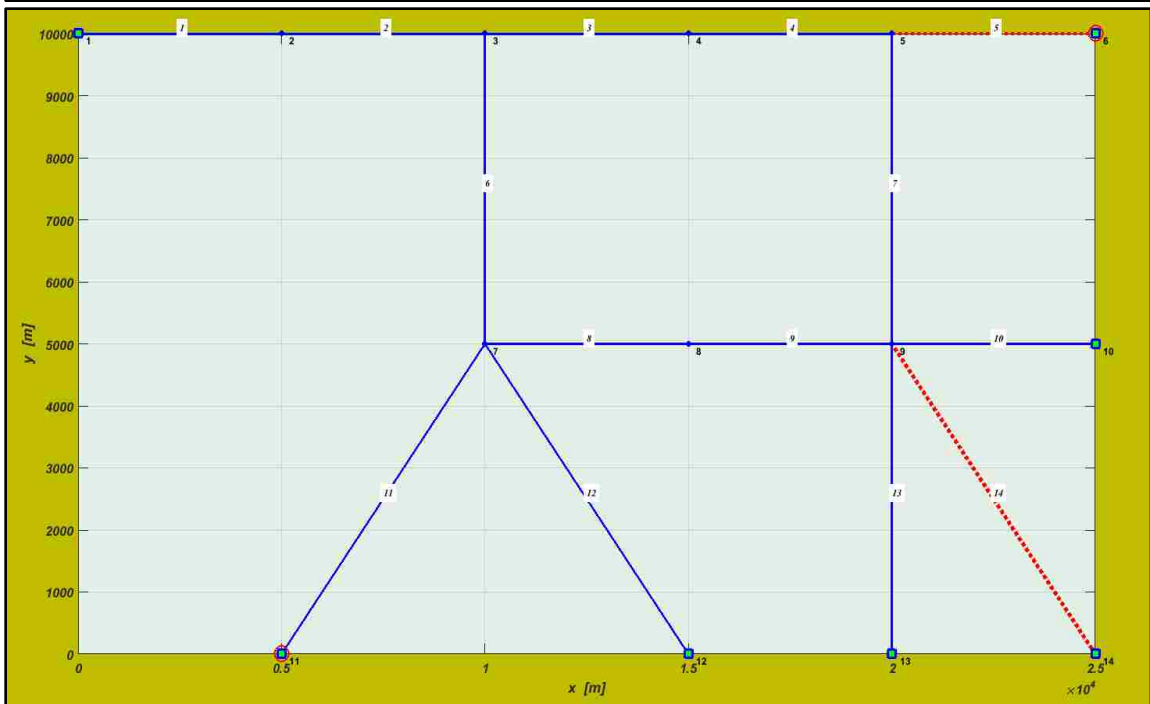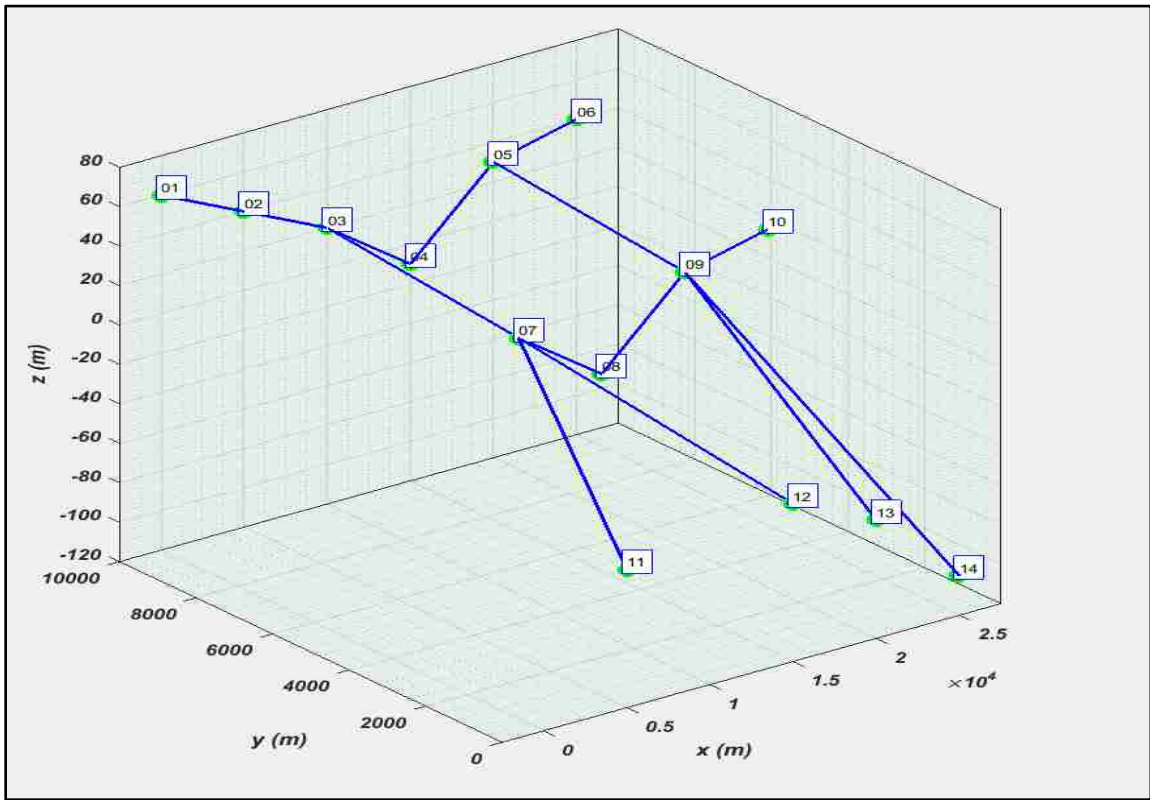
Figure 6.1: Layout of the investigated network

Pipe	Connectivity	Nodal Coordinates			D(mm)	e (mm)	h (m)
		X(m) (*1000)	Y(m) (*1000)	Z(m)			
1	1-2	0	10	60	400	0.5	10
2	2-3	5	10	40	400	0.5	-
3	3-4	10	10	20	300	0.5	-
4	4-5	15	10	-10	300	0.5	-
5	5-6	20	10	30	300	0.5	-
6	3-7	25	10	40	300	0.5	180
7	5-9	10	5	10	300	0.5	-
8	7-8	15	5	-20	300	0.5	-
9	8-9	20	5	20	300	0.5	-
10	9-10	25	5	30	300	0.5	190
11	7-11	5	0	-50	300	0.5	270
12	7-12	15	0	-40	300	0.5	260
13	9-13	20	0	-60	300	0.5	280
14	9-14	25	0	-100	300	0.5	320

Table 6.1: Data network
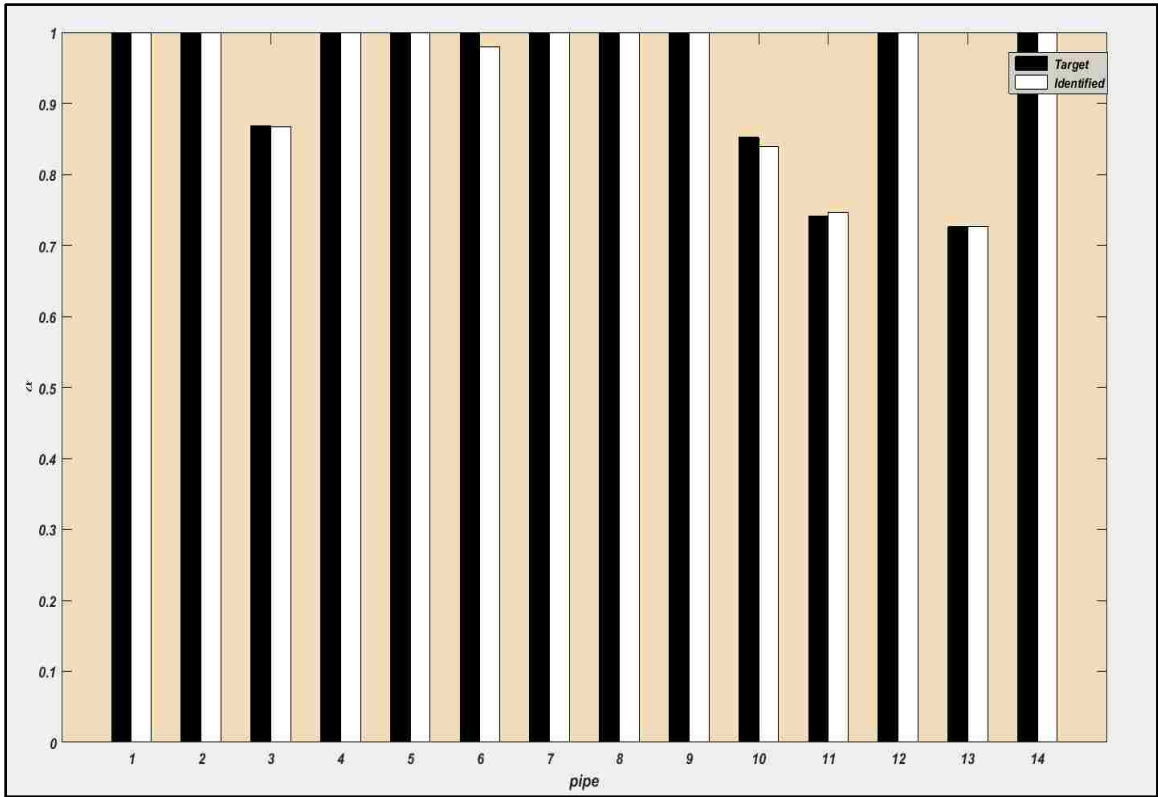
Figure 6.2: Results of the blockage identification procedure

Pipe	Alpha real	Alpha identified	Error%
1	1	1	0
2	1	1	0
3	0.868	0.866	0.186
4	1	1	0
5	1	1	0
6	1	0.979	2.051
7	1	1	0
8	1	1	0
9	1	1	0
10	0.852	0.839	1.507
11	0.741	0.746	0.661
12	1	1	0
13	0.726	0.727	0.108
14	1	1	0

Table 6.2: Error percentage in the results of identification

Results of the statistical identification													
Pipe	1	2	3	4	5	6	7	8	9	10	11	12	13	14
μ	0.99	0.99	0.88	0.98	0.99	0.99	0.97	0.99	0.99	0.86	0.74	0.99	0.74	1
$\sigma\%$	1.27	0.92	3.32	3.04	1.11	0.17	4.62	1.10	2.46	3.49	1.83	0.58	2.69	0

Table 6.3: Results of the statistical identification

Figure 6.3: Results of the statistical analysis

6.2.2 Description of the Second Case Study

The proposed methodology is demonstrated on the artificial network shown in Figure 6.4. The network consists of 15 pipes and 15 nodes. The crude oil is extracted from the subsea reservoirs located at nodes 7, 8, 9, 12, 13, 14 and 15, where the pressure i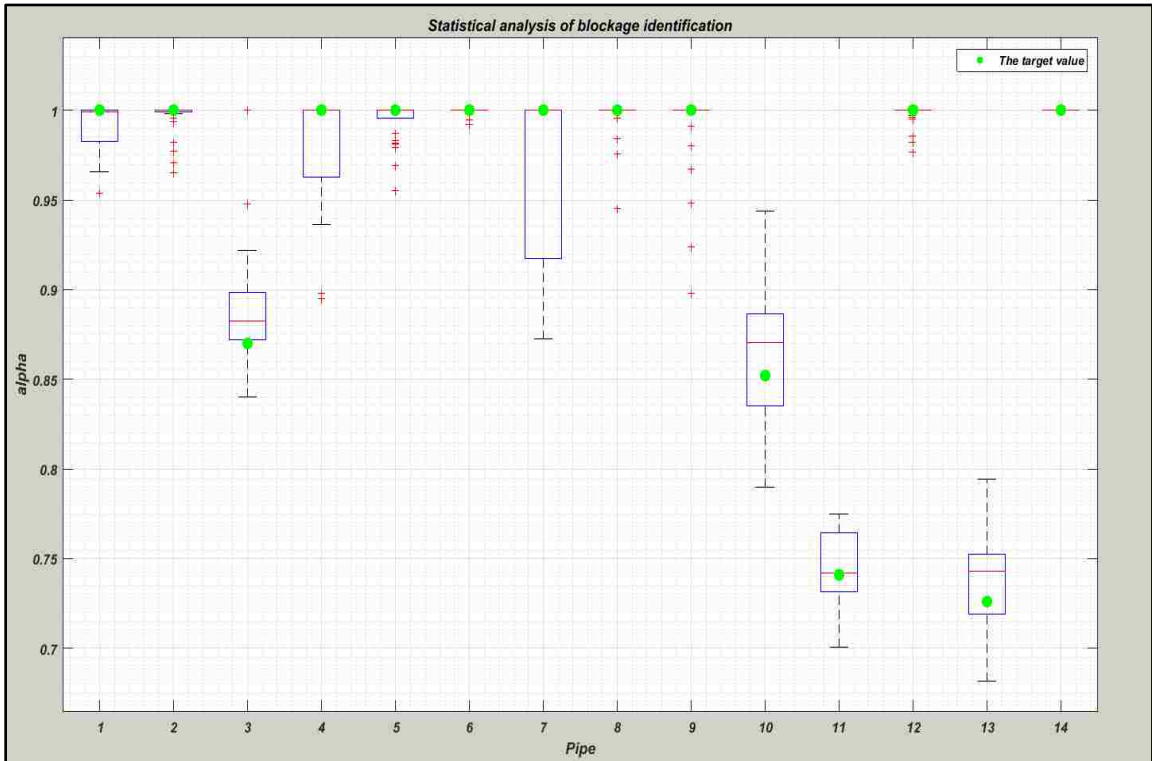s imposed. The pressure head is also imposed at node 1, where the crude oil is collected. The necessary input data of the investigated network are collected in Table 6.4. In this application the temperature of the crude oil in each pipe is computed in terms of the mean value of the temperature at the inlet and outlet nodes of the pipe itself. When the nodal elevation equals or is greater than 0, the temperature at this node is considered to be 22º. Otherwise, it is assumed to vary between 15º and 22º. The examined scenario is characterized by blockages in pipes 3 (30% blockage over 30% L), 4 (50% blockage over 30% L), 8 (50% blockage over 50% L) and 12 (30% blockage over 75% L). Flow data is collected at all pipes except pipes 1, 2, 3, 8, 10 and 11, whereas the nodal pressure head is measured at all nodes.

The results in terms of identified residual diameters are collected in Figure 6.5. The error percentage for such system is shown in Table 6.5. For the investigated scenario, the results show that the technique was able to detect all the 4 occluded pipes, without false positives and with notable accuracy in such a large-scale system. Also, the statistical analysis in terms of mean value μ and standard deviation σ of the parameter α for each pipe are illustrated in Table 6.6, and are graphically presented in Figure 6.6 by using a Box-and-Whisker plot. As it can be seen, even though the mean values for the blocked pipes are slightly greater than the exact target values, the proposed technique was able to identify the last 3 obstructed pipes (i.e., 4, 8 and 12) with a very low dispersion. However, the statistical

144

analysis was not accurate in identification the exact value in terms of the mean of pipe 3. It can be concluded that the small percentage of blockage (30%) deposited in a short portion of the pipe length (i.e., 30% L) introduces difficulty for the suggested methodology to sense the exact value of the obstruction.
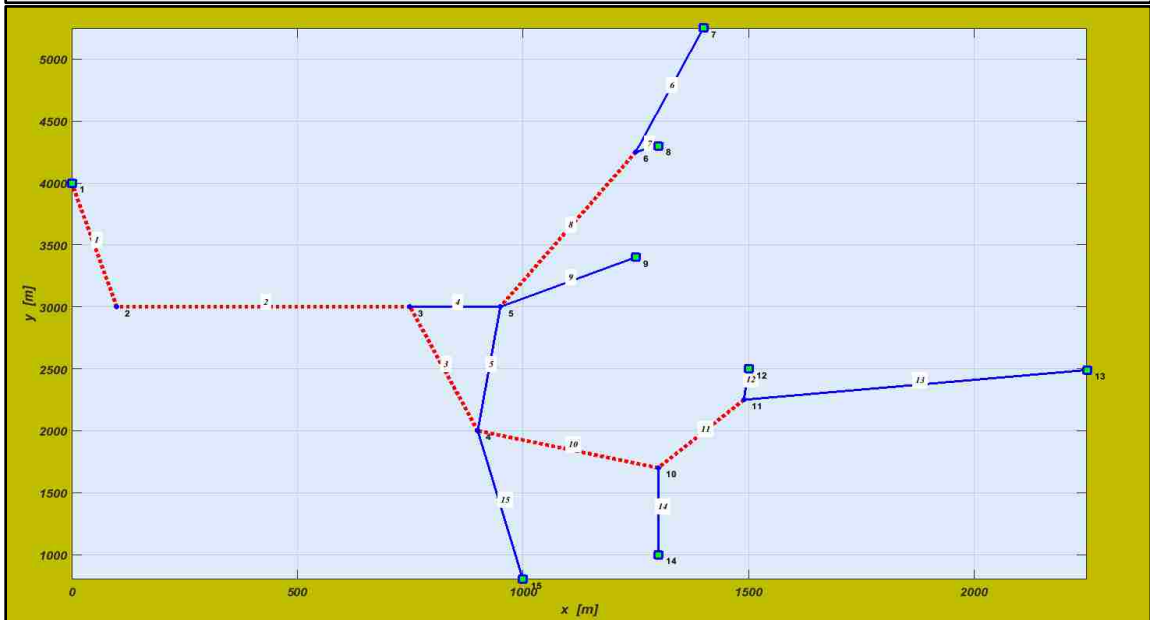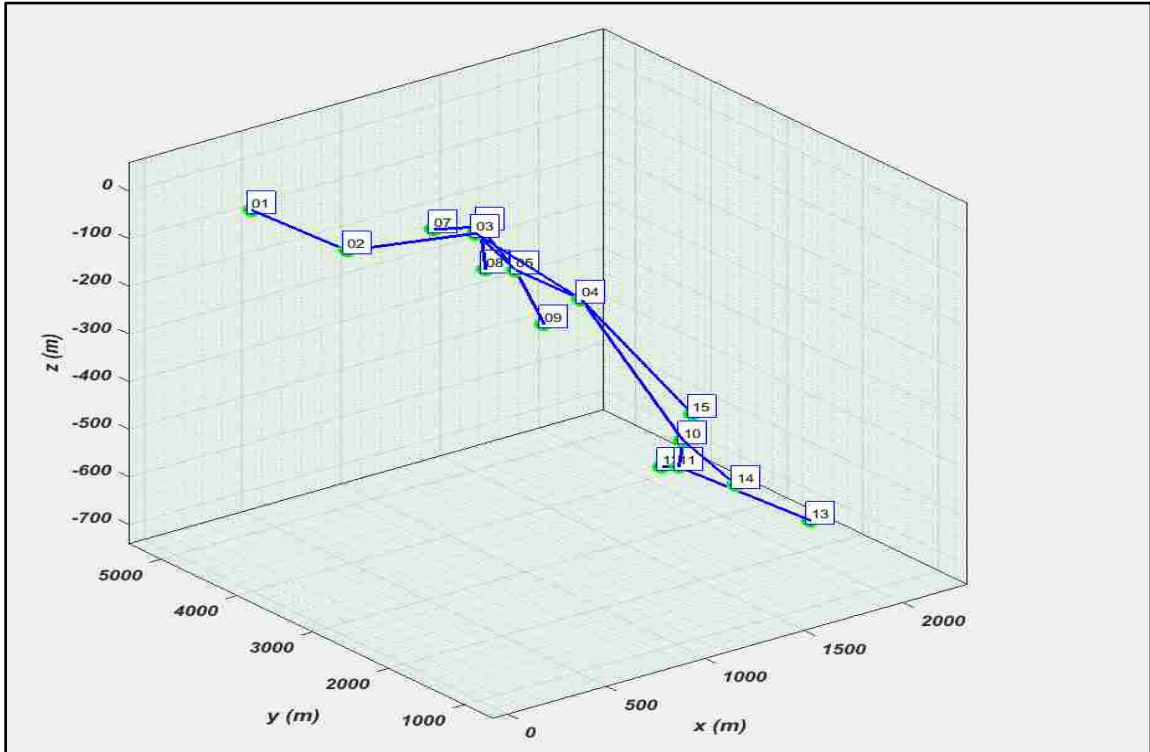
Figure 6.4: Layout of the inspected network

| Pipe | Connectivity | Nodal Coordinates | | | D(mm) | e (mm) | h (m) |
		X(m) (*1000)	Y(m) (*1000)	Z(m)			
1	1-2	0	4	60	400	0.05	10
2	2-3	0.1	3	40	400	0.05	-
3	3-4	0.75	3	0	350	0.05	-
4	3-5	0.9	2	-80	350	0.05	-
5	4-5	0.95	3	-100	350	0.05	-
6	6-7	1.25	4.25	-140	350	0.05	-
7	6-8	1.40	5.25	-240	300	0.05	450
8	5-6	1.30	4.30	-240	300	0.05	450
9	5-9	1.25	3.40	-280	300	0.05	490
10	4-10	1.30	1.70	-400	300	0.05	-
11	10-11	1.49	2.25	-520	300	0.05	-
12	11-12	1.50	2.50	-540	300	0.05	790
13	11-13	2.25	2.49	-740	300	0.05	990
14	10-14	1.30	1.00	-440	300	0.05	690
15	4-15	1.00	0.80	-240	300	0.05	450

Tabel 6.4: Network data
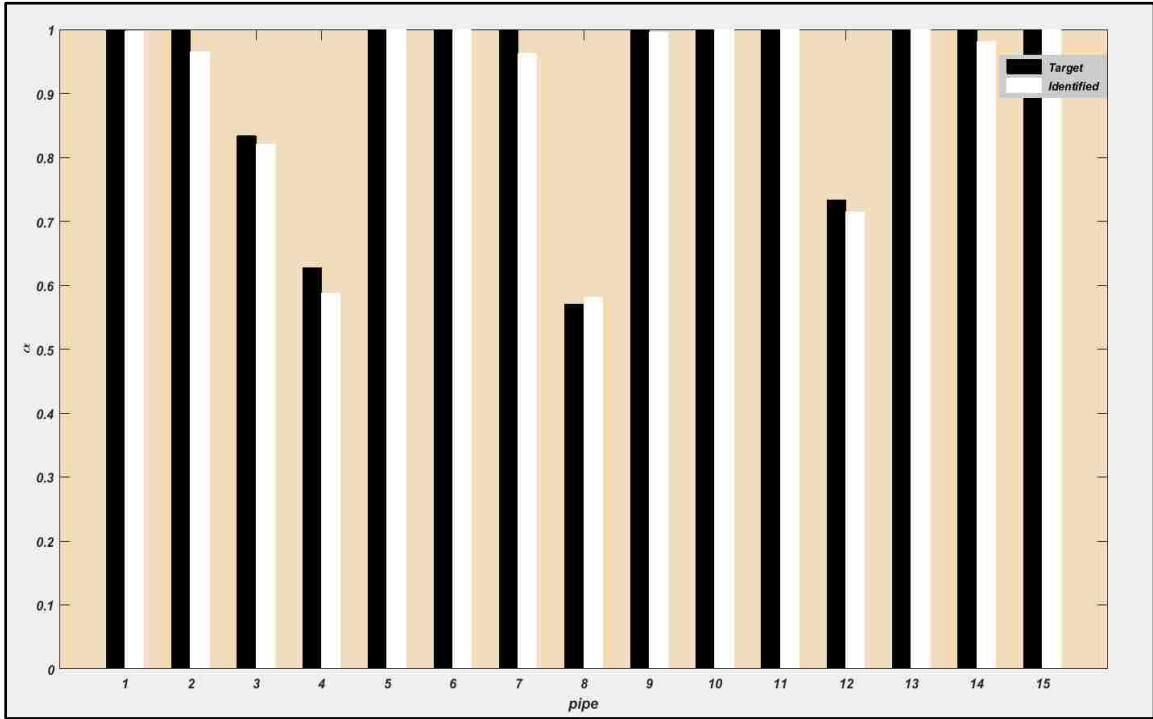
Figure 6.5: Results of the blockage identification procedure

Pipe	Alpha real	Alpha identified	Error%
1	1	0.997	0.278
2	1	0.964	3.527
3	0.834	0.821	1.532
4	0.627	0.588	6.333
5	1	0.999	0
6	1	0.999	0
7	1	0.962	3.804
8	0.571	0.581	1.704
9	1	0.996	0.439
10	1	0.999	0
11	1	1	0
12	0.733	0.714	2.587
13	1	1	0
14	1	0.980	1.968
15	1	0.999	0

Table 6.5: Error percentage in the results of identification

Results of the statistical identification

Pipe	1	2	3	4	5	6	7	8	9	10	11	12	13	14	15
μ	0.99	0.94	0.94	0.55	0.99	0.99	0.96	0.60	0.99	0.99	0.99	0.82	0.99	0.99	0.98
$\sigma\%$	0.79	7.41	6.37	15.12	0.93	1.06	4.31	5.13	21.83	1.93	1.60	12.15	0.31	0.65	3.48

Table 6.6: Results of the statistical identification
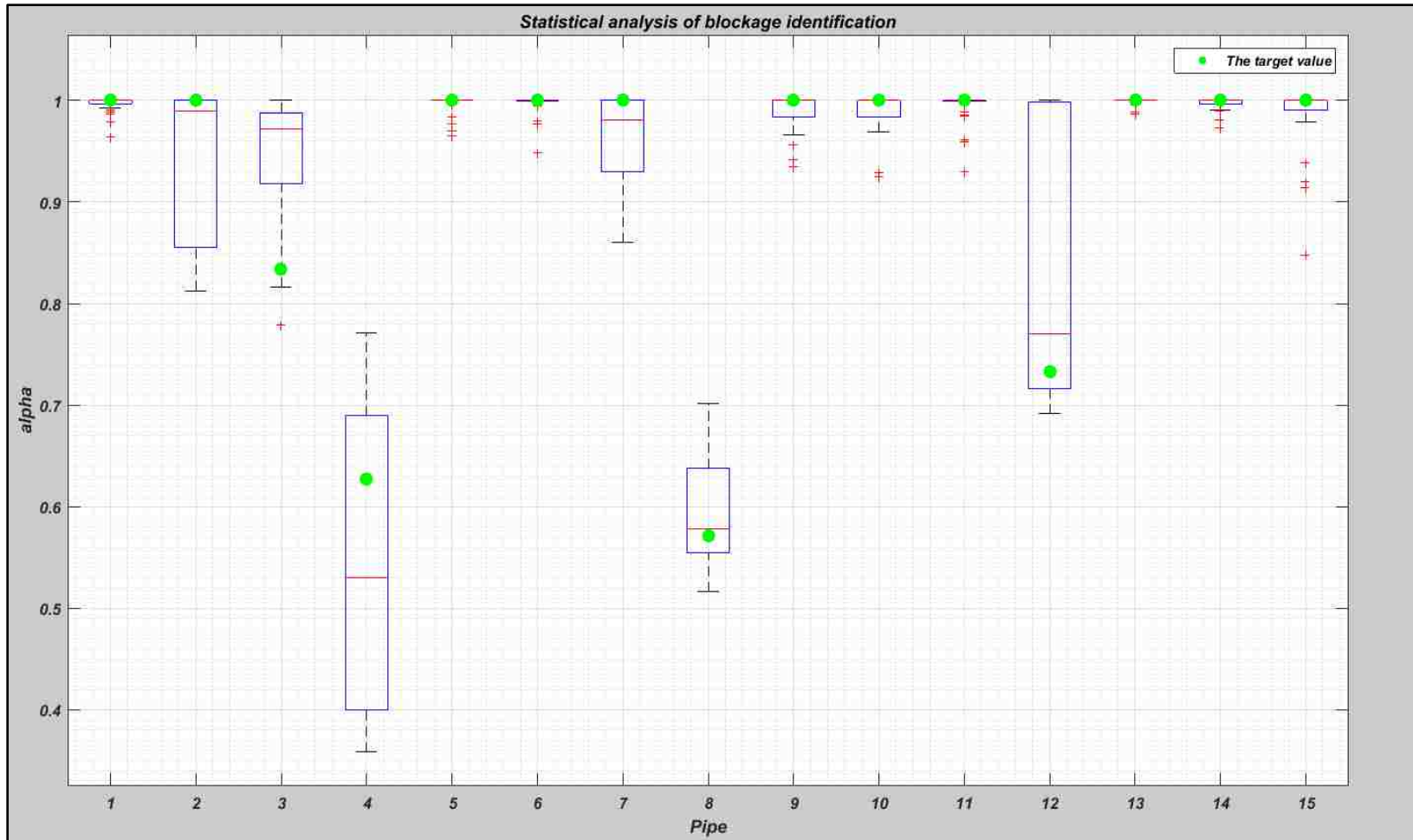
Figure 6.6: Results of the statistical analysis

This chapter provides a fundamental proof demonstrating the accuracy and robustness of the suggested procedure. The two examples proved the possibility to use the proposed technique with different occlusion scenarios and network layouts. The presented numerical applications showed that the proposed methodology was able to identify the blockage without false positives. Results, in fact, show a very good correspondence between the respective target values of alpha and those identified by the procedure. Overall, it can be noted that the methodology was capable to obtain a reasonable degree of accuracy, nonetheless some of the measurements were not available!

CHAPTER 7

CONCLUSIONS AND FUTURE DEVELOPMENTS

7.1 Conclusions

A technique to identify blockages that create a serious damage in pipeline networks has been presented. The proposed methodology provides a quantitative assessment of the blockage severity. The suggested procedure based on a finite element method along with Genetic Algorithms is used to obtain the results of the identification. The proposed technique identifies the blockage as a result of the optimization of the residual diameters by minimizing the discrepancy between the measured and simulated nodal pressure heads and pipe flows.

The study investigates several pipeline networks experimentally and numerically. By looking at the results of the analysis, the proposed technique has shown a very good accuracy in the identification of the residual diameters in terms of parameter α. Overall, the empirical and numerical applications discussed throughout this study have proved the accuracy and robustness of the suggested procedure. Also, the proposed technique needs simple measurements that do not affect the normal operational conditions and at the same time are affordable. Thus, it is advantageous to use such technique rather than others that are explained in this study, which require sophisticated measurements and are costly.

Technically, the methodology has presented a good sensitivity and a reasonable degree of accuracy in detection of clogged pipes, even when some nodal pressure head and pipe flow measures are not available. The results of the numerical and experimental applications have provided a general information about the location of the blockage, but cannot characterize the exact size of the obstruction in terms of length and residual diameter, but only combination of the two. The results of the identification procedure proved the validity of the proposed technique both experimentally and numerically. Also,

parametric studies have been conducted to improve the accuracy and sensitivity of such methodology. The analytical results have shown that the proposed procedure can be used broadly with any network (complex, simple, looped, branched, underwater, underground or in desert).

Further improvements by developing the finite element model can be implemented, to simulate the flow in each pipe in the case of multi-phase fluid.

7.2 Future Developments

Several suggestions and ideas can be taken into consideration to make the proposed technique used widely without any limitations for future studies. Below are some of the ideas that can be interesting to examine:

- Adjust the proposed technique to work either with single-phase fluids or with multi-phase fluids in non-steady state.

- Take into consideration the case of non-uniform blockage in the entire pipe as it is in reality.

- Make the technique more advanced, to include dynamic measurements that can be collected easily.

- Improve the technique to cover two goals: 1) detect the blockage location and 2) apply further steps to remove the blockage.

- Improve the performance of GAs by implementing one of the recent advanced and modified methods that have been suggested, such as Search Space Reduction Method (SSRM) or improved Genetic Algorithm utilizing Migration and Artificial Selection (iGAMAS).

- Introduce a precise objective function that does not depend on any penalty factor.

References

Adewumi, M. A., Eltohami, E. S., & Solaja, A. (2001). Possible detection of multiple blockages using transients. *Tc*, *170*(344), 5.

Bocchini, P., Marzani, A., & Karamlou, A. (2014). Blockage Detection in Pipeline Networks for Gas and Oil. In *Shale Energy Engineering 2014: Technical Challenges, Environmental Issues, and Public Policy* (pp. 676-683).

Bathe, K. J. (1982). Finite element procedures in engineering analysis.

Bayley, F. J. (1958). An Introduction to Fluid Dynamics. *Great Britain.*

Colombo, A. F., Lee, P., & Karney, B. W. (2009). A selective literature review of transient-based leak detection methods. *Journal of Hydro-environment Research*, *2*(4), 212-227.

Duan, H. F., Lee, P. J., & Tuck, J. (2014). Experimental investigation of wave scattering effect of pipe blockages on transient analysis. *Procedia Engineering*, *89*, 1314-1320.

Gen, M., & Cheng, R. (2000). *Genetic algorithms and engineering optimization* (Vol. 7). John Wiley & Sons.

Goldstein, R. J. (1983). Fluid Mechanics Measurements.

Heeley, D. (2005). Understanding Pressure and Pressure Measurement. *Freescale Semiconductor Application Note*.

Holland, J. H. (1975). Adaptation in natural and artificial systems. An introductory analysis with application to biology, control, and artificial intelligence. *Ann Arbor, MI: University of Michigan Press*.

Introduction to Process Optimization. (n.d.). Retrieved from http://www.siam.org/books/mo10/mo10_sample.pdf

Koh, C. G., & Perry, M. J. (2009). *Structural Identification and Damage Detection using Genetic Algorithms, Structures and Infrastructures Book Series, Vol. 6*. Crc Press.

Lee, P. J., Vítkovský, J. P., Lambert, M. F., Simpson, A. R., & Liggett, J. A. (2008). Discrete blockage detection in pipelines using the frequency response diagram: numerical study. *Journal of Hydraulic Engineering*, *134*(5), 658-663.

Malhotra, R., Singh, N., & Singh, Y. (2011). Genetic algorithms: Concepts, design for optimization of process controllers. *Computer and Information Science*, *4*(2), 39.

Marzani, A., Mazzotti, M., Bocchini, P., Viola, E., di Lullo, A., Mantegazza, T., & Pagliuca, G. (2013). Ident cation of blockages in pipe networks via a simple and non-invasive technique based on steady-state measurements and Genetic Algorithms.

Mohapatra, P. K., Chaudhry, M. H., Kassem, A., & Moloo, J. (2006). Detection of partial blockages in a branched piping system by the frequency response method. *Journal of fluids engineering*, *128*(5), 1106-1114.

Mazzotti, M., Marzani, A., & Bocchini, P. (2008). Finite element formulation for parameter identification problems. *University of Bologna, Bologna, Italy*.

Meles, Claudio. (2014). Blockages Pipeline Networks Detection. *Thesis*

Papaevangelou, G., Evangelides, C., & Tzimopoulos, C. (2010, July). A new explicit relation for the friction coefficient in the darcy-weisbach equation. In *Proceedings of the Tenth Conference on Protection and Restoration of the Environment* (Vol. 166, pp. 6-09).

Sattar, A. M., Chaudhry, M. H., & Kassem, A. A. (2008). Partial blockage detection in pipelines by frequency response method. *Journal of Hydraulic Engineering*, *134*(1), 76-89.

Scott, S., & Yi, J. (1999). Flow testing methods to detect and characterize partial blockages in looped subsea flowlines.

Scott, S. L., & Satterwhite, L. A. (1998). Evaluation of the backpressure technique for blockage detection in gas flowlines. *TRANSACTIONS-AMERICAN SOCIETY OF MECHANICAL ENGINEERS JOURNAL OF ENERGY RESOURCES TECHNOLOGY*, *120*, 27-31.

Viola, E., & Bocchini, P. (2013). Non-destructive parametric system identification and damage detection in truss structures by static tests. *Structure and Infrastructure Engineering*, *9*(5), 384-402.

Vasava, P. R. (2007). *Fluid flow in T-junction of pipes* (Doctoral dissertation, LAPPEENRANTA UNIVERSITY OF TECHNOLOGY).

Wang, X. J., Lambert, M. F., & Simpson, A. R. (2005). Detection and location of a partial blockage in a pipeline using damping of fluid transients. *Journal of water resources planning and management*, *131*(3), 244-249.

Yuan, S. W. (1967). Foundation of Fluid Mechanics.

Zienkiewicz, O. C., Taylor, R. L., & Taylor, R. L. (1977). *The finite element method* (Vol. 3). London: McGraw-hill.

Appendix

The implementation of the proposed technique via MATLAB program is summarized as follows:

1- The Input File Template for Any Pipeline Network

```
% Blockage detection

diary off; close all; clear; clc;
addpath ./bin

% Units
% length:      m
% time:        sec
% temperature: °C

%% Type of analysis and fluid

param.analysis = 1; % 1=simulated measures; 2=real measures
param.fluid    = 2; % 1=water; 2=crude oil (ask if you need to expand the library in physicprop)
param.toll = 1e-5;  % tollerance on the residuals for convergence
param.maxiter = 50; % maximum number of Newton-Rapson iterations

%% Network layout and characteristics

% nodal coordinates
%          X        Y          Z
nodes = [                        ];

% pipe connectivity
%       node i   node j
LCO = [             ];

% Pipe characteristics
%        L         D       e         KL         T
pipes = [                              ];
% you can create function to compute the pipe length or it is possible to
% put the pipe length directly

% Temperature of fluid and surroundings
%         Tf Ts
T.pipes = [    ];

% Measured nodal temperatures
%       node   T (°C)
T.meas = [         ];

% Reservoirs

%        nodo    h (m)
himp = [              ]; % Define as B.C
```

```matlab
% Demands
%         node   Q(m^3/sec)
Qimp = [               ]; % Define as B.C

%% Blockages



%                 Pipe  %length  %residualD  eb
simul.blockages = [                          ];




%% Measurements

%indexes of pipes for which a measurement is available
hmeas = [  ]';
Qmeas = [  ]';


%% Impose noise on mearurements (for param.analysis = 1)

simul.noiseh = 5;    % percentage noise level on h
simul.noiseQ = 5;    % percentage noise level on Q

%% Measured quantities (for param.analysis = 2)

measures.h = []; %vector of measured pressure heads (has to be consistent with hmeas)
measures.Q = []; %vector of measured flows (has to be consistent with Qmeas)

%% Optimization parameters of GAs

optimparam.PopulationSize = 200;
optimparam.Generations = 100;
optimparam.StallGenLimit = 2000;
optimparam.StallTimeLimit = 60*60;
optimparam.TolFun = 1e-13;

%% Run identification

[ alpha ] = pineblid( param, optimparam, nodes, LCO, pipes, T, himp, Qimp, hmeas, Qmeas, eb, simul, measures );
```

2- A Box-and-Whisker plot

```matlab
%% Statistical analysis
clc; clear; close all;
g=xlsread('Results.xlsx','sheet3','B156:U165');
%% plot box and whisker plot
% boxplot(g','PlotStyle','compact')
% hold on
boxplot(g')
grid on
xlabel('Pipe');
ylabel('alpha')
title('Statistical analysis of blockage identification')
grid minor
hold on

%% Target values
X=[1 2 3 4 5 6 7 8 9 10];
Y=[1 1 0.7414 1 1 1 1 0.53554 1];
sz=100;
scatter(X,Y,sz,'g','filled')
hold on
%% scaled-dawn
XX=[0.985550962 1 0.810199854 0.996079619 0.96769615 0.977193896 0.93 0.868559407 0.57 0.650768317];
scatter(X,XX,sz,'p','b','filled')
legend('The target value','Scaled-dawn value')
```

3- Missing Measurements Comparison through Images

```matlab
clc;close all; clear;
x1=xlsread('Results.xlsx','sheet7','D4:M13');
x2=xlsread('Results.xlsx','sheet7','D20:M29');
x3=xlsread('Results.xlsx','sheet7','D32:M41');
x4=xlsread('Results.xlsx','sheet7','D44:M53');
x5=xlsread('Results.xlsx','sheet7','D56:M65');
x6=xlsread('Results.xlsx','sheet7','D69:M78');
x7=xlsread('Results.xlsx','sheet7','D82:M91');
x8=xlsread('Results.xlsx','sheet7','D95:M104');

figure
subplot(2,2,1)
image(x1,'CDataMapping','scaled')
colorbar
%colormap
xlabel('pipe'); ylabel('Blocked pipe'); title('\alpha=0.8')
subplot(2,2,2)
image(x3,'CDataMapping','scaled')
colorbar
%colormap(gray(2000))
xlabel('pipe'); ylabel('Blocked pipe'); title('\alpha=0.7')
subplot(2,2,3)
image(x5,'CDataMapping','scaled')
colorbar
%colormap(gray(2000))
xlabel('pipe'); ylabel('Blocked pipe'); title('\alpha=0.6')
subplot(2,2,4)
image(x7,'CDataMapping','scaled')
colorbar
%colormap(gray(2000))
xlabel('pipe'); ylabel('Blocked pipe'); title('\alpha=0.5')
```

Biography of the candidate

Mohanad Khazaali was born in August, 1989. He grew up in Al- Dewaniyah city that is located in the southern part of Iraq. He has a strong and close relationship with his family, which consists of his parents and six siblings. His father, Abdulzahra Khazaali, is a high school graduate who served in the army for a few months prior 2001. Now, he is working as a driver to support his family. The writer's mother, Balasim Hissan is working as a teacher in a primary school. She graduated from the Educational Diploma Institute in 1987 and was offered teaching job instantly. Mohanad has two brothers and four sisters with a decent education.

Mohanad Khazaali confronted many challenges that affected his path to education, but he successfully overcame all them. In June 2007 to June 2011, he earned his bachelor's degree from the college of engineering located in his city. He was a hardworking and persistent student among his peers; he was at the top of his class. During his study, he received several awards from different organizations. In 2011, he received an award from the dean of Al-Qadisiyah University for his dedicated work and his optimal achievements. Sadly, at the time he graduated, Iraq faced an economic crisis and many companies were shut down; it was hard to find a job. However, he was lucky to get a job offer from Al-Maskit Alafkee company- a reputed private company in Al-Dewaniyah, Iraq, which specializes in sewage system pipelines design and implementation. He was qualified to work as a supervisor engineer in the company for almost three years (June 2011 to December 2013). Later on, in 2013, Mohanad got a permanent job in the Ministry of Education as a supervisor engineer to oversee school buildings design and implementation. Meanwhile, he was awarded scholarship by Higher Committee for Education

Developments in Iraq (HCED)\ prime minster office through a competitive process to pursue his Master's degree. He got accepted by Lehigh University (USA) to do his Master's degree in structural engineering. Mohanad Khazaali started his academic program in August 2015, and he graduated in May 2017. His academic progress throughout these two years was good. Mohanad would like to continue with his effort to gain more knowledge through the doctoral degree. He got an opportunity by Lehigh University with support from his advisor (Paolo Bocchini) to do his Ph.D. and will start in August 2017.